Universidade de Aveiro Departamento de Electrónica, Telecomunicações e Informática,
2015

Marina Daniela da Cruz Jordão

Sistemas de Caracterização para Aplicações RFID

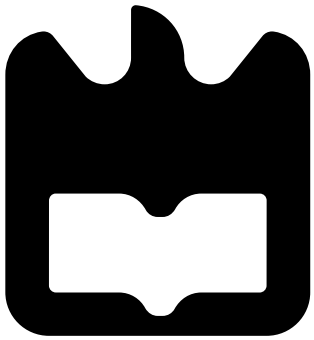

Aos meus Pais e irmã,

Marina Daniela da Cruz Jordão

Sistemas de Caracterização para Aplicações RFID

Characterization Systems for RFID Applications

Dissertação apresentada à Universidade de Aveiro para cumprimento dos requesitos necessários à obtenção do grau de Mestre em Engenharia Electrónica e Telecomunicações, realizada sob a orientação científica do Professor Doutor Nuno Miguel Gonçalves Borges de Carvalho, Professor Catedrático do Departamento de Electrónica, Telecomunicações e Informática da Universidade de Aveiro e sob co-orientação científica do Doutor Pedro Miguel Duarte Cruz, Investigador Doutorado do Instituto de Telecomunicações, poló de Aveiro

o júri / the jury

presidente / president

Professor Doutor João Nuno Pimentel da Silva Matos
Professor Associado do Departamento de Electrónica, Telecomunicações e Informática da Universidade de Aveiro

vogais / examiners committee

Professor Doutor Rafael Ferreira da Silva Caldeirinha
Professor Coordenador do Departamento de Engenharia Electrotécnica da Escola Superior de Tecnologia e Gestão do Instituto Politécnico de Leiria (arguente)

Professor Doutor Nuno Miguel Gonçalves Borges de Carvalho
Professor Catedrático do Departamento de Electrónica, Telecomunicações e Informática da Universidade de Aveiro (orientador)

agradecimentos / acknowledgements

Um agradecimento especial aos meus pais e irmã por todo o apoio prestado afim de alcançar os meus objetivos.

Agradeço também a toda a minha família e amigos pelo apoio contínuo em todo o meu percurso académico.

A todos os meus colegas e amigos, que tive o prazer de conviver durante o meu percurso na Universidade de Aveiro, um grande obrigado, pois sem a vossa ajuda e força esta etapa teria sido bem mais complicada.

Muito obrigado ao meu orientador, Professor Doutor Nuno Miguel Gonçalves Borges de Carvalho, ao meu co-orientador, Doutor Pedro Miguel Duarte Cruz e ao colaborador, Investigador Diogo Carlos Alcobia Ribeiro, por todo incentivo, disponibilidade e ajuda durante toda a realização desta dissertação.

Um agradecimento especial ao João Santos e ao André Prata, assim como, a todos os membros do Instituto de Telecomunicações, por todo o auxílio prestado.

Obrigada!

Palavras-Chave

Radio Communication, Wireless Power Transmission, Energy Harvesting, RF-DC, Mixed-Domain, PXI, LabVIEW, RFID

Resumo

Esta dissertação surge no âmbito da colaboração do Instituto de Telecomunicações com a National Instruments (NI), com o intuito de desenvolver soluções de caracterização e medida para conversores RF-DC. Estas soluções de caracterização pretendem garantir uma otimização deste tipo de circuitos, que é a base dos sistemas de Wireless Power Transmission and Electromagnetic Energy Harvesting.

Pretende-se assim recorrer a código Laboratory Virtual Instrumentation Engineering Workbench (LabVIEW) e aos módulos PCI eXtensions for Instrumentations (PXI) da NI com o objetivo extrapolar estes sistemas de medida para aplicação de leitura e medida de Tags Radio Frequency Identification (RFID).

Assim sendo, nesta dissertação pretende-se desenvolver um sistema de caracterização do RFID usando o LabVIEW, ou seja, um leitor de RFID.

Palavras-Chave

Rádio Comunicações, Wireless Power Transmission, Energy Harvesting, RF-DC, Mixed-Domain, PXI, LabVIEW, RFID

Abstract

This dissertation has the collaboration of the Telecommunications Institute with National Instruments, in order to develop solutions for characterization and measurement for RF-DC converters. These characterization solutions are intended to ensure optimization of this type of circuit, which is the basis of Wireless Power Transmission and Electromagnetic Energy Harvesting systems.

It is intended to use LabVIEW code and the PXI modules from NI with the goal of extrapolating these measurement systems to read and measure the RFID Tags.

Therefore, this dissertation is focused on RFID characterization using the LabVIEW, in other words, RFID reader.

Contents

List of Figures

List of Tables

List of Acronyms

ASK Amplitude Shift Keying

BLF Backscatter-link frequency

CRC Cyclic-Redundancy Check

CW Continuous Wave

DC Direct Current

DFT Discrete Fourier Transform

DR Divide Ratio

DSB-ASK Double-sideband amplitude shift keying

EIRP Equivalent Isotropically Radiated Power

EPC Electronic Product Code

ERP Effective Radiated Power

ETSI European Telecommunications Standards

FAM Front-end Adapter Module

FCC Federal Communications Commission

FFT Fast Fourier transform

FHSS Frequency Hopping Spread Spectrum

FM Frequency Modulation

FM0 Bi-phase space

FPGA Field Programmable Gate Array

FrT Frequency tolerance

GPS Global Positioning System

HF High Frequency

IoT Internet of Things

IQ In-phase/Quadrature

ISM Industrial, Scientific and Medical

ISO International Standards Organization

IT Instituto de Telecomunicações

LabVIEW Laboratory Virtual Instrumentation Engineering Workbench

LF Low Frequency

MIT Massachusetts Institute of Technology

NI National Instruments

OOK (On/Off Key)

PC Protocol control

PIE Pulse Interval Encoding

PR-ASK Phase-reversal amplitude shift keying

PXI PCI eXtensions for Instrumentations

PXISA PXI Systems Alliance

PW Pulse With

RTcal Interrogator-to-Tag calibration symbol

RF Radio Frequency

RFID Radio Frequency Identification

RN16 16-bit Random or pseudo-Random Number

RX Receiver

SSB-ASK Single-sideband amplitude shift keying

Tari Type A Reference Interval

Tpri Backscatter-link pulse-repetition interval

TRcal Tag-to-Interrogator calibration symbol

TX Transmiter

UHF Ultra High Frequency

USA United States of America

USB Universal Serial Bus

VI Virtual Instrument

VSA Vector Signal Analyzer

VSG Vector Signal Generator

WPT Wireless Power Transfer

XPC Extended Protocol Control

Chapter 1

Introduction

A characterization approach based on specific PXI instrumentation is developed using measurement solutions for RF-DC converters, Radio Frequency Identification (RFID) and so on. These tests and measurement solutions are important to guarantee the optimization of circuits, mainly when the energy efficiency needs to be maximized, being such a key point in wireless power transmission and electromagnetic energy harvesting.In order to use these characterization systems in useful applications, the first thing to be done was to apply it to RFID applications. In this sense, the excitation of an RFID tag should be done following a convenient protocol. This is why the first approach was to design an RFID reader that could be embedded into the characterization instrument.

The PXI platform is a useful tool in this scenario, because it has the ability of implement test and measurement applications, for any type of purposes. The LabVIEW programming is a fundamental requirement to work with PXI, because it is a graphical programming with the big advantage of the code becoming easier to understand and, for this reason, the programmer productivity is increased.

For this purpose, an RFID reader and the respective LabVIEW code has been developed, in order to demonstrate the applicability of modular instrument. Two architectures have been implemented, one based on a stimulus-response strategy and another based on real-time interrogator emulation strategy. The RFID reader uses International Standards Organization (ISO) 18000-6C RFID communication protocol, which operates in the 860-960 MHz frequency range. Thus, it is important to create an RFID reader application, in order to demonstrate that this kind of applications are very useful to make RFID tag tests, measurements and to read tags.

All things considered, in the course of this dissertation another application emerges for RFID technology that is very significant, nowadays. The spectrum analyzer is a regular measure instrument used in Radio Frequency (RF) laboratories, and the most recent instruments have the benefit of having a spectrogram application view too. In fact, the spectrogram view allows to have a different overview of spectrum, and this is a big advantage in RF world.

Another considering aspect is the fact of seeing what is present in Ultra High Frequency (UHF) RFID spectrum. In RF laboratories sometimes it is useful to know if signals exist near frequencies that we are working on. So, building a spectrum analyzer and spectrogram application is a goal of this dissertation too, because it is another measure system application using the PXI, and, at the same time, an application case of RFID reader.

Nowadays, Wireless Power Transfer (WPT) is a hot topic because is a technique which

makes the transmission of electrical power from one device to another device. Therefore, with this technique the power-charging problem can be resolved. According to this fact, build an RF-DC measurement system is a requirement to read and to optimize the efficiency of these circuits. Thus, building an RF-DC measurement system using LabVIEW code is purpose of this dissertation too.

1.1 Motivation

The RFID [Dob07] [Rob05] technology was used in the Second World War in radar systems by several countries, like Germany, England,Japan and the United States of America. The radar system was developed by the Scottish physicist Sir Robert Alexander Watson-Watt. He also developed an airplane identification system with British Army's help during the Second World War, in 1935. For this reason, transmitters were implanted in airplanes that gave different answers to the radar. These signals were received from radar stations on ground and, this way, the transmission of the response signal was started, which identified the airplane as friendly. It was then created the first radio frequency identification. The Massachusetts Institute of Technology (MIT) and other research institutes, in 1999, started the study about an architecture with radio frequency technology, to apply on product identification applications. The first radio frequency identification was then created. As a result of this study, Electronic Product Code (EPC) was defined. EPC defines a product identification architecture using radio frequency signals, later called RFID.

After all, RFID brings to technology an easy and cheap way to do object identification, which is very useful and it is currently used in industry applications. Nowadays, because of these reasons, applications which allow test if tags work or not, applications that allow to make distance test about RFID tags and read the tags have an important role in industry.

The PXI platform and the LabVIEW code are fundamental tools in measurement system, developed by National Instruments NI. These two tools were particularly designed to measure and control systems and, for this reason, the PXI platform is the right choice to develop RFID reader systems.

Some works were made in this specific area [Ins15a] [Nik09] [Ins13a], and below a brief description about these issues is made.

1.1.1 LabVIEW-Based UHF RFID Tag Test and Measurement System Review

As it was mentioned before, some works were made in RFID tag test and measurement. An example of this, is this paper [Nik09], which describes an UHF RFID tag test and measurement using the PXI and the LabVIEW code. In this work, the authors report how the system was built and the results obtained. Beyond the PXI, the system is based on RF signal generator, composed by a PXI-5421 (which generates an arbitrary waveform) and a RF up-converter PXI 5610. The system is also composed by a RF signal analyzer, with a PXI-5600 (RF downconverter) and the digitizer PXI-5620.

Two important lessons were learnt. The first one, is the RF signal generator and the RF signal analyzer in this system present a limitation about synchronization, which is very important to detect tag response. The reason why this happens is because the system has separated RF local oscillators (LO). The second lesson is about the LabVIEW processing

time, which has longer duration than the time limits which imposed different phase relations in receiver chain.

The analysis of this paper was very important for this dissertation, because it was a starting point to understand how this dissertation work could be implemented.

1.1.2 Advanced RFID Measurements: Basic Theory to Protocol Conformance Test Review

Another substantial contribution is an article [Ins13a] developed by NI, with the purpose of giving to scientists in the research and commercial environments, a test and measurement system for tags. Firstly, the RFID theory is shortly explained and then the tag testing methodology. After that, a brief introduction about tags, antennas and communication protocols.

As a matter of fact, with this article some doubts about an RFID reader system have been resolved, because the information about this topic is explained in a simple way. In this article, two very useful architectures were learnt (explained in chapter 3) to apply in this dissertation. Thus, this article was important to understand how these architectures could be applied in this dissertation, as well as, to observe the big difference between these two and their complexity.

These two papers/articles were very important to start this dissertation and make some decisions because many initial questions were clarified.

1.2 Objectives

In this dissertation it is intended to develop an RFID reader system capable of giving some information to the user about RFID tags and an RF-DC measurement system, more specifically:

- `Test the tag functionality`: detect if tag can reply or not;
- `Make distance measurement test`: get the maximum distance which tag can reply;
- `Make power measurement test`: detect the minimum power which is needed for tag reply;
- `Read the tag`: get the tag EPC;
- `Make a spectrum analyzer and spectrogram application`: analyze and see what happens in the UHF RFID spectrum for all frequency bands worldwide;
- `Make an RF-DC measurement system`: get a_1, b_1, S_{11}, Direct Current (DC) voltage and efficiency of RF-DC circuits.

To develop the RFID application, the PXI platform and the LabVIEW code are requirements. An RFID reader is supposed to be built in UHF range (860 MHz - 960 MHz) and the ISO 18000-6C RFID communication protocol is used. In downlink, the Pulse Interval Encoding (PIE) with the (On/Off Key) (OOK) modulation is used and in uplink the Bi-phase space (FM0) coding is used. The RFID system is supposed to be built for United States of

America (USA) range and for a dense-interrogator environment, because it is more difficult to fulfill these specifications, than the European specifications. It makes the project more challenging.

For sure, the goal of this dissertation is not only to repeat that which has been done in this topic (RFID reader with PXI platform) in some articles, but the intention to build an RFID simple system capable of improving some of these works. It is a big purpose to create a useful tool, for RF laboratory, able to measure, test and read RFID tags, in a simple way to the user. Another purpose is to build an application which allows to view the RFID power spectrum, in a user-friendly fashion. Regarding RF-DC circuits, it is important to know the parameters values (incident wave (a_1), reflected wave (b_1) and thus, S_{11} (reflection coefficient)) of these circuits, because this way the RF-DC circuits optimization can be done, with a LabVIEW application for this purpose.

1.3 Organization of the Dissertion

This document is divided into 6 chapters, including this introductory chapter:

- `Chapter 2 - Technical Background`: In this chapter, an introductory explanation is made of the concepts used in this dissertation.
- `Chapter 3 - Archictures and Specifications`: There is an intention to explain the architectures used to build the RFID system and understand the choices made about some system specifications.
- `Chapter 4 - Implemetation`: The development and the implementation of the RFID reader is explained in this chapter.
- `Chapter 5 - Results`: The dissertation results are demonstrated in this chapter.
- `Chapter 6 - Conclusion and Future Work`: The conclusion of this dissertation is done and ways to improve this work in the future are also mentioned.

1.4 Original Contributions

This dissertation work provided the opportunity to participate in CONFTELE 2015, 10^{th} Telecommunications Conference held in Aveiro between September 17^{th} - 18^{th}. A scientific paper was written, M. Jordão, D. Ribeiro, P.M. Cruz, N.B. Carvalho, " *RFID Characterization System based on LabVIEW*" and this one was accepted and presented in poster form, in the conference. The paper can be seen in Appendix A and the poster can be seen in Appendix B.

Chapter 2

Technical Background

This chapter is devoted to explain the baseline topics used in the course of this dissertation. Firstly, a brief overview of RF communications will be given. The PXI platform is very important, due to the fact that this element controls all system. The LabVIEW programming because it is the key element used to develop all system. The RFID is a technology which allows to identify many objects and is very useful in our days, in many applications, for instance in industry. The protocol ISO 18000-6C is explained in detail, because it is the primary tool to start developing the RFID reading system.

2.1 RF Communications

The RF communications [Ins07] is used in wireless communications like phone, television, radio, satellite and so on, to transmit and to receive information. The operation range [Ana09] of RF communication can be separated in several ranges, but the most common are concentrated in the low end range (3 kHz - 3 GHz). This information can be seen in more detail in Table 2.1, but in summarised form.

Frequency (Hz)	**Applications**
30 - 3 k	Submarine communication
3 k - 30 k	Communication for military purposes
30 k - 300 k	Navigation and international radio stations
300 k - 3 M	National radio stations
3 M - 30 M	Radio stations and radiotelephone
30 M - 300 M	Frequency Modulation (FM) radio stations radio and Television stations
300 M - 3 G	Television stations, mobile phones and air traffic control by radar
3 G - 30 G	Mobile phones, radar, communication satellite and Global Positioning System (GPS)
30 G - 300 G	Space Station

Table 2.1: Operation range in RF communications.

The radio frequency waves are electromagnetic and are able to send energy, which allows communication without using cables. The information sent can be analog or digital. The analog signals have a big number of messages and the corresponding waveforms might not

be all acquaintances. The digital signals have a detection of a finite number of waveform acquaintances.

The modulation process allows to send information using frequency. A carrier is a radio signal not modulated, which is an analog waveform that can be modulated to transmit information. Several types of modulation exist and which one is more useful depends on the application scenario. The modulation can be in amplitude, frequency or phase.

The transmitter and the receiver are fundamental elements in RF communications, because they allow to send and receive information, and for this reason the antennas are crucial elements in radio communications, because they are the interface to the air. To send a signal in RF communications, a big process happens, the coding of information, the modulation, the upconversion process, the downconversion process and the demodulation part (can be seen in Figure 2.1), but other techniques are useful in RF communications like filtering, interpolation, In-phase/Quadrature (IQ) modulation and many others.

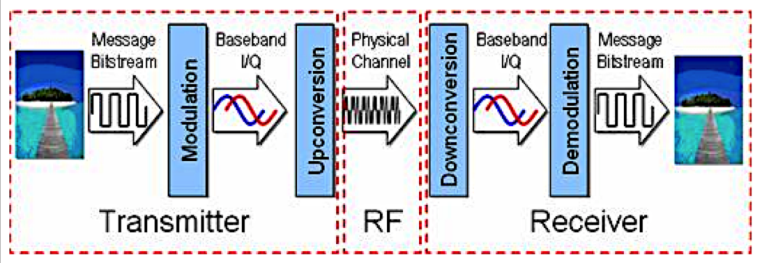

Figure 2.1: Block diagram of communication system [Ins07].

Some aspects are required to send information in RF communications and the IQ modulator is one of them. The IQ modulator is a useful tool for RF communications, because it allows to modulate signals to send information, and for this reason it is very used in RF systems. So, can be concluded that to make RF communications is required take into account these aspects, because is a complex process.

2.2 PXI Platform

The PXI [Ins14b] platform from NI is a high performance computer. This platform was developed in 1997 and is administered by PXI Systems Alliance (PXISA), group of companies which has a goal to promote and control the specifications of PXI. This system is designed to provide reliable and easily configurable measurement solutions. For these reason, it is a great solution for electronic test equipment, automation system and modular laboratory instruments.

The PXI chassis allows to put some slot modules, with different types of functions, so the PXI has the ability to add different types of front ends to work like receivers and transmitters, and has the possibility of processing with Field Programmable Gate Array (FPGA).

A bigger advantage of PXI is timing and resources synchronization, because this equipment contains a 10MHz system reference clock, a PXI trigger bus, a start trigger bus and a slot-to-slot local bus to address the need for advanced timing and synchronization. Thus, the 10MHz reference clock can be exported and sharing it with other devices.

In particular, PXI from NI, affords modules for instrumentation, data aquisition, commutation, movement, vision, advanced sincronization and interface with other buses.

All things considered, a PXIe-1085 [Ins15b] was used in this dissertation, which is present in Figure 2.2.

Figure 2.2: Instituto de Telecomunicações (IT)'s PXI platform system from NI.

2.2.1 PXI Modules

The PXI platform has the ability to add different types of front-ends to work like receivers and transmitters and has the possibility of processing the data in FPGAs. These modules are internally connected to a FlexRIO FPGA module. In this dissertation, two RF Front-end Adapter Module (FAM)'s from NI were used to connect to the PXI.

NI 5792

The NI 5792 [Ins13c] is an RF receiver adapter module, which connects to PXI and uses a FPGA module. This module has five connectors, an input receiver, an input and an output clock, an input and an output local oscillator. The module specifications are briefly shown in Table 2.2.

RF frequency range	200 MHz to 4.4 GHz
ADC	14-bit dual channel at 250 MS/s
Phase noise	<95 dBc/Hz, 10 kHz offset
Dynamic range	>106 dB
Instantaneous bandwidth	200 MHz

Table 2.2: NI 5792 specifications.

NI 5793

The NI 5793 [Ins13d] is an RF transmitter adapter module, can be connected with PXI using a FPGA module. This module has five connectors, an input trnasmitter, an input and an output clock, an input and an output local oscillator. The module specifications are on the following Table 2.3.

RF frequency range	200 MHz to 4.4 GHz
DAC	16-bit dual channel at 250 MS/s (500 MS/s with 2x interpolation), I and Q
Phase noise	<95 dBc/Hz, 10 kHz offset, 2.4 GHz carrier
Transmiter (TX) output power	7 dBm at 2.2 GHz
Instantaneous bandwidth	200 MHz

Table 2.3: NI 5793 specifications.

NI PXI 5652

The NI PXI 5652 [Ins06] is a RF signal generator with a frequency range of 500 kHz to 6.6 GHz. This module has modulation capability and can be seen in Figure 2.3.

Figure 2.3: NI PXI 5652 [Ins06].

2.2.2 NI myDAQ

NI myDAQ [Ins] is an electronic device from NI which allows received and read data, in other words, data aquisition. This device connects with computers by an Universal Serial Bus (USB) interface and this way can be done measurements and analysis of signals, easily. Figure 2.4 shows this device.

Figure 2.4: NI myDAQ [Har13].

2.3 LabVIEW Programming

The LabVIEW software package [Ins13b] [Ins98] is a graphical programming developed by NI, which contains tools to design, to implement measurement and control systems. This language was created in 1986, initially, for the Macintosh operating system, but, nowadays, it exists for Windows, Linux and Solaris operating systems too. LabVIEW language follows

a data flow model, which makes it very functional for data acquisition and handling of information. This programming language is very useful for measurements, processing, signals analysis, control and tests. To interact with user, this language contains a front panel (interface) and a block diagram to develop the graphic code of the program. Figure 2.5 shows an example of LabVIEW programming, which is a calculator program. As it can be seen, the program contains the block diagram and the front panel, which allows the user to interact with the Virtual Instrument (VI).

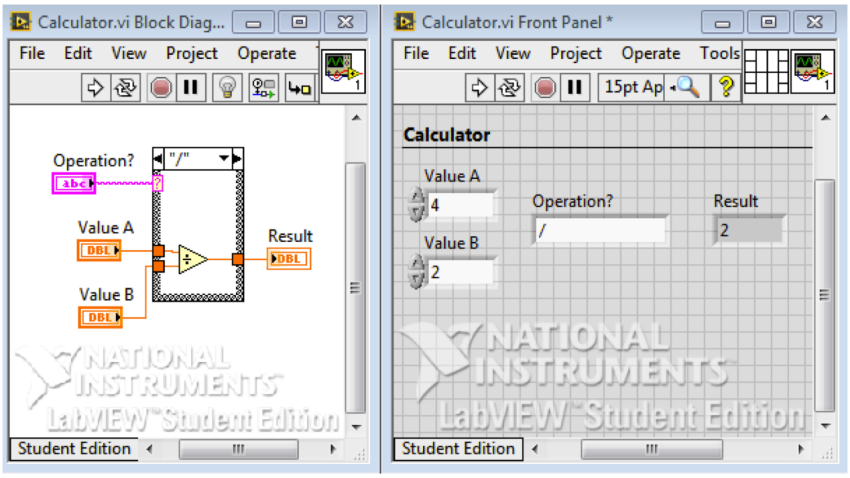

Figure 2.5: LabVIEW programming example.

The VIs are programs which contain other subVIs inside (functions which contain other functions). As a result, each program can be used for another program, or, can just be used stand alone. Each VI can be connected to another VIs, by connectors (lines) that make the VIs dependents from each other. The big advantage of this, are VIs which do not depend on others and can be execute in first place. Thus, the program becomes more efficient, with less time of execution.

One of the great LabVIEW programming advantages is the fact it allows the increase of productivity, because with the block diagram interface it is simple to view the entire code, create and to develop. This programming was used in this dissertation, because it is simple and compatible with most of the selected sub-systems, since it is very helpful in measurement systems also, and by the fact that it is used in PXIe-1085 from NI.

In summary, the LabVIEW is a great tool to develop graphical code, although the first steps in this programming language are quite confusing. The reason why this initial difficulty is present, in most part of beginner's LabVIEW users, is due to the fact that developers are more familiar with written programing languages than graphical. When it is required to adapt all programming concepts to the graphical programming languages, some difficulties appear, at this moment. So, the big initial difficulty is to make the connection between the ordinary concepts of programming languages, for instance, built an array, with the respective blocks in LabVIEW programming.

2.4 RFID Theory

RFID [VDHP07], is a technology that uses radio frequency waveforms for identification approaches. This identification method allows to store a serial number that identifies a person, object or another type of information within the tag. The RFID system is based on interrogator (reader) and tag communication. Due to this fact, this technology much used and adaptable in many tasks, which makes this technology very used in industry and stores to know information about objects. Next, a brief description about this technology is made.

2.4.1 Operating Mode

An RFID system [Dob07] [MKS11] [GS1] consists of two main elements, the reader and the tag. The reader is responsible for all communication between tag (or tags) and reader, and is responsible to read the information that the tag contains. Therefore, if problems exists in reader and tag communication, the reader has the responsibility of managing all communication and solving all problems. This way, the reader is much more complex than the tag, and, for this reason, the reader has a much higher cost than the tag, as well as bigger dimension. However, the tag is an element of low complexity, small size and low cost, which only has to answer the entire communication process managed by the reader. The system also contains antenna (monostatic), or antennas (bistatic), which function to transmit and receive information between the reader and the tag.

The tag transmits the own information by sending the signal from integrated circuit to the reader. The reader converts the radio waves, from RFID, to digital information. After this, the information can be read and understood by a computer. Figure 2.6 gives an insight about the RFID working principle.

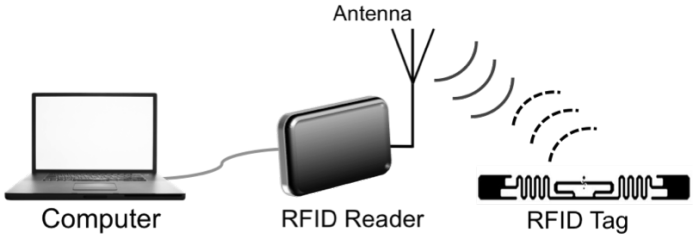

Figure 2.6: RFID operating mode.

2.4.2 Types RFID Tags

There are three types of RFID tags [Dob07] [Cis08], depending on the internal power:

- `Active tag` - has own power source (internal battery), which feeds the chip and the communication signal. This tag has a large data storage capacity, can resist harsh environments, has a higher cost and can be read at large distances.

- `Passive tag` - works with the energy which is sent through the reader, the energy received is used to send the stored data to the reader. It has a small number of elements, a simple constitution, a longer period of operation and requires no maintenance, which

makes it very cheap. However, the passive tag, compared with active tag, has a shorter range, because it has no internal battery.

- `Semipassive tag` - has a battery, but that is only activated when it receives a signal from the antenna/reader. Thus, battery power is typically used only for the chip feeding, while the energy used for communication is received by antenna/reader. So, these tags have a range value between passive tag and active tag.

Nevertheless, tags can be classified according to the storage type in internal memory. There are three types of tags, according to the storage type [Pra08] [Jou]:

- `Read only (RO)` -the data is written only one time, when it is manufactured, and the data cannot be changed. However, these tags can be read several times, which make them very useful for commercial applications, for this reason, typically they are passive.
- `Write Once, Read many (WORM)` - are written when they are manufactured, but can be changed a few times, in a limited number.
- `Read-Write (RW)` - can be reprogrammed many times, which make these tags more advantageous. Because of this reason, they contain a flash memory and usually are used in environments which need to update information recurrently.

Thus, the right tag must be selected depending on the reading range, the environment, and other factors.

2.4.3 Frequency Bands and Protocols

The RFID systems operate in several bands, which are related to Industrial, Scientific and Medical (ISM) bands. The ISM bands [Ban94] have a control by the regulatory authorities of each country due to the fact that they have obligations relating to spectrum. The Table 2.4 shows the distribution of UHF RFID frequencies bands worldwide [Dob07].

RFID systems can also be classified by frequency band like in Low Frequency (LF), High Frequency (HF), UHF and Microwave. The LF systems, which operate at 125-134 kHz, and the HF systems, which operate at 13.56 MHz, are both inductive. For higher frequencies there are two common bands, the UHF systems, which operate at 860-960 MHz, and the microwaves, which operate at 2.4-2.5 GHz, and both are radioactive.

To accomplish communication between the tag and the reader it is necessary to respect several rules, and these rules are present in a protocol. It is possible to see some RFID communication protocols [Ins13a] [Dob07] in Table 2.5. These protocols are related with readers and tags communication frequency and were created by ISO.

2.4.4 Power Transmit Mask

To achieve an RFID communication between reader and tag, some regulations for radio-frequency emissions are needed to respect, like the maximum power transmitted (Effective Radiated Power (ERP)). The RFID operates in several bands (ISM bands), like as was mentioned before, and the entities are responsible to check the specifications, in each country.

Worldwide, two big entities are responsible for doing it, the European Telecommunications Standards (ETSI) (Europe) and the Federal Communications Commission (FCC) (USA) [RFI09]. Table 2.6 shows the difference between the two regulatory entities.

Country	Frequency (MHz)
USA, Canada	902-928
Mexico	915
Argentina, Chile, Costa Rica, Dominican Republic, Uruguay	902-928
Brazil	902-907.5, 915-928
Europe	865-868
South Africa	865.6-867.6, 917-921
China	917-922
Thailand	920-925
Korea	908.5-914
Japan	952-954
Taiwan	922-928
Malaysia	866-869
Singapore	923-925, 866-869
Austalia	918-926
New Zealand	864-868

Table 2.4: Distribuition of UHF RFID frequencies bands worldwide.

	Frequency	Tag Type - Protocols
LF	125-134 kHz	Passive - HiTag, ISO11784/5, 14223, ISO18000-2
HF	5-7 MHz	Passive - iPico DF/iPx, ISO10536
HF	13.56 MHz	Passive - ICODE, ISO14443, ISO15693, ISO18000-3 MIFARE, Tag-IT, TIRIS
UHF	850-950 MHz	Passive - EPC class 0, EPC class 1, Intellitag, ISO18000-6A, Title 21, S918, Ucode
UHF	850-950 MHz	Semipassive - AAR S918, EZPass, Intelleflex, Maxim, Title 21
UHF	860-960 MHz	Passive - EPC GEN II, EPC class 0, EPC class 1, Intelitag tolls, ISO18000-6A,B and C, Rail, Title 21
Microwave	2.4-2.45 GHz	Active - ANSI 371.1, ISO18000-4
Microwave	2.4-2.45 GHz	Passive - Intellitag, ISO18000-4
Microwave	2.4-2.45 GHz	Semipassive - Alien BAP, ISO18000-4

Table 2.5: Relationship between RFID communication protocols and frequency bands.

	ETSI	FCC
Bandwidth of the transmission channels	200 kHz	500 kHz
Distance between transmission channels	600 kHz	None, because the transmission channels are adjacents
Maximum power transmitted	2 W ERP (33.01 dBm)	4 W ERP (36.02 dBm)
Reader operation frequency	865-868 MHz	902-928 MHz

Table 2.6: ETSI and FCC specifications.

The Frequency Hopping Spread Spectrum (FHSS) allows to transmit the radio signals and allows to change the carrier through several frequency channels too. This technique is used in FCC (see Figure 2.7) and has two big advantages, difficulty to interception and sharing bandwidth with many types of conventional transmitters and with minimal interference. Thus, this technique is used by FCC. Figure 2.8 represents the technique used by ETSI.

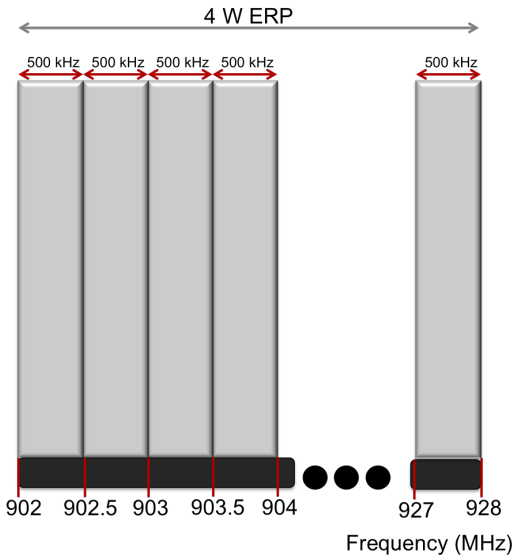

Figure 2.7: USA UHF RFID regulation by FCC.

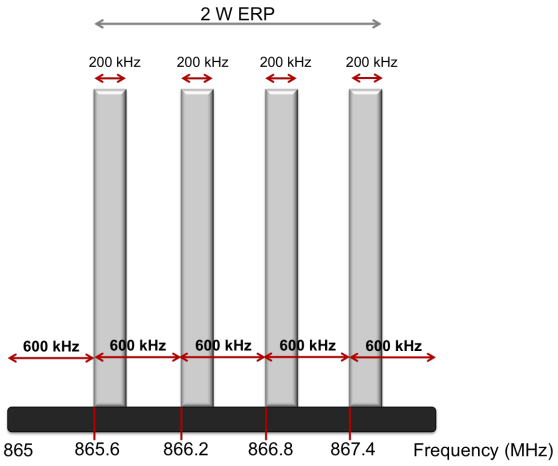

Figure 2.8: European UHF RFID regulation by ETSI.

Therefore, each type of environment has a transmit mask to respect, and can be applied different types of power transmit mask. These masks [GS115] are for a single-interrogator environment, a multiple-interrogator environment or a dense-interrogator environment.

- `Single-interrogator environment` - in this case it is only taken into account the european UHF RFID regulation, because there is only one reader.

- `Multiple-interrogator environment` - several readers exist in the environment. The interference in the adjacent channels needs to be respected.
- `Dense-interrogator environment` - each channel is occupied with a reader. So, tags can be read when all adjacent channels are occupied.

2.4.5 Relevance to the Internet of Things

The Internet of Things (IoT) [VF13] is a growing issue. This big technology revolution is the Telecommunication future, in order to provide the connection between the daily routine objects, with a big control system, through the internet (see Figure 2.9). Thus, data of several objects can be controlled and registered.

However, besides using the internet to send data, about object information, it is necessary to be constantly reading information of these objects. The RFID tags allow to acquire the information, at home, in commerce, in factories, for instance, and allow to know the object localization. Because of these reasons, the RFID tags are the perfect choice for this scenario [Jou15]. In fact, some tags have the ability to read the information recurrently (Read-Write Tags), which make these tags very useful for IoT applications.

Nevertheless, the economic factor is very important in any kind of business, the RFID tags are much easier to develop and do not require maintenance. Thus, systems which allow to make a successful tags reading and make efficient measurement tag tests are also associated to all this great revolution. So, this makes the tags and, consequently, the readers (to read the tag information) a big focal point of IoTs, in the near future. Therefore, it is foreseen that the IoT will make the RFID tags technology grow, as well as, the RFID readers, more and more.

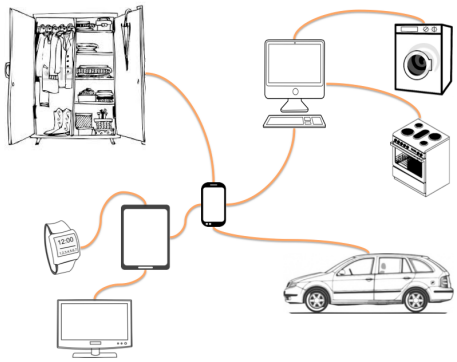

Figure 2.9: IoT concept.

2.5 Protocol RFID ISO 18000-6C

The protocol is an agreement which allows to connect and establish communication between two systems. To develop an RFID reader, in this dissertation, is used the ISO 18000-6C protocol, EPC Generation-2 Class 1 UHF (EPC Gen-2) [GS115]. This protocol was developed by EPC Global Organization and operates in 860 MHz - 960 MHz frequency range.

Thus, a tag identification can be done, using an RFID reader and this protocol. To read a tag it is required to know the parameters which allow to read the tag information. The

EPC [EPC13] gives an exclusive identification for an object. This attribution is made by EPC global, a company which makes a unique identification product. The EPC is encoded on RFID tag, for all kinds of applications, and this way it is possible to identify many different objects. In Figure 2.10 it is possible to observe the EPC structure.

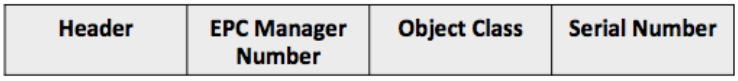

Figure 2.10: EPC structure.

The header identifies the length, type, structure, version and generation of the EPC. The EPC manager number is the entity responsible for maintaining the subsequent partitions. The object class identifies a class of product. The serial number is a unique identifier number for each product.

An interrogator (reader) to interact with tags employs three operations, the select operation, the inventory operation and the access operation. The select is responsible for choosing the one or more tags in a given population. The inventory (or inventory round) is responsible for identifying an individual tag. The access is responsible for communicating with a tag which was already identified.

Nevertheless, in this dissertation only the inventory round is used, because it is intended to get the tag identification. Firstly, it is send a Query command, then the tag replies with a 16-bit Random or pseudo-Random Number (RN16) command. After that, the reader sends the ACK command, which contains the same RN16 command which was sent by the tag. The tag, receives the ACK command and sends the Protocol control (PC), EPC and PacketCyclic-Redundancy Check (CRC). Finally, if EPC is valid, the reader sends to tag the QueryRep command, if not, sends the NAK command.

In this protocol, the reader sends information to the tag, which modulating a RF carrier using a Double-sideband amplitude shift keying (DSB-ASK), Single-sideband amplitude shift keying (SSB-ASK) or Phase-reversal amplitude shift keying (PR-ASK), and using PIE. When the reader sends the information to the tag (R→T), the tag starts to operate because of this modulated RF carrier, and this way, the tag is capable to send his own information to the reader. After this, the reader receives the tag backscattered reply (T→R). To communicate, the tags use the amplitude, or phase modulation of the RF carrier, by backscatter. The FM0 and Miller are used by the tag like the encoding format to response to the reader.

The following subsections will explain the RFID protocol details.

2.5.1 Modulation

In modulation [Col] process, the signal characteristics are modified to transmit information, through the carrier wave, and these modifications can be in frequency, amplitude or phase. In this protocol can be used DSB-ASK, SSB-ASK, PR-ASK, to send information from the reader to the tag (R→T). The DSB-ASK modulation is less efficient, however it is easier to develop with OOK. The SSB-ASK is more complex than DSB-ASK, because it requires an IQ modulator, but gains in terms of spectral efficiency. In SSB-ASK and DSB-ASK, the power efficiency present in this modulation depends on the modulaton index. To decrease the carrier to noise in a narrowband, the PR-ASK is a nice solution, because of that the power transmitted to tag is increased.

The Amplitude Shift Keying (ASK) is a digital modulation technique, which uses the variation of the RF carrier amplitude in accordance with baseband digital input signal. So, to represent logic level '0' is used 0 and to represent the logic level '1' is used the Acos(2πf). The A is the amplitude and the f is waveform frequency.

The OOK modulation is a very popular modulation index [JA]. The digital OOK modulation is simple and is an easy form of ASK modulation. This modulation uses two symbols to represent logic level '1' and '0', where both have different amplitudes. For this reason, the carrier frequency assumes a certain amplitude (voltage level), and, this way, represents the logical level '1'. The logic level '0' is represented by zero amplitude (voltage level), like Figure 2.11 shows. The big advantage of this modulation is the transmission of zero symbol. When a zero is sent, it does not need to transmit any waveform, the signal remains in zero, and this way, allows conserve energy. Nevertheless, this modulation is very sensitive to undesired signals.

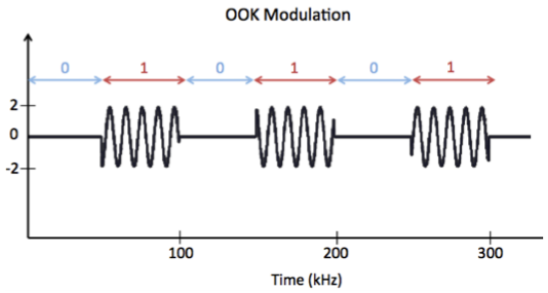

Figure 2.11: OOK modulation.

2.5.2 Pulse Internal Encoding

In encoding process, the message is converted into symbols. PIE [YZC09] (see Figure 2.12.) is used to easily do the information demodulation in tag, where the information comes from the RFID reader (R→T).

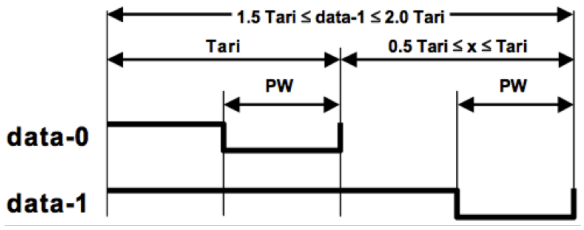

Figure 2.12: PIE.

Basically, this encoding intends to represent the '0' and '1' symbols (data 0 and data 1). To do this, variable pulse lengths are used to transmit digital information. According to the ISO 18000-6C protocol, tags are required to respond to commands. The data rate is specified by Type A Reference Interval (Tari) value, the time interval required to transmit a zero bit. The Tari value is between 6.25μs and 25μs. The Pulse With (PW) minimum value is MAX(0.265Tari, 2) and the maximum value is 0.525Tari. So, the data-0 is represented by two logic levels, '1' and '0', and the data 1 is also represented by two logic levels, '1' and '0'.

However, in data 0 and data 1, the logic level '0' is represented by PW value. In data-0, the logic level '1' is also represented by PW, in constrast to data 1, because the logic level '1' has bigger duration (see Table 2.7).

Logic level	**'1'**	**'0'**
data-0	Tari-PW	PW
data-1	**Minimum**: 1.5Tari **Maximum**: 2Tari	PW

Table 2.7: PIE symbols duration.

2.5.3 FM0 and Miller encoding

The FM0 [Dob07] inverts baseband phase at every symbol boundary. The tag can code information with FM0 or Miller, to send to reader (T→R).

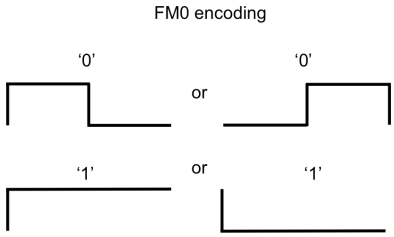

Figure 2.13: FM0 encoding.

This encoding (FM0) works like a transition in the middle of the '0' symbol, but does not exist a transition in the middle of the '1' symbol. Figure 2.13 shows the FM0 encoding and Figure 2.14 shows the FM0 generator state diagram, which occurs four possible stages, S1, S2, S3 and S4.

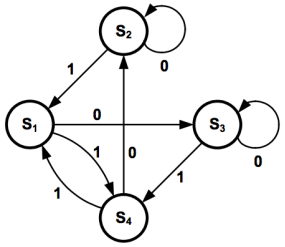

Figure 2.14: FM0 generator state diagram [GS115].

In the Miller [GS115] encoding, the signal FM0 is multiplied by a square wave, using 2, 4 or 8 factor for each FM0 symbol. In this encoding, between two data-0 symbols exists an inversion of phase and the same happens in middle of data-1 symbol. In Figure 2.15 can be seen the Miller-signaling state diagram.

In FM0 encoding, the S2 and S3 stages represent the data-0 symbol, and the S1 and S4 stages represent the data-1 symbol. The relation between them remains in (2.1) and (2.2).

$$S_1 = -S_4 \tag{2.1}$$

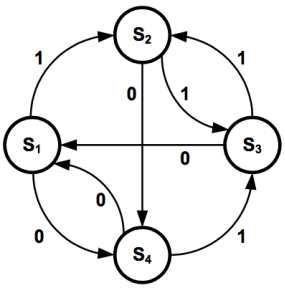

Figure 2.15: Miller-signaling state diagram [GS115].

$$S_2 = -S_3 \tag{2.2}$$

In Miller encoding, the S4 and S1 stages represent the data-0 symbol, and the S2 and S3 stages represent the data-1 symbol. The relation between them is the same that in (2.1) and (2.2). So, the big diference between FM0, Miller 2, 4 and 8 is the number of transitions in each symbol, and can be seen in Figure 2.16. The FM0 is typically used because of its is easiness of implementation.

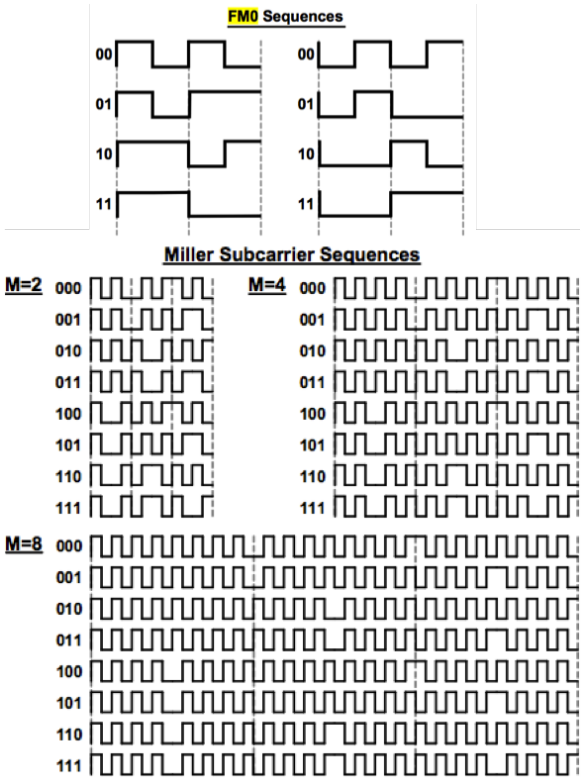

Figure 2.16: Miller-signaling state diagram as compared to FM0 state diagram [GS115].

2.5.4 Preamble and Frame-sync

To send commands from reader to tag (R→T) some fields need to be used. Thus, to send any command from reader to tag a preamble has to be sent (see Figure 2.17) or a frame-sync (see Figure 2.18). The preamble precedes the Query command, which makes this one the initiator of the inventory round. The frame-sync precedes the ACK, NAK, QueryAdjust and QueryRep commands. As can be seen in Figure 2.17, the preamble contains four parts, the delimiter, the data-0, the Interrogator-to-Tag calibration symbol (RTcal) and the Tag-to-Interrogator calibration symbol (TRcal). The preamble and frame-sync are very similiar, however, the frame-sync has not the TRcal part.

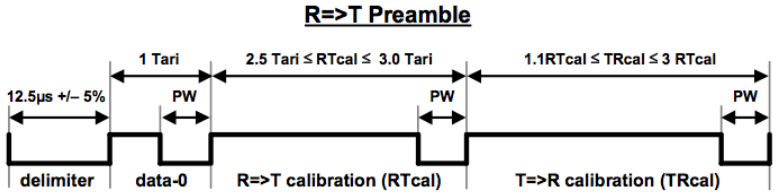

Figure 2.17: Preamble [GS115].

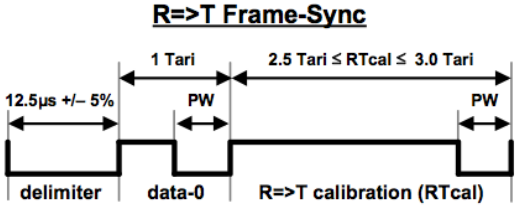

Figure 2.18: Frame-sync [GS115].

To calculate each parameter that composes the preamble and frame-sync the values in Table 2.8 have to be used.

Parameter	Value
Tari	6.25 μs≤Tari≤ 25 μs
PW	MAX(0.265Tari) ≤PW≤ 0.525Tari
delimiter	12.5 μs +/- 5%
data-0	Tari
RTcal	2.5Tari≤RTcal≤ 3Tari
TRcal	1.1RTcal≤TRcal≤ 3RTcal

Table 2.8: Parameters which set the preamble and frame-sync.

Therefore, to send information from tag to the reader (T→R) the communication starts with a FM0 preamble (see Figure 2.19). This preamble is different from the preamble in R→T communication. It may start or not with a pilot tone (depends on the Query command sent by tag in the beginning of the communication). The pilot tone is formed for 12 data-0

symbols. After pilot tone (or if no pilot tone) there are 6 static symbols (1 0 1 0 v 1, v means violation). After these 6 symbols, the command sent from tag to the reader appears.

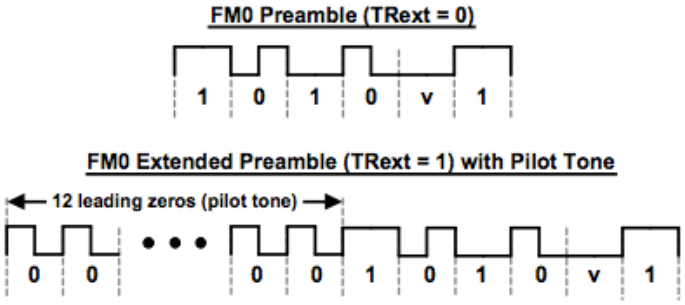

Figure 2.19: FM0 Preamble [GS115], with (bottom) and without (top) pilot tone.

2.5.5 Protocol commands

To do the communication between the reader and the tag some commands are exchanged. That happens in inventory round part, which was implemented in this dissertation.

ACK

The ACK command is sent to the tag (R→T) in order to inform that the RN16 command was received and is valid. Therefore, when the reader receives the RN16 command from tag, the ACK command is sent to inform the tag, containing the same RN16 information. Thus, the ACK command is composed by 18 bits, 2 statics bits (01) and the 16 bits (the same bits in RN16 command) (see Table 2.9). Nevertheless,a Frame-sync is sent before the ACK command.

	Command	**RN**
# of bits	2	16
description	01	Echoed RN16 or handle

Table 2.9: ACK command [GS115].

After the ACK command is sent, the tag replies with PC, EPC and PacketCRC, which makes a total of 96 bits.

NAK

The NAK command, such as the ACK command, is preceded by a Frame-sync. This one, has the purpose to inform the tag that the EPC received is not valid. When this happens, the tag does not reply to this command. NAK is composed by 8 specific bits (see Table 2.10).

PC, EPC and PacketCRC

The PC, EPC and PacketCRC command (see Table 2.11)) is composed by 96 bits and is sent from the tag to the reader (T→R), after the reader sends to the tag (R→T) an ACK

	Command
# of bits	8
description	11000000

Table 2.10: NAK command [GS115].

command. This command contains the tag EPC, which gives an exclusive identification for each tag. Like in the other commands, this one is preceded by a FM0 preamble.

	PC, EPC and PacketCRC command
# of bits	96

Table 2.11: PC, EPC and PacketCRC command.

Query

The Query command is responsible for initializing the communication between reader and tag, and is preceded by a preamble. This command contains all the communication configurations between reader and tag, and due to this reason, the Query command starts the inventory round. Table 2.12 shows all fields that form this command, which is composed by 22 bits.

Tag replies to the Query command with a RN16 command.

QueryAdjust

The QueryAdjust command is preceded by a Frame-sync and is composed by a total of 9 bits (see Table 2.13). The purpose of this command is to adjust the Q parameter value.

The tag replies with a RN16 command, after being sent a Query Adjust command.

QueryRep

QueryRep command informs the tag to decrease one unit in your slot counter. Thus, when the slot counter reaches the zero value, the tag knows that it is your time to be read. This command is also preceded by a Frame-sync and has 4 bits, which can bee seen in Table 2.14.

When a Query command is sent to the tag, the tag replies with a RN16 command.

RN16

The RN16 command (see Table 2.15) is composed by 16 bits randomly generated and is sent from the tag to the reader (T→R), after reader sends to tag (R→T) a Query command. FM0 preamble precedes this command.

2.5.6 Power Transmit Mask

This protocol can be applied on three power transmit masks, the single-interrogator environment, the multiple-interrogator environment (see Figure 2.20) and the dense-interrogator environment (see Figure 2.21). Table 2.16 depicsts the specifications for multiple-interrogator and for dense-interrogator environments.

Fields	Definition	# of bits	Bits
Command	Starts the Query command.	4	1000
DR	Sets Backscatter-link frequency (BLF) value.	1	0: DR=8 1: DR=64/3
M	Number of subcarriers per symbol.	2	00: M=1 01: M=2 10: M=4 11: M=8
TRext	Sets if preamble from tag has pilot tone or not.	1	0: No pilot tone 1: Use pilot tone
Sel	Sets which tags reply.	2	00: All 01: All 10: ∼SL 11: SL
Session	Session number.	2	00: S0 01: S1 10: S2 11: S3
Target	Select the type of tags that respond to this command.	1	0: A 1: B
Q	Sets the number of slots in the round.	4	0-15
CRC	A 16-bit CRC code that a tag calculates over its PC, optional XPC word or words, and EPC and backscatters during inventory.	5	CRC-5

Table 2.12: Query command fields.

Fields	Definition	# of bits	Bits
Command	Starts the QueryAdjust command.	4	1001
Session	Selects the inventory round number session.	2	00: S0 01: S1 10: S2 11: S3
UpDnt	Adjusts the Q parameter.	3	110: Q=Q+1 000: No change to Q 011: Q=Q-1

Table 2.13: QueryAdjust command fields.

In multi-interrogator environment, the channel R represents the channel used to send information, the channel S represents other channel than R and the P represents the power of a particular channel. To fulfill the power transmit mask, when any information is sent in channel R, the relation between power in channel S and channel R is shown in Table 2.16.

In dense-interrogator environment, the R_{BW} represents the R channel bandwith and the S_{BW} represents the S channel bandwith. The F_0 is the offset frequency and the F_c is the

Fields	Definition	# of bits	Bits
Command	Starts the QueryRep command.	2	00
Session	Selects the inventory round number session.	2	00: S0 01: S1 10: S2 11: S3

Table 2.14: QueryRep command fields.

	RN16
# of bits	16

Table 2.15: RN16.

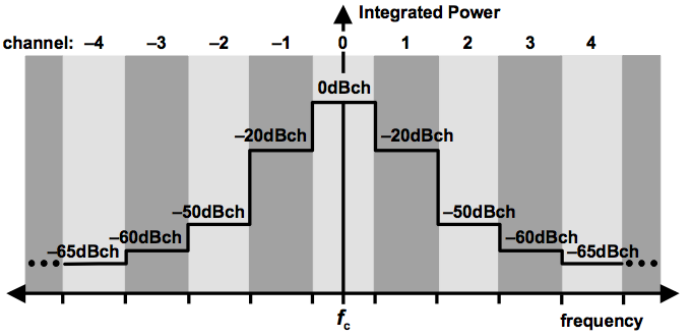

Figure 2.20: Transmit mask for multiple-Interrogator environment [GS115].

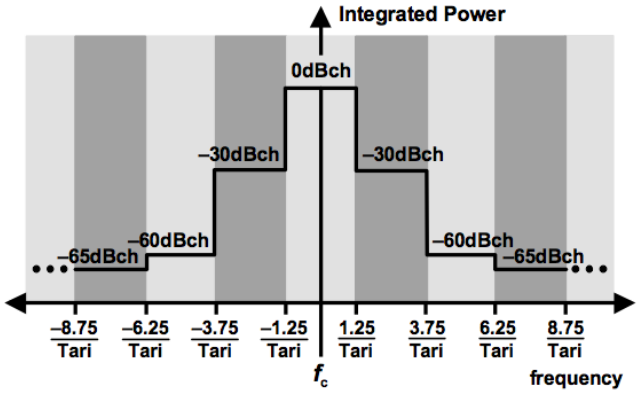

Figure 2.21: Transmit mask for dense-Interrogator environment [GS115].

carrier frequency. In this environment, the ratio between channel S, which is centered in (n.F_0)+F_c, (n is an integer) should be respected.

2.5.7 Link Timing

In order to fulfill the communication between reader and tag, time limits need to be respected. In Figure 2.22 it is possible to understand the relation between commands and time.

Multi-interrogator environment	Dense-interrogator environment
|R-S|=1: $10log_{10}$(P(S)/P(R)) < -20 dB	|n|=1: $10log_{10}$(P(S_{BW})/P(R_{BW})) < -30 dB
|R-S|=2: $10log_{10}$(P(S)/P(R)) < -50 dB	|n|=2: $10log_{10}$(P(S_{BW})/P(R_{BW})) < -60 dB
|R-S|=3: $10log_{10}$(P(S)/P(R)) < -60 dB	|n|>2: $10log_{10}$(P(S_{BW})/P(R_{BW})) < -65 dB
|R-S|>3: $10log_{10}$(P(S)/P(R))< -65 dB	

Table 2.16: Values to respect in power transmit mask [GS115].

During inventory round, it is required to have a continuous wave between each command, sent by the reader. This happens because the tag to get energized and thus, be able to reply to reader commands.

First, the Query command is sent and tag replies with the RN16 command, and at the same time, the T1 must be respected. T1 represents the immediate time that tag can reply, after tag receives a command.

Then, after tag sends a RN16 command, the reader has to send a ACK command with a maximum time limit of T2. T2 represents the time that reader has to demodulate a signal from tag and send a new one. After reader sends the ACK command, the tag has to reply with a PC, EPC and PacketCRC, until T1 time. When reader receives the PC, EPC and PacketCRC, the T2 time is the limit time for reader to send the QueryRep command, or the NAK command. If the T1 and T2 are exceeded, the communication ends. Thus, the times are one of the most important requirement for the communication between reader and tags.

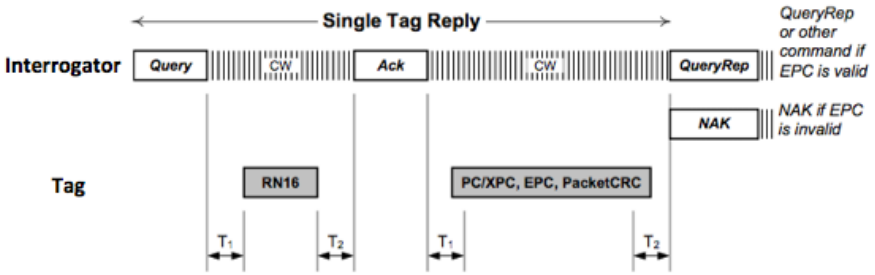

Figure 2.22: Link timing [GS115].

To calculate the T1 and T2 times, the formulas in Table 2.17 are used, which depend on the Backscatter-link pulse-repetition interval (Tpri), Frequency tolerance (FrT) and RTcal values. It should be noted that the Tpri value is calculated according (2.3) and the BLF value is related to (2.4), which will be explained in next section.

$$\text{Tpri} = \frac{1}{\text{BLF}} \tag{2.3}$$

2.5.8 Backscatter Link Rates and CRC

The BLF value is the symbol frequency sent by the tag. In FM0 encoding the BLF value is the data-rate. The (2.4) specifies the relationship between BLF, Divide Ratio (DR) and

Parameter	Minimum	Nominal	Maximum
T1	MAX(RTcal,10Tpri) ×(1-|FrT|)-2μs	MAX(RTcal,10Tpri) ×(1+|FrT|)+2μs	MAX(RTcal,10Tpri)
T2	3.0 Tpri		20.0Tpri

Table 2.17: Link timing parameters [GS115].

TRcal. Table 2.18 shows the link frequencies and tolerances specified for DR of 64/3 and the Table 2.19 shows the same information for a DR of 8.

$$\text{BLF} = \frac{\text{DR}}{\text{TRcal}} \tag{2.4}$$

BLF	TRcal (μs +/- 1%)	FrT (nominal temp)	FrT (extended temp)	Frequency variation during backscatter
33.3	640	+/-15%	+/-15%	+/-2.5%
33.3<TRcal<66.7	320<BLF<640	+/-22%	+/-22%	+/-2.5%
66.7	320	+/-10%	+/-15%	+/-2.5%
66.7<TRcal<83.3	256<BLF<320	+/-12%	+/-15%	+/-2.5%
83.3	256	+/-10%	+/-10%	+/-2.5%
83.3<TRcal≤133.3	160≤BLF<256	+/-10%	+/-12%	+/-2.5%
133.3<TRcal≤200	107≤BLF<160	+/-7%	+/-7%	+/-2.5%
200<TRcal≤225	95≤BLF<107	+/-5%	+/-5%	+/-2.5%

Table 2.18: Tag-to-Interrogator link frequencies for DR=64/3 [GS115].

BLF	TRcal (μs +/- 1%)	FrT (nominal temp)	FrT (extended temp)	Frequency variation during backscatter
17.2≤TRcal<25	320<BLF≤465	+/-19%	+/-19%	+/-2.5%
25	320	+/-10%	+/-15%	+/-2.5%
25<TRcal<31.25	256<BLF<320	+/-12%	+/-15%	+/-2.5%
31.25	256	+/-10%	+/-10%	+/-2.5%
31.25<TRcal<50	160<BLF<256	+/-10%	+/-10%	+/-2.5%
50	160	+/-7%	+/-7%	+/-2.5%
50<TRcal≤75	107≤BLF<160	+/-7%	+/-7%	+/-2.5%
75<TRcal≤200	40≤BLF<107	+/-4%	+/-4%	+/-2.5%

Table 2.19: Tag-to-Interrogator link frequencies for DR=8 [GS115].

The CRC is a parameter used by reader and tag to validate commands in R→T and T→R communication, respectively. The CRC can be the CRC-5 and CRC-16. The first one is explained in Table 2.20 and the second one is explained in Table 2.21

Length	Polynomial	Preset	Residue
5 bits	x^5+x^3+1	01001_2	00000_2

Table 2.20: CRC-5 [GS115].

CRC Type	Length	Polynomial	Preset	Residue
ISO/IEC 13239	16 bits	$x^{16}+x^{12}+x^5+1$	$FFFF_h$	$1D0F_h$

Table 2.21: CRC-16 [GS115].

2.5.9 Short Protocol Overview

After the protocol has been explained, it is possible to make a short overview, to understand better the protocol process more easily. Figure 2.23 presents a short overview of some protocol steps.

First a Query command is created, which starts the communication between the reader and the tag. In Figure 2.23 it is possible to observe each parameter, which composes the Query command. However, it should be noted that the preamble part before the Query command is missing. After building the Query command, the coding process starts. As it can be seen, a 1 symbol is encoded with a data-1, and a 0 symbol is encoded with a data-0. As was explained before, the data-1 and the data-0 have different duration. Then, the modulation process starts, and, after that, the command is ready to send, the Query command, to the tag (in this example the OOK modulation was used).

The tag replies with a RN16 command and then this one is decoded. To decode the RN16 command, the tag sends a FM0 preamble, which may contain a pilot tone, or not, sends six symbols, and lastly, sends the RN16. Then, the information from tag is read, using FM0 or Miller encoding (in figure example FM0 encoding was used).

Thereafter, although it is not present in Figure 2.23, the reader starts to build the ACK command, and uses the same process until sending this one to tag. The tag replies with PC, EPC and PacketCRC command, using the same process in RN16 command, like as explained before.

The figure allows to better understand how protocol works and specify all protocol steps, in a summarised form.

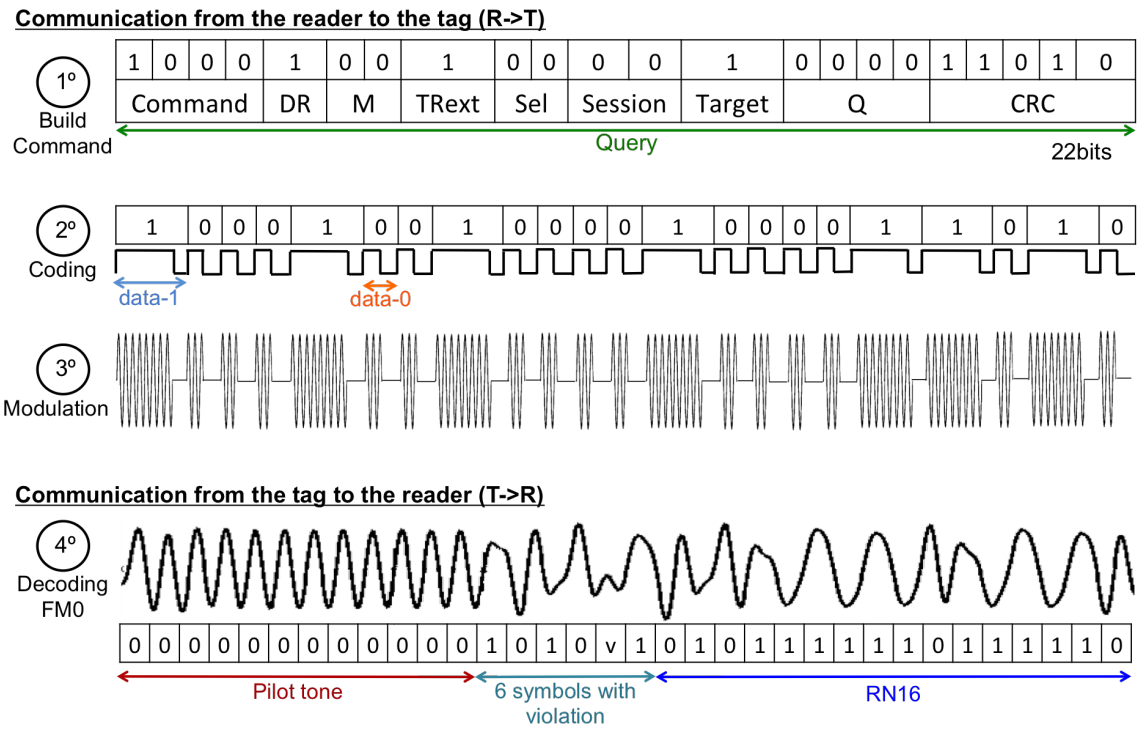

Figure 2.23: Short protocol overview process.

Chapter 3

Architectures and Specifications

The purpose of this chapter is to explain the reason why the elements that compose the RFID reader system were chosen, explain the architectures which were used to develop the system and explain the choice of the specifications to test the system.

To develop the RFID reader, like any other system, it is necessary, first of all, to make technical decisions. The technology to use, the equipments, the architecture of the system, the programming language, in other words, the hardware and the software are fundamental choices to initiate the development of system, to make it more efficient as possible. In addition, a specific issue is the communication protocol that should be implemented respecting several details, as explained in previous chapter.

Therefore, the first element taken into account, in this dissertation, was the PXIe-1085 from NI, because it was intended to provide one application for that measurement instrument. For this reason, the LabVIEW programming language was used to develop the entire system.

Subsequently, the ISO 18000-6C communication protocol was selected, as mentioned before. This choice was made because this communication protocol operates in UHF range, 860 MHz - 960 MHz, the range that is intended to develop the RFID reader. It is intended to get the tag identification, and to do this, it is only necessary the Inventory Round part of the protocol. The Figure 3.1 shows how the Inventory Round works, and how it will be implemented in this dissertation.

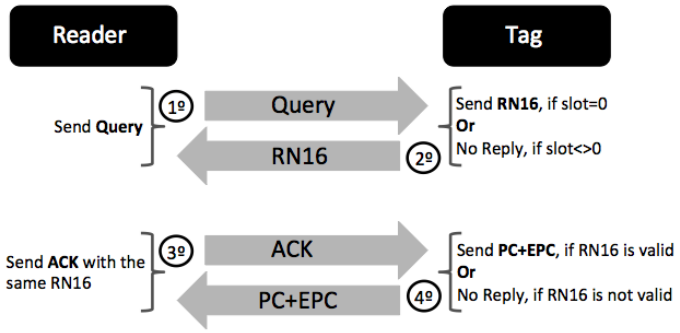

Figure 3.1: Communication between reader and tag.

As shown in Figure 3.1, the Query command is sent to tag with all configurations which are required to communicate. Then, the tag replies with a RN16 command, in case the slot

to read tag is zero. If the slot is not zero, the tag does not respond. The reader receives the RN16 and sends the ACK command to tag, with the same RN16. The tag, if ACK command contains a valid RN16, replies with PC and EPC. If ACK command does not contain a valid RN16, the tag does not respond. This way, the EPC is obtained, from tag.

Thus, after understanding how protocol works, the study process was started about architectures, which allowed to develop simple and reconfigurable RFID reader, using some resources commonly available in laboratory environment. The two architecures used in this dissertation were a stimulus-response architecture and a real-time interrogator emulation architecture, which are described below.

The architectures used to build the spectrum analyzer and spectrogram application and the RF-DC measurement system will also be explained later on.

3.1 Stimulus-Response Architecture

To develop an RFID reader, using LabVIEW programing, a stimulus-response [Ins13a] architecture was used. In this architecture, the Vector Signal Generator (VSG) interrogates the tag with a Query command and, simultaneously, sends a digital marker to trigger the Vector Signal Analyzer (VSA). This way, the VSA captures the signal backscattered signal by the tag, and processes the information, in PXI.

This architecture was chosen because it is freely available in IT's RF laboratory facilities. In Figure 3.2 it is possible to observe the block diagram which was used to develop the RFID reader with stimulus-response architecture.

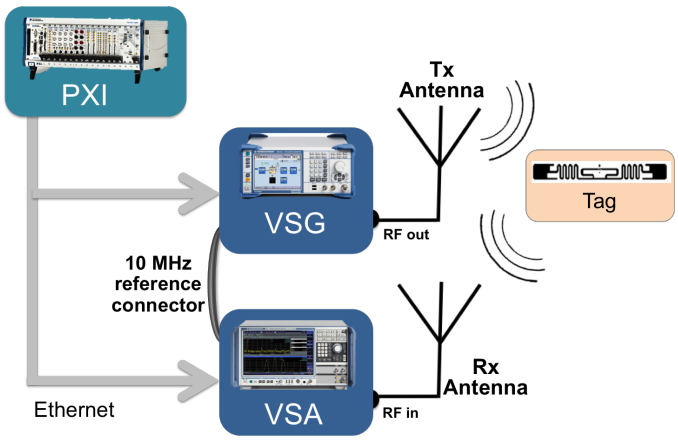

Figure 3.2: Block diagram of stimulus-response architecture.

In Figure3.2 it is possible to observe that the system has as principal element the PXIe-1085, which is responsible to control all system process. The PXIe-1085 is connected to VSG and VSA by ethernet. In this dissertation, the SMJ100A VSG was used, from Rohde & Schwarz, which operates until 3 GHz. The VSA used was FSW Signal and Spectrum Analyzer, from Rohde & Schwarz, which operates from 2 kHz to 8 GHz. The VSG and VSA are connected by 10 MHz reference connector. The transmission antenna are connected to VSG, antenna which is responsible for sending the signal to tag. To acquire the signal from tag, a reception antenna was connected to VSA. The transmission and reception antennas,

which were used are shown in Figure 3.3. These antennas (transmission and reception) are equals, so the specifications [KAT] are equal too, and can be seen in the Table 3.1.

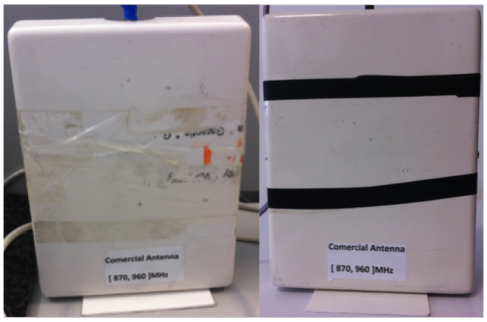

Figure 3.3: Transmission and reception antennas.

	Antennas specifications
Description	736624 Kathrein Antenna
Operating Frequency	870 MHz - 960 MHz
Polarization	Vertical
Gain	7 dBi

Table 3.1: Transmission and reception antennas specifications.

Figures 3.4 and 3.5 show the tags that were used for system test. The first tag is ALN-9640 Squiggle Inlay [Tec14a], from IDSolutions and it is a high performance general purpose RFID inlay for use in a wide variety of applications. The second one is ALN-9654 G INLAY [Tec14b], from Alien Technology, and is an ultra-high-performance. Both tags work in RFID UHF range, 840 MHz - 960 MHz, with ISO 18000-6C protocol, and they contain the same chip [Tec14c].

Figure 3.4: Tag from IDSolutions.

Figure 3.5: Tag from Alien Technology.

After deciding which elements to integrate the stimulus-response architecture, the flowchart of LabVIEW program was developed, which can be seen in Figure 3.6.

First, the Query command is created, which initializes the communication between the reader and the tag. Then, the while loop is started, responsible for controlling the power value, which wakes up the tag. It should be noted that, the program can be initialized by a frequency chosen by the user.

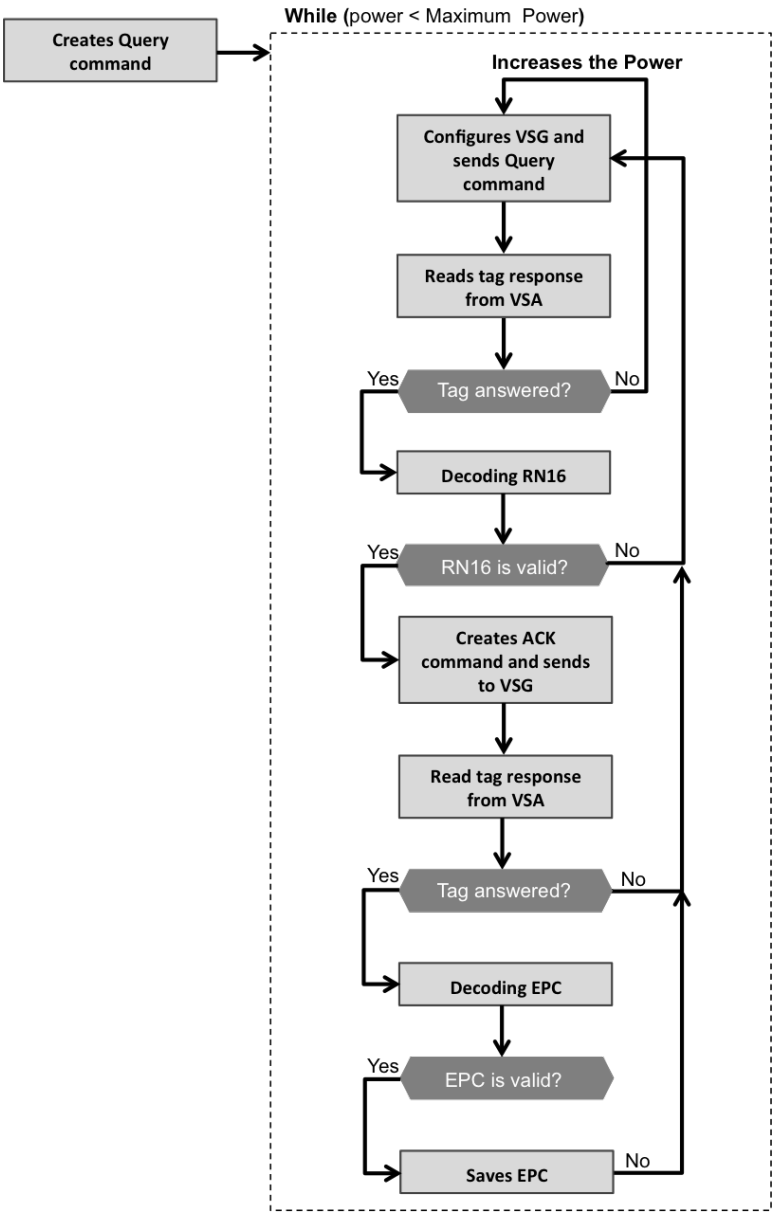

Figure 3.6: Flowchart of the stimulus-response architecture program to develop LabVIEW code.

The maximum limit of transmission power defined by FCC is 4 W (36.02 dBm). However, the VSG is limited in output power capabilities and does not fulfill the maximum specs, but in any case, an external driver could be used.

This while loop begins to configure the VSG, and after that sends the Query command to VSG. The VSA starts to capture data since the VSG sends a Query command to tag. So, this way, the VSA captures the RN16 command, which was sent by tag. If the VSA does not detect any tag response, the system increases the power, and then sends the Query command to tag again. If, VSA detects tag response, the PXI starts to decode the RN16. Even if, the decode was not valid, all process starts again (send Query command to VSG), although the

power value is kept. If the decode is valid, then creates the ACK command and sends it to VSG. Again, the VSA is used to capture data from tag, and if tag does not respond, a Query command is sent with same power value. Also, if tag responds, the EPC decoding is started. Once again, if the EPC decoding is not valid, starts to send a Query command with same power. If the EPC is valid, then the EPC is saved and the program over. In other words, at this moment, the tag was read with success.

However, when this architecture started to be developed in laboratory, a big limitation was quickly found. Due to the fact that it is required to select the file in VSG, when a command is sent to VSG, it became unsustainable to send ACK command in time. After decode RN16, create the ACK command and send to VSG the file must be selected in VSG, manually. So, obviously, the time of microseconds (T2) between the tag and reader to complete all communication expires. Therefore, this architecture has a big limitation, because it does not allow to do all tag reading process, so the flowchart present in Figure 3.6 can not be applied, because of this limitation.

Thus, because of this limitation, the flowchart was changed. The reason is because it was necessary to adapt the program to this limitation, and this way, the program became more simple. Thereby, the flowchart used is present in Figure 3.7.

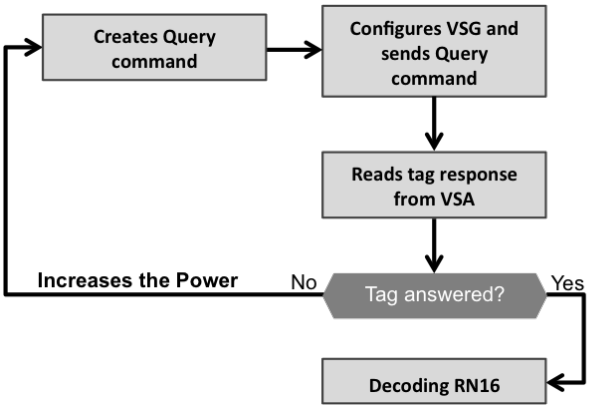

Figure 3.7: Flowchart of the stimulus-response architecture program to develop LabVIEW code simplified.

It should be noted that the while loop is not present in program because when any change happens, it is required to send the file to VSG, and to select the file in VSG manually. So, the while loop is not required. Each time the program needs to be run, manual interaction is required with the VSG, so,the LabVIEW program is only needed to run once, and this way, the while loop is not required. The code can be seen in Figure 3.8. First, the preamble is built, then, the Query command is converted into baseband signal. After, the continuous wave is done, and all sequence is merged. Finally, the code is sent for VSG block, which contains all VSG configuration and sends the data to VSG.

The VSA code is in other VI, because it is only required to run when the user selects the file in VSG. This code can be seen in Figure 3.9. In this figure is seen that, besides the VSA configuration, after capture the data from VSA, the RN16 block makes the decoding of data from tag, and then, the ACK block develops the ACK command.

In summary, the Query command was created first, then it was sent the Query command to VSG, and the user selects the file, which contains the Query command in VSG. The user,

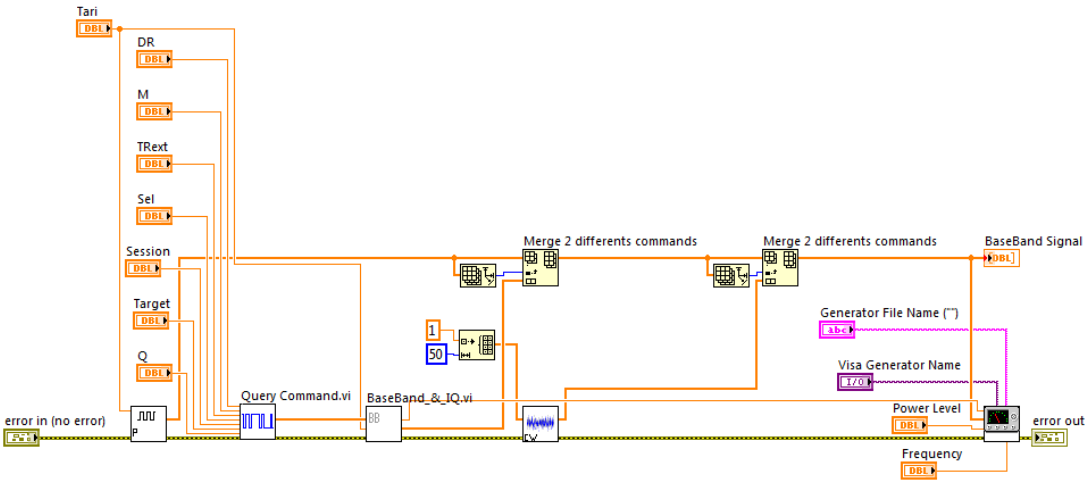

Figure 3.8: LabVIEW code of VSG.

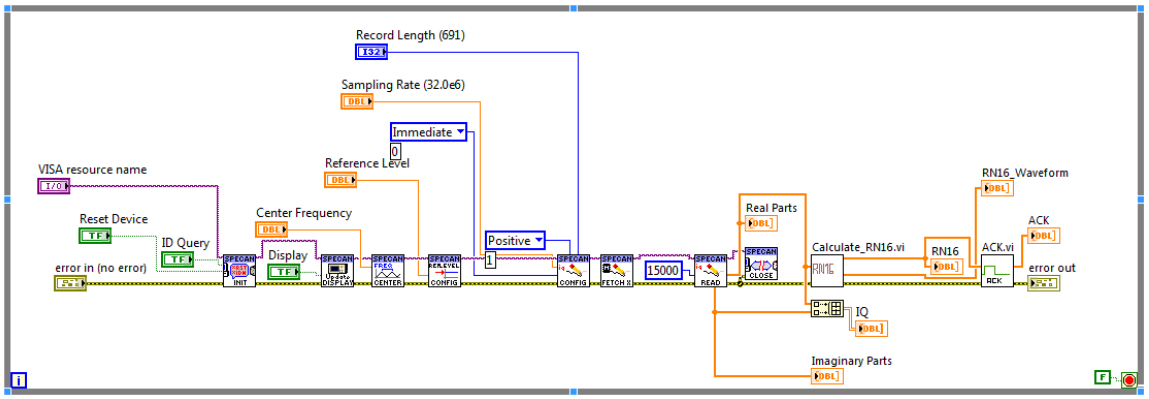

Figure 3.9: LabVIEW code of VSA acquisition.

after selecting the file, starts the VSA, in other VI. This VI is responsible for reading the tag response and decoding the RN16, which was sent by tag.

However, despite this limitation, this architecture allows to send the Query command and receive the tag response (RN16). Although, this part of communication is not enough to get the EPC, but is enough to make communication tests and measurement with tags. In other words, this system is useful to test tags response, and it is also useful to perform tag distance tests. So, this architecture, in spite of not allowing to develop a complete RFID reader, allows to develop an UHF RFID tag test and measurement system.

3.2 Real-Time Interrogator Emulation Architecture

Due to the fact that the communication times between reader and tag were not fullfilled in stimulus-response architecture, it was necessary to find another alternative.

Thereby, the real-time interrogator emulation architecture [Ins13a] was chosen to the RFID reader system. The reason for this choice is that the RF modules uses the PXI FPGAs,

and this way is able to decode and retransmit commands faster, than in the other architecture (VSG and VSA), between reader and tag.

Although, this architecture was used in this dissertation, the FPGA processing was not employed, so existing FPGA LabVIEW example blocks were used in order to facilitate the implementation. In this sense, to choose a transmitter and a receiver that allows to send commands between reader and tag. Therefore, to the RFID reader system, a RF Transmitter and RF Receiver were chosen, instead of a VSG and a VSA, respectively.

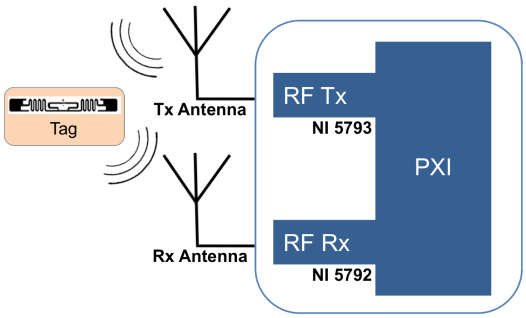

Figure 3.10: Block diagram of real-time interrogator emulation architecture.

As it can be seen in Figure 3.10, the block diagram is more simple than in stimulus-response architecture. The TX module configuration code and Receiver (RX) configuration code were divided in three blocks, in order to optimise the system performance. Thus, the three parts were not shown in this dissertation. Although, can be said that these blocks only contains the configuration of the RF modules.

The PXIe-1085 is the key element which realizes all system processing, and is connected to both RF modules. This way, RF transmitter, NI 5793, and RF receiver, NI 5792, modules, were used, both from NI and connected with PXI chassis (can be seen in Figure 3.11).

Figure 3.11: PXI with NI 5792 and NI 5793.

The NI 5792 and NI 5793, radio frequency receiver and transmitter, respectively, are both adapter modules designed to work in FPGA module, in PXI.

The transmission antenna is connected to RF transmitter, NI 5793, which sends the signal to tag. The reception antenna receives signal from tag, and is connected to RF receiver, NI 5792. It should be noted, that the transmission antenna and the reception antenna are the

same ones represented in stimulus-response architecture, as well as the test tags. Thereafter, the LabVIEW code was developed, which controls all system, the respective flowchart can be seen in Figure 3.12

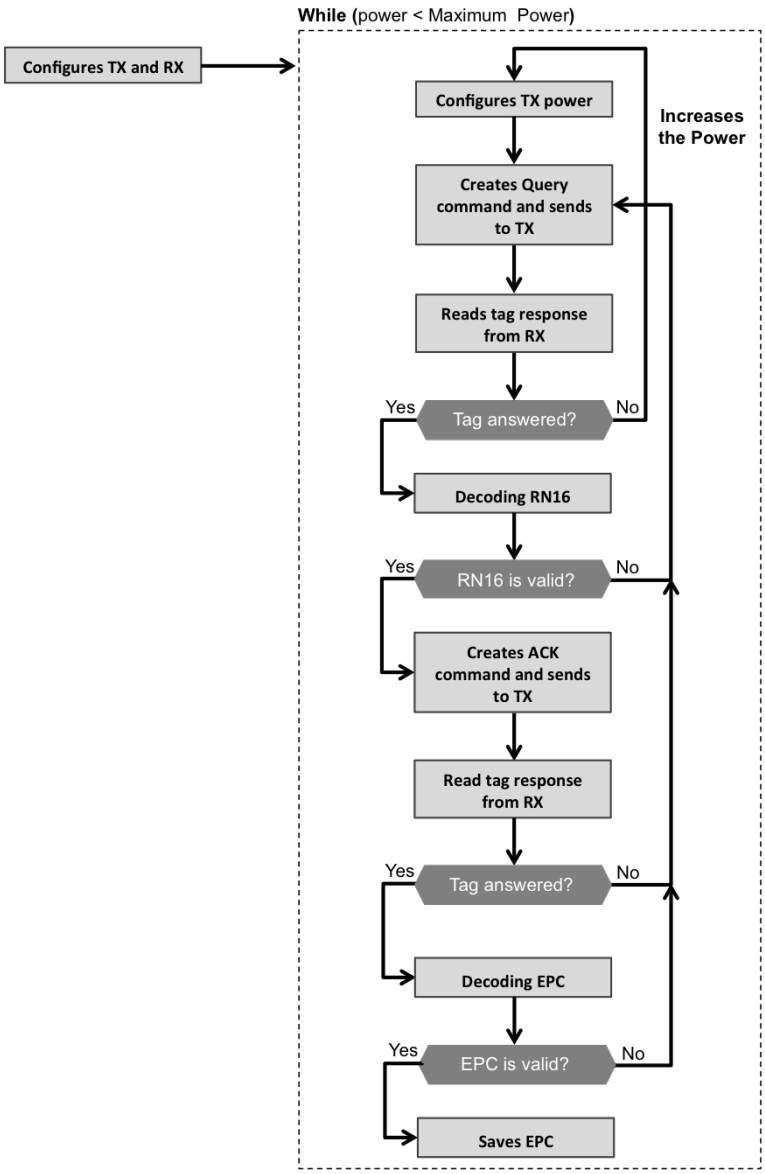

Figure 3.12: Flowchart of the real-time interrogator emulation architecture program to develop LabVIEW code.

As it can be seen, in first place, the TX and RX modules, NI 5793 and NI 5792, were configured because this configuration is only needed to be done one time. Then, the while loop is started which controls the power value sent to tag. After that, the TX module, NI 5793, is configured with the first power value, which was configured by the user. It should be noted that frequency can be initialized by the user. The same process about maximum power limit used in stimulus-response architecture was applied in this architecture.

After, the TX module was configurated with power value, the Query command was created

and sent to TX. At this moment, the RX module started to acquire the tag response. If tag does not reply, the power value is increased and all process starts again. Else, if tag replied, the RN16 decoding is done and is verified, if the decoding is valid. Furthermore, if RN16 decode is not valid, the Query command is sent again to TX, with the same power value. Else, if RN16 is valid, the ACK command is created. Then, the ACK command is sent to TX and, one more time, the RX acquires the tag reply. If tag does not reply, all process starts again, with the same power value. If not, the EPC decoding is made. If the EPC decoding does not valid, all process repeats again, as was mentioned before. Again, if the EPC decoding is valid the EPC data is saved, and the program is ended.

It should be noted that all kind of code that could be done without needing to be done depending on previous blocks, was made in order to optimize the system runtime. In Figure 3.13 the use of LabVIEW code can be seen.

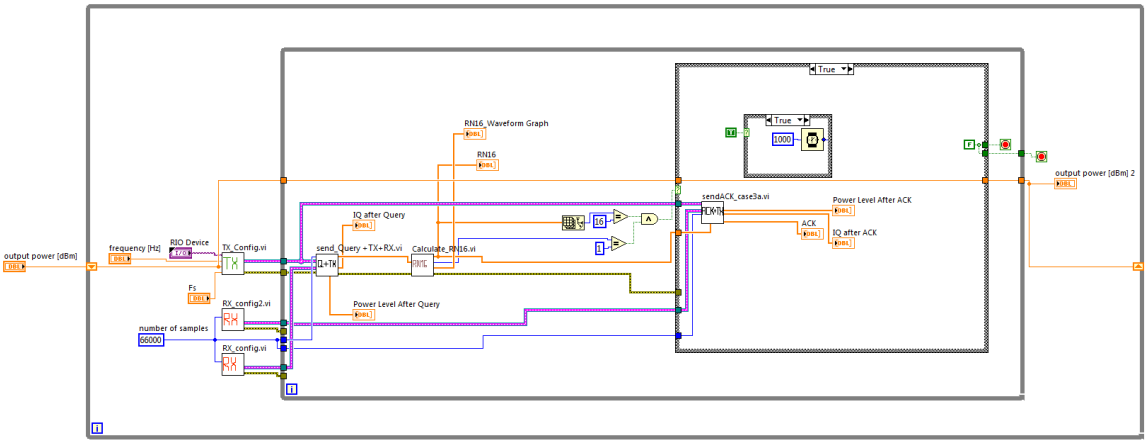

Figure 3.13: LabVIEW code of real-time interrogator emulation architecture.

Nevertheless, developing this architecture without FPGA processing led to the same problem that of stimulus-response architecture. This happened because using the PXI to process all code, is not considered real-time process. It is only real-time process if it is made in FPGA. This way, it has not succeeded in fulfilling all the communication between reader and tag, because the T2 is not fulfilled.

In conclusion, the FPGA processing is fundamental to develop all protocol steps. Once again, only the RN16 reply was obtained from tag. Thus, like in stimulus-response architecture it was only possible to develop a tag test and a measurement system.

It should be said that all this process was very important to better understand how RF modules and PXI work even though FPGA processing was not used.

The time required to send data to the RF transmitter module, the time that is necessary to capture data from the RF reception module, the time required to send data into the FPGA and the time required to capture samples from both RF modules, are several features that enabled a more intensive study of how all these processes occurred.

In summary, this study brought a greater knowledge about PXI and RF modules, NI 5793 and NI 5792 and it can be conclued that with this archictecture it was easier to make tag measurement and tests.

3.3 Specifications

To build an RFID reader some decisions were needed to be made about system specifications. The main specifications to be accomplished by the RFID reader are in Table 3.2

Reader carrier frequency	915 MHz
Bandwidth of the transmission channel	500 kHz
Distance between channels	None, because the transmission channels are adjacents
Maximum output power	4 W ERP
Sampling frequency	100 MHz
Environment	Dense-Interrogator
Modulation	SSB-ASK (OOK)
Encoding	PIE
Coding	FM0

Table 3.2: RFID reader specifications.

The 915 MHz carrier frequency was used, because the system was designed for USA range. The USA range differ between 902 MHz and 928 MHz, and 915 MHz is the middle value. Each channel has a bandwidth of 500 kHz, and that was a reason to choose a USA range. The distance between channels does not exist because in USA case the channels are adjacents.

The sampling frequency chosen is 100 MHz, since with this value it is possible to have more samples to build the signal and this way prevent the aliasing.

The power allowed for USA range the maximum power transmitted is 4W (36.02 dBm) ERP. Nevertheless, this value is easily changeable by the user, if desired.

The SSB-ASK and OOK modulation was used in this dissertation. The reason why this modulation was chosen is because the SSB-ASK is more spectrally efficient, but is more complex and requires an IQ modulator. The PIE and the FM0 coding were used because of protocol specifications.

Also, others values were chosen to fulfill the protocol. The Tari value chosen was 16 μs because it is the middle value between 6.25 μs and 25 μs (values defined in the protocol). For PW value was chosen 8 μs (Tari/2), because this way the data-0 has the same duration for both logic levels '1' and '0'. The RTcal value chosen was the 2.75Tari (44 μs), because it is the middle value between minimum and maximum, and, for the same reason, for the TRcal was chosen 2.05RTcal (90.2 μs). For the data-1 was chosen the 1.75Tari value, because it is the value between maximum and minimum.

It should be noted that all commands have the same duration for data-0 and data-1 symbols. In fact, the RFID reader has been built for the user who can change the carrier frequency easily.

3.4 Application Use Case (Spectrum Analyzer)

In RF communications there are several instruments which are fundamental to generate and analyze RF signals. The spectrum analyzer [VTS13] is an important tool in RF world, because it allows to analyze the signals in frequency domain and to see the harmonics components. This way, this instrument allows to see the amplitude of the signal, in y axis, and

the frequency signal, in x axis. Other information can be read about the signal, like time, power and voltage, besides frequency.

Nowadays, it is more and more usual to see the spectrum analyzers instruments with an extra tool like spectrogram. The spectrogram is light decompostion technique which analyzes the power spectral density. So, the spectrogram is used to indicate the intensity variation of the power spectral density, which allows to analyze in detail the composition of signal, according to the colour variation.

For this reason, an UHF RFID spectrum analyzer was developed with the purpose of understanding what happens in this specific frequency range during the operation of an RFID reader and tag communication. Thus, a LabVIEW application that shows the power spectrum and its spectrogram representation has been built. This was implemented for each worldwide standardized UHF frequency band.

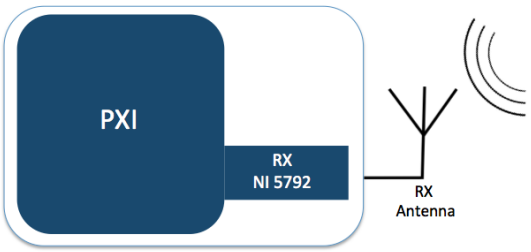

Figure 3.14: Block diagram of spectrum analyzer application.

The application developed was very useful when analysing details on the RFID signal produced in the frame of this dissertation. The big advantage of this application is to see in a much faster way the power spectrum and the spectrogram of UHF RFID frequency band, without using other laboratory instruments.

In Figure 3.14, it can be seen the block diagram of the system, which includes the PXI platorm with the necessary PXI receiver board connected to an antenna for the UHF band.

3.5 RF-DC measurement system

As mentioned before, the RF-DC converters are being every time more used because of their importance in the WPT world [XA15] [JCR14]. For this reason, an RF-DC measurement system was developed in order to read the circuits outcomes and to permit its optimization. Figure 3.15 shows the block diagram of this system.

As can be seen, the system is composed by a PXI, to control all system and two couplers, from Marki Microwave, to read the incident (a_1) and reflected (b_1) waves, by connecting these coupled waveforms to two RX modules on the PXI (NI 5792). Also, the system contains an RF signal generator (NI 5652) and a NI myDAQ which reads the DC voltage from RF-DC circuit, and it is connected to PXI through an USB interface.

To develop the LabVIEW code of RF-DC measurement system, the flowchart present in Figure 3.15 was followed. It is intended to have an application to measure the parameters of the RF-DC circuit, and this way getting the best result in each case. So, two while loops were created in order to sweep the frequency and the power at the RF port. After this, the

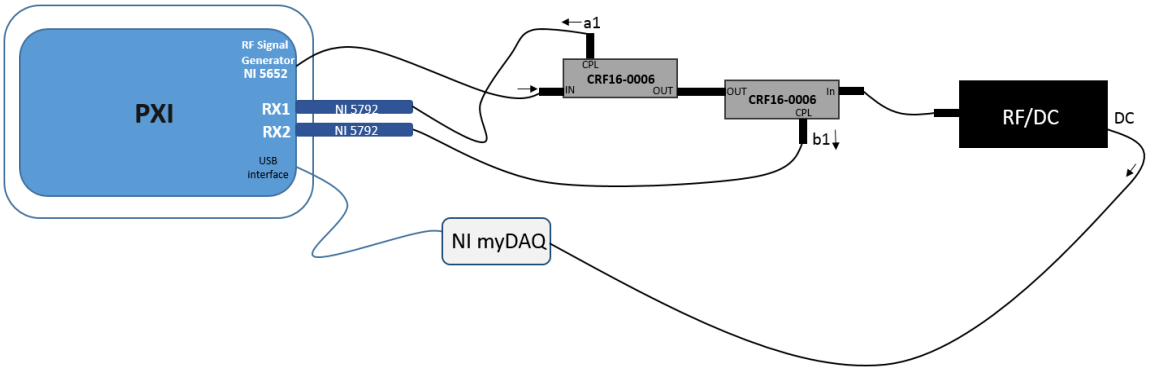

Figure 3.15: Block diagram of RF-DC measurement system.

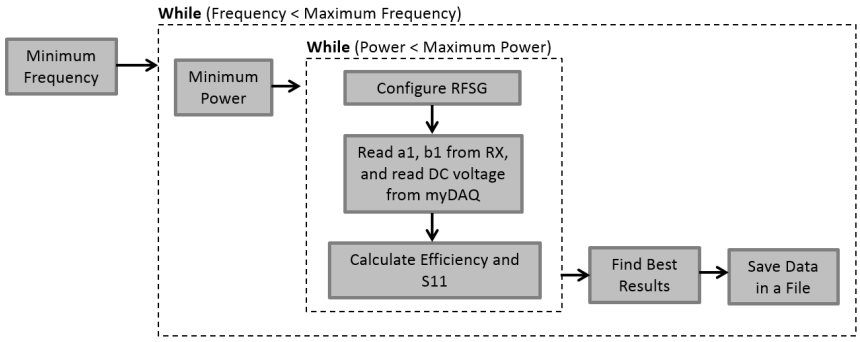

Figure 3.16: Flowchart of RF-DC measurement system.

NI PXI 5652 module is activated. Next, the RX modules are read in order to get the a_1 and b_1 waveforms, and then, allowig not only the calculation of the RF-DC conversion efficiency, but also the RF matching performance (known as S_{11}). Finally, for each input power level a file is created with all information. This system was developed to show that RF-DC measures in PXI can be done and this way, this work can be a step to develop a robust measurement system.

In chapter 4 will be explained how this system was implemented.

Chapter 4

Implementation

In this chapter focuses in detail how the whole RFID reading system has been built. So, it is intended to explain all RFID implementation, since the construction of the commands to be sent to the tag, until the decoding of the signals read from the tag, using LabVIEW code. The implementation how spectrum analyzer and spectrogram and the RF-DC measurement system were implemented is explained too.

4.1 Commands Development for R→T Communication

The first thing to be done in RFID reader system was the development of the commands, because these start the reader tag communication (R→T). As explained under, in subsection 2.5, before sending any command from reader to tag (R→T) and from tag to reader (T→R), it is required a preamble and frame-sync, depending on the cases. For this reason, the development of the preamble and the frame-sync in communication (R→T) was started.

4.1.1 Development of the Preamble and the Frame-sync

Figure 2.17 shows, in chapter 2, how the preamble is composed by four parameters, the delimiter, the data-0, the RTcal and the TRcal.

As mentioned in section 3.3, the 100 MHz was used as the sampling frequency. It is intended to generate the number of samples required to do the preamble time. However, each parameter of preamble has a specific duration. So, it was necessary to calculate each parameter separately to built the preamble. The (4.1) was used to calculate the number of samples of each parameter, and this equation allows to calculate the number of samples using the ratio between the parameter duration with the sampling time (Ts).

$$Number of samples = \frac{Duration}{T_s} \tag{4.1}$$

Table 4.1 shows the number of samples of each parameter, which compose the preamble, using the (4.1).

Frame-sync is composed by the same parameters than preamble, as was mentioned in section 2.5.4, though does not have the TRcal parameter. Hence, the frame-sync has the same values for delimiter, data-0 and RTcal, than preamble. The total duration value of frame-sync is 72.5 μs and 7250 samples.

	Duration (μs)	**Number of samples**
delimiter	12.5	1250
data-0	logic level 1 = 8 logic level 0 = 8 total = 16	logic level 1 = 800 logic level 0 = 800 total = 1600
RTcal	logic level 1 = 36 logic level 0 = 8 total = 44	logic level 1 = 3600 logic level 0 = 800 total = 4400
TRcal	logic level 1 = 82.2 logic level 0 = 8 total = 90.2	logic level 1 = 8220 logic level 0 = 800 total = 9020
Total	162.7	16270

Table 4.1: Preamble values.

Whereupon, was developed the respective LabVIEW code for coding the preamble and frame-sync. Figure 4.1 shows the implementation results of preamble and frame-sync. As can be seen, the duration in number of samples, of each parameter of the preamble, and the frame-sync, as well as, the total duration, was achieved. So, it is easy to understand that Table 4.1 values, match with Figure 4.1 values.

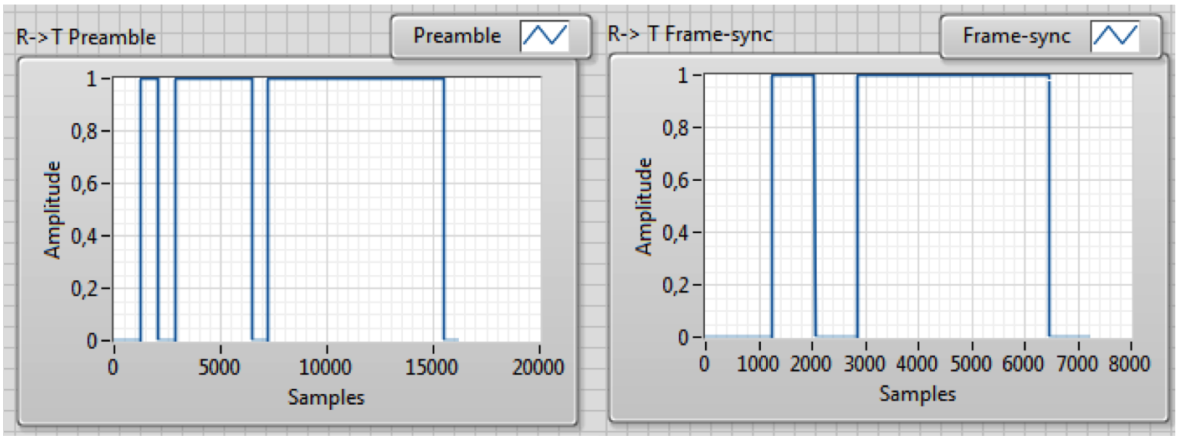

Figure 4.1: Preamble and frame-sync results in LabVIEW code.

The next step was modulate the preamble and frame-sync with a waveform with 1 MHz of frequency. Then, a low pass filter was applied in order to secure that the power transmit mask is fulfilled. The way how this filter was developed is explained in this chapter afterwards.

Finally, the last step of preamble and frame-sync building was done the IQ modulator. The way how IQ modulator was developed and the reason why it was used is explained after in this chapter. The final result of preamble and frame-sync can be seen in Figure 4.2.

After the end of the preamble and frame-sync implementation, the development of the Query command began.

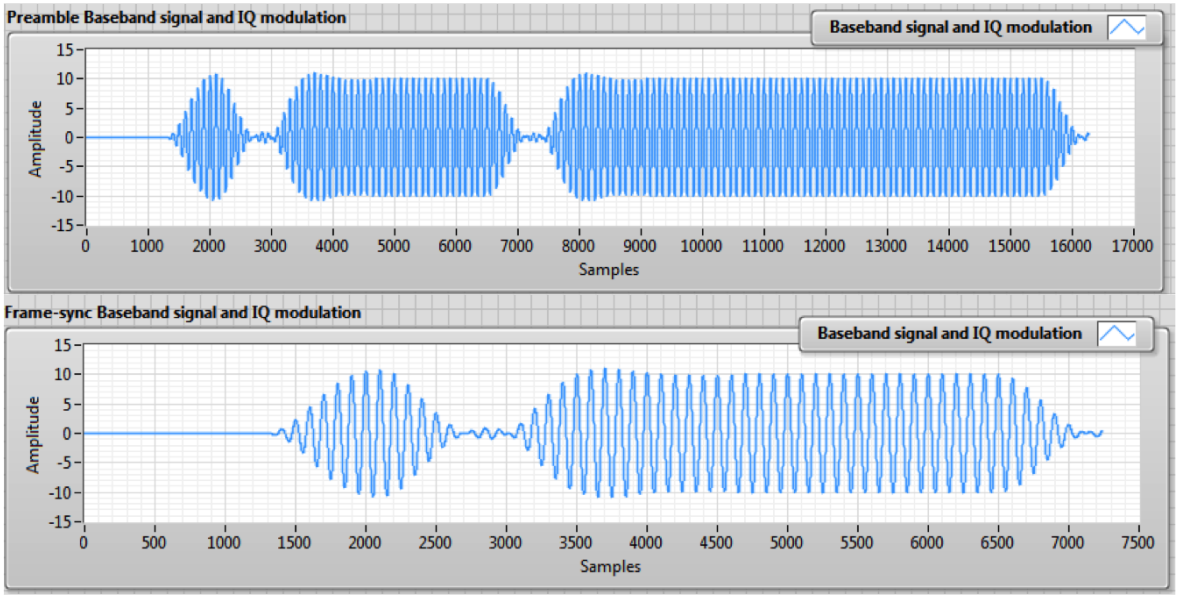

Figure 4.2: Preamble and frame-sync baseband results, with a low pass filter and an IQ modulator in LabVIEW code.

4.1.2 Development of Query Command

The Query command, like as explained in subsection 2.5.5, is composed by 22 bits. The same process to build the preamble and the frame-sync was applied to build the Query command.

As explained before, for each tag, the Query command parameters are different, so it is required to configurate these parameters. The interface to configure the Query command parameters to specify one tag, in LabVIEW code, can be seen in Figure 4.3.

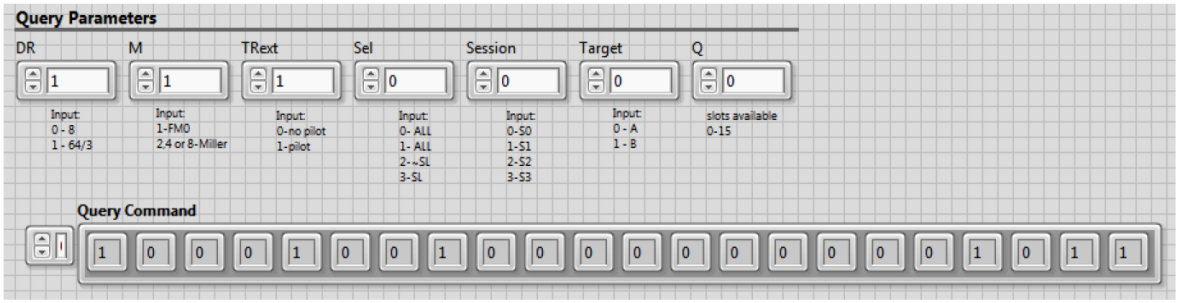

Figure 4.3: User interface for specify the Query command parameters in LabVIEW code.

To build the Query command, in number of samples, the same process was used as in preamble and frame-sync. The Query command is composed by zeros and ones symbols, so, in Table 4.2 can be seen the duration, and the number of samples, of data-0 and data-1.

Figure 4.4 shows an example of Query command. This example contains 6 zero symbols and 16 one symbol, so the total number of samples should be 42400, as can be seen in Figure 4.4.

Then, like in preamble and frame-sync process, a low pass filter was applied in the Query

	Duration (μs)	Number of samples
data-0	logic level 1 = 8 logic level 0 = 8 total = 16	logic level 1 = 800 logic level 0 = 800 total = 1600
data-1	logic level 1 = 20 logic level 0 = 8 total = 28	logic level 1 = 2000 logic level 0 = 800 total = 2800

Table 4.2: Query command values.

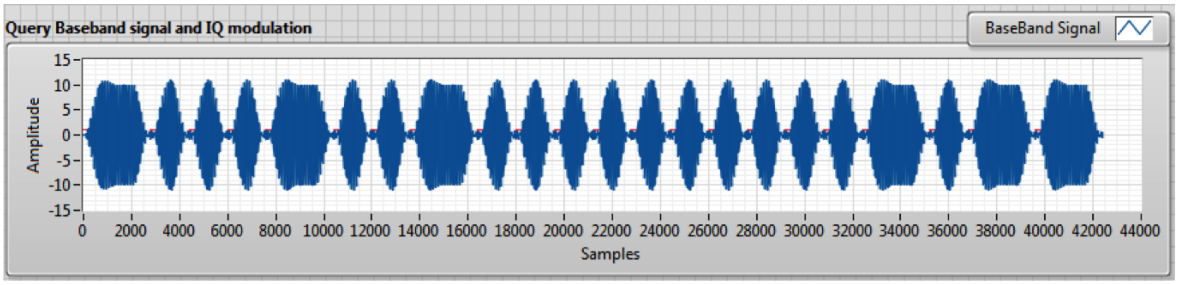

Figure 4.4: Example of Query command LabVIEW code.

command, and then a IQ modulator. It is also important to notice, that before sending the Query command, a preamble is sent.

4.1.3 Development of ACK Command

The same procedure was used to implement the ACK command. So, the ACK command, which contains 18 bits and uses data-0 and data-1 symbols to coding it, was built the same way as Query command. The result can be seen in Figure 4.5. It should be noted that the data-0 and data-1 have the same duration than in Query command implementation, obviously.

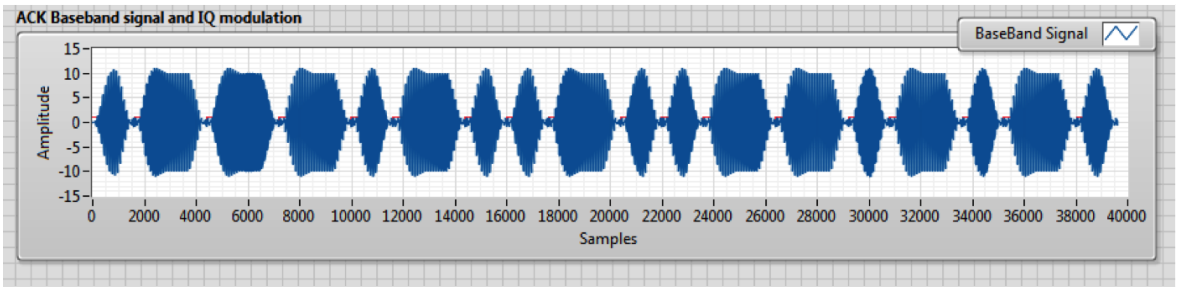

Figure 4.5: Example of ACK command in LabVIEW code.

Although, as mentioned in subsection 2.5.5, the ACK command is composed by RN16. This ACK command example, contains one RN16 command sent by tag. This example, which contains 9 zero symbols and 9 one symbols, has the total number of samples of 39600. It is noted that, before sending an ACK command, a frame-sync was sent. Once again, after building the ACK command into number of samples, a low pass filter and an IQ modulator were applied.

However, in this dissertation, the Query and the ACK commands were only used in R→T communication, because with just these two commands it is possible to obtain the tag EPC. It is noted that this is just one ACK example command, because in each tag communication, the tag sends the RN16 randomly.

4.2 Low Pass Filter for R→T Communication

To fulfill the power transmit mask, a low pass filter was required to develop. To build the low pass filter in LabVIEW, a data-0 symbol [San14] was generated in LabVIEW code. Then, the data-0 symbol was sent to the VSG and a spectrum analyser was used to see the impact of the filter in power mask.

Before using this method, to choose the best filter for the system the matlab filter design was used. However, it was conclued that the filter simulated in matlab has a different behavior in LabVIEW. So, because of this reason, the trial and error method was used to find the best low pass filter. After many tries was conclued that the better filter to fulfill the power transmit mask is a filter with cut-off frequency of 90 kHz and with a order value of 3.

Thus, a filter block was implemented in LabVIEW which was configured like a low pass filter and this one can be seen in Figure 4.6.

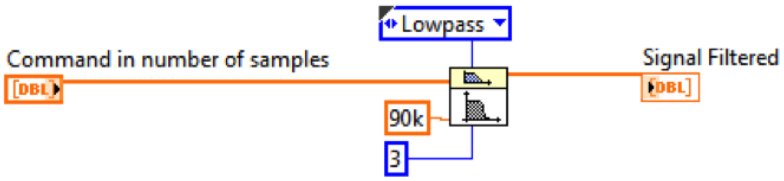

Figure 4.6: Implementation of low pass filter in LabVIEW code.

As can be seen in Figure 4.7, there is a big difference in the signal with and without filter, and in chapter 5, the results of power transmit mask using this filter are presented.

4.3 IQ Modulator

The IQ [Ins14a] is a crucial element in RF communications, which allows to represent a signal in a complex form. The IQ allows to give the information, when any changes happen in phase, or amplitude, in a sine wave. Thus, using the IQ modulator, these changes in phase, or amplitude, can be used to encode information, in other words, modulation. The I part is composed by (4.2), and the Q part is composed by (4.3), where A means amplitude.

$$I = A.\cos(angle) \tag{4.2}$$

$$Q = A.\sin(angle) \tag{4.3}$$

IQ modulation is one modulation technique, which I is the phase component and Q is the quadrature component. It is an efficient way to transfer information, allows modulate a carrier and turn into waveform, and can change the carrier frequency slightly. This way, the

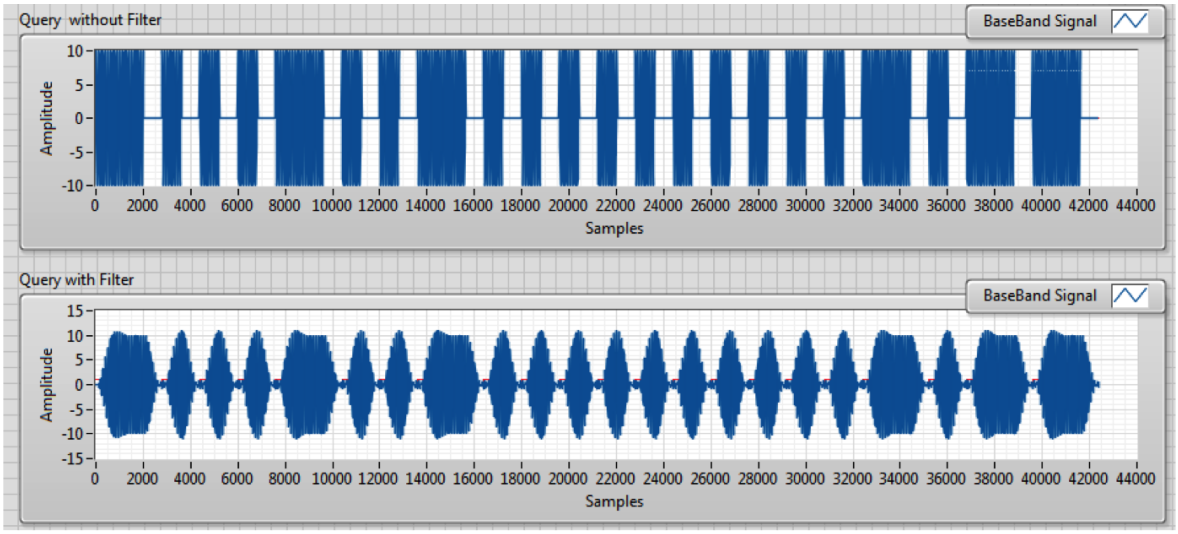

Figure 4.7: Difference between a Query command without a low pass filter and with a low pass filter.

signal can be treated as a phasor modulating. Can be seen in Figure 4.8 a block diagram of IQ modulator, which explains how the IQ modulator works.

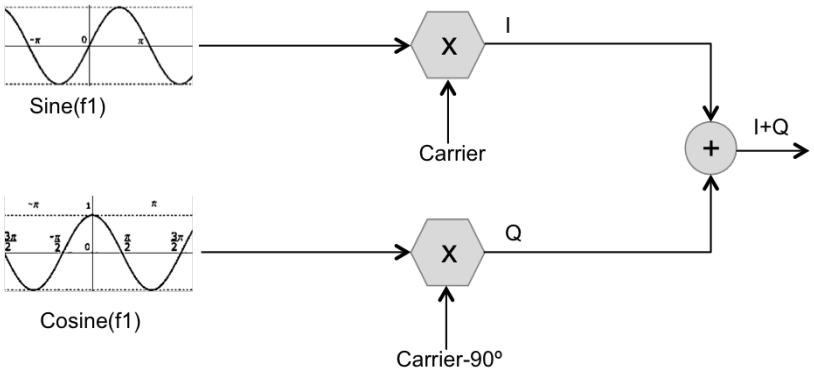

Figure 4.8: IQ modulator block diagram.

First, a sine with frequency f1 is generated and a cosine with the same frequency. Then, the sine is multiplied by a carrier, and the cosine is multiplied by the same carrier, but with 90 degrees phase shift. Finally, the I and Q component are added.

The LabVIEW code used to develop the IQ modulator can be seen in Figure 4.9 and, should be noted that a command being filtered appears, and then the IQ modulator is made, as mentioned in subsection 4.1.1, subsection 4.1.2 and subsection 4.1.3. First, a sine and a cosine are created, using appropriate LabVIEW blocks, then, the signals from sine and cosine blocks are waveforms, so they need to be converted in a double. After this, the signal (command), in number of samples, is multiplied by sine (I) and cosine (Q). Thus, the I and Q components are created, and finally, the I component (real part) and Q component (imaginary part) pass into a block which make these two in a complex number. So, after this process, the RF signal is ready to be sent.

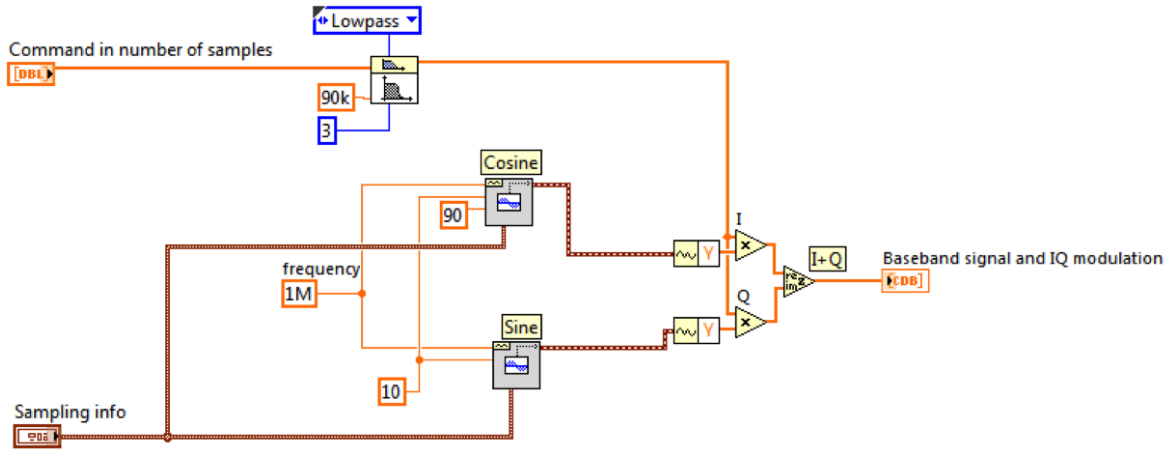

Figure 4.9: IQ modulator used in LabVIEW code.

4.4 VSG and VSA Configuration

To interact with VSG and VSA, appropriate LabVIEW blocks (drivers) were used. Each configuration block of the VSG (see Figure 4.10) and the VSA (see Figure 4.11) has an established role. To send the information to VSG, the data is required to pass by an IQ modulator, before. As was mentioned in section 4.3, the IQ modulator was made after building the commands, so it is not required to do it in this VI.

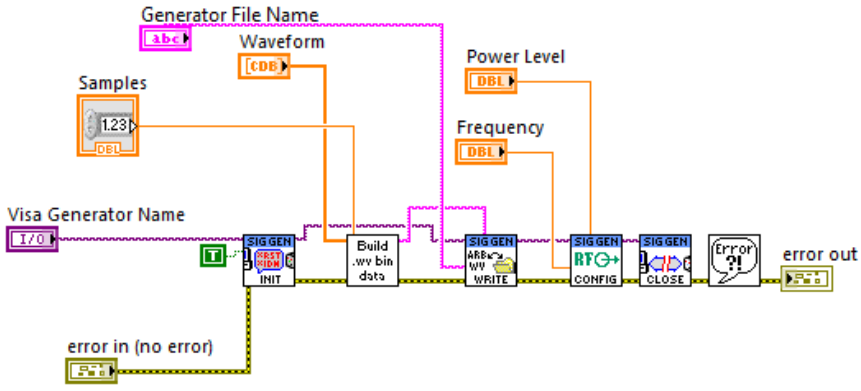

Figure 4.10: VSG configuration in LabVIEW code.

In VSA, when data is received from the equipment, to decode the tag information (on the specific case of this dissertation) is only part needed is the real part, so the IQ demodulator is not required.

4.5 Decoding Information from Tag T→R

To decode the tag information, three big VIs were made: the tag information decoding, the autocorrelation and the FM0 decoding. The LabVIEW code of these three processes can be seen in Figure 4.12, and each one of them have, inside, the corresponding LabVIEW

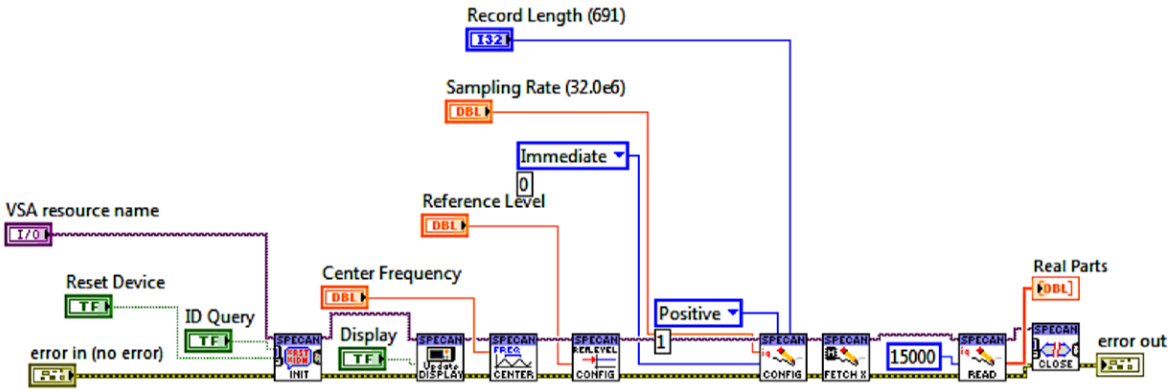

Figure 4.11: VSA configuration in LabVIEW code.

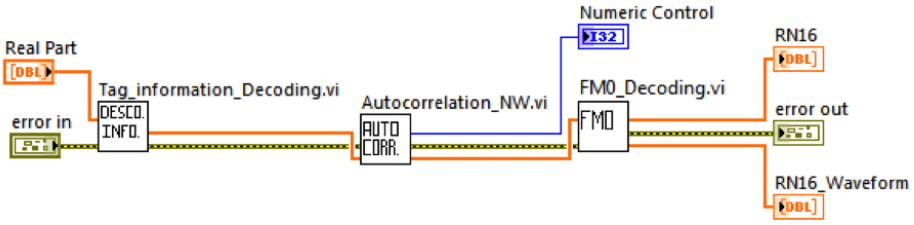

Figure 4.12: LabVIEW code for decoding tag information.

code. The first block has as purpose to process the information received from tag. The autocorrelation block compares the information received with a sequence already known, this way it can decode the symbols. The last block, FM0 decoding, reads the information and gets the command information.

4.5.1 Tag Information Decoding

The sign received by tag is present at carrier frequency of 15 MHz and it was needed to calculate the interest sign. So, using the (2.4), the BLF value was calculated, to a DR value of 64/3 and a TRcal value of 90.2 μs. It should be noted that, the tag used in this experience, has a DR value of 64/3. The BLF value calculated was 236.5 kHz, thus, the interest sign is present in 15.236 MHz frequency. Can be seen in Figure 4.13 the sign received from tag with a carrier frequency of 15 MHz and the interest sign in 15.2365 MHz.

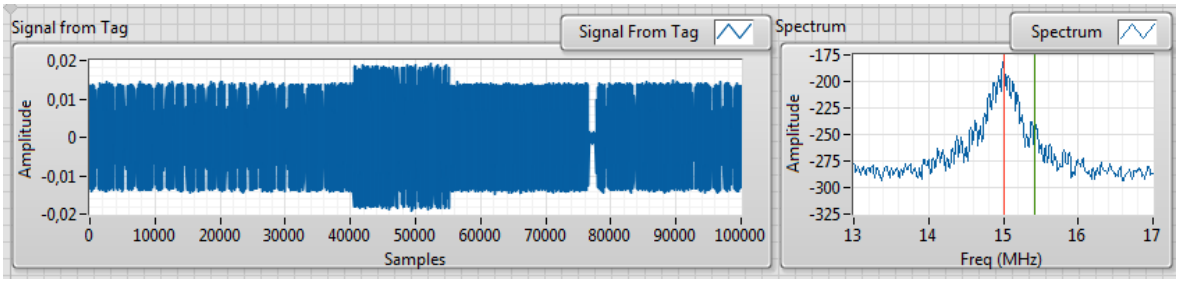

Figure 4.13: Signal received from tag.

To decode the interest sign, some procedures were required to do, more specifically, an envelope detector, followed by filters [San14]. To sum up this process, the Figure 4.14 shows the block diagram of envelope detector and filters, and each one of these blocks is described below.

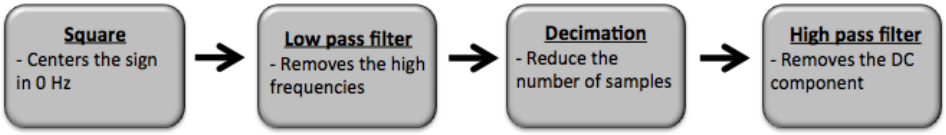

Figure 4.14: Block diagram of envelope detector followed by filters.

In Figure 4.15 can be seen the corresponding LabVIEW code.

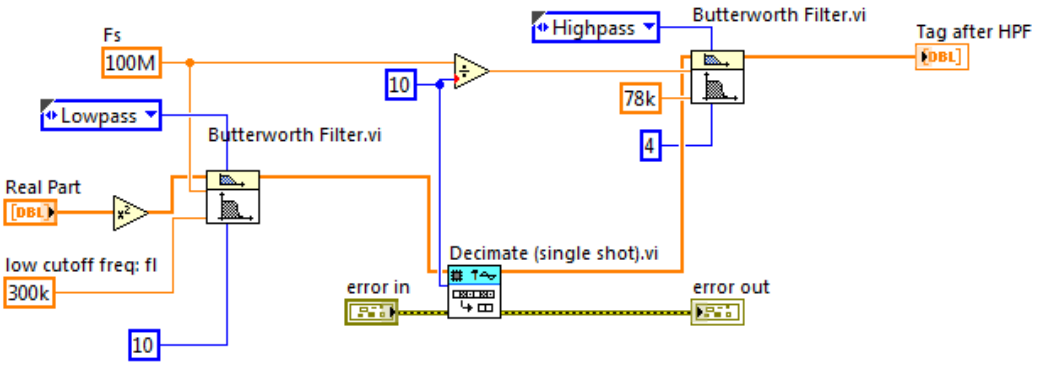

Figure 4.15: LabVIEW with square, low pass filter, decimation and high pass filter.

Square

To do an envelope detector, a square process is used, which creates a DC component, centering the signal in 0 Hz. Thus, the sign passes from 15 MHz to 0 Hz, and this way, the interest sign passes to 236.5 kHz.

So, to square the sign to make this explanation, in LabVIEW code, a square block was used, which computes the square of the sign value. The result can be seen in Figure 4.16, and, as was expected, a DC component was created and the interest sign is in 236.5 kHz.

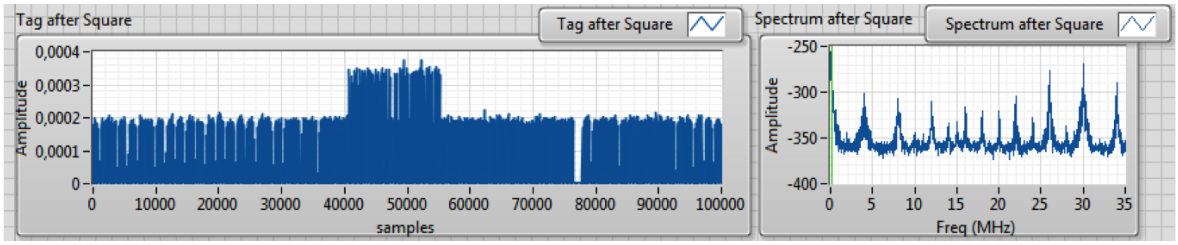

Figure 4.16: Signal after pass by squaring.

Low pass Filter

The low pass filter [The04] cut the high frequencies, until a specific cut-off frequency and allows to pass the low frequencies. The filters can have different order and can be different types. In this dissertation, the low pass filter was used to remove the high frequencies, because the interest sign stays in zero frequency. In LabVIEW code, a specific filter block was used and was configured with filter specifications. To choose the low pass filter specifications some calculations were made.

To remove the high frequencies it was necessary take into account the interest sign, which is present in 236.5 kHz frequency. Some experiences were made to find the best low pass filter. As was said before, the filter simulation in matlab was not used because the behavior of filter in LabVIEW is different. Thereby, the low pass filter with a cut-off frequency of 300 kHz and with a 10 value order was used, because with these specifications the interest sign bandwith is covered. A butterworth filter was chosen, because this one has a flat frequency response and has less ripple than other types of filters, and these are the reasons why this filter was chosen. In Figure 4.17 can be seen the signal, after having been filtered, by a low pass filter, which contains the interest signal in 236.5 kHz.

Figure 4.17: Signal after pass by a low pass filter.

To sum up, the low pass filter was correctly developed and applied.

Decimation

The decimation process [Tan08] [ZT94] has the purpose to reduce the sampling rate. This process permits to obtain less samples, and this way allows to interpret the data more easily and efficiently. To reduce the sampling rate an integer factor (M) is used and the equivalent equation is present in (4.4):

$$y(m) = x(mM) \tag{4.4}$$

The x(n) represents the data sequence and y(m) is the downsample sequence obtained by x(n), for all M samples. So, in decimation occurs the sampling rate reduction from Fs to Fs/M, where Fs is the sampling frequency. Figure 4.18 shows an example of decimation.

Nevertheless, it should be noted that the alising can occur in decimation, so the M factor must be carefully chosen.

In this dissertation, the decimation was used to reduce the samples and this way facilitate the interest sign analysis, and, for this reason, make decoding faster. Thus, was used the integer factor (M) of 10, so the sampling frequency was reduced to 10 MHz. It is possible to observe the result in Figure 4.19. Comparing with Figure 4.17 it is easy to conclude that the number of samples in Figure 4.19 is less 10 factor (Fs/M, 100 MHz/10) than Figure 4.17. The 10 factor value was chosen, because with this value the aliasing does not happen and

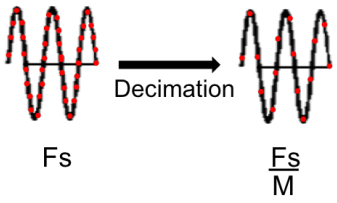

Figure 4.18: Example of decimation process.

the number of samples is significantly reduced. In LabVIEW code, a specific block was used which does the decimation.

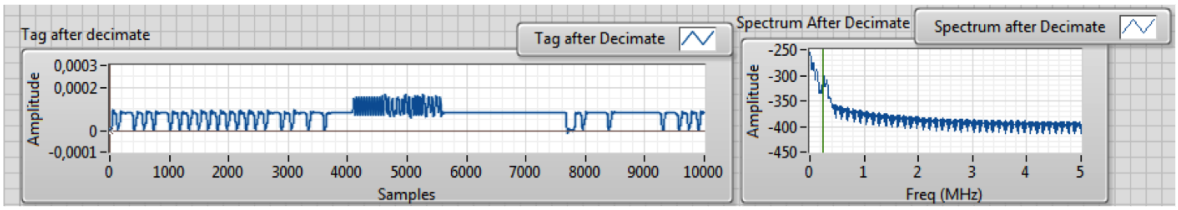

Figure 4.19: Signal after pass by decimation.

High Pass Filter

The high pass filter [The04] cut the low frequencies, until a specific cut-off frequencies, and allows to pass the high frequencies. As was mentioned in low pass filter, the high pass filters can have different order and can be different types.

In this dissertation, the high pass filter was used to remove the DC component, so, this way, the interest sign is the only one that is analyzed. So, the interest signal is present on 236.5 kHz frequency, and, for this reason, the high pass filter must have a cut-off frequency less than this value. To choose the right cut-off frequency, for the high pass filter, some experiences were made, and in the end, the high pass filter with 78 kHz and with 4 order value was chosen. A butterworth filter was chosen for the same reason than in Low pass filter.

In LabVIEW code, a specific filter block was used and was configurated with filter specifications. In Figure 4.20 can be seen the signal after being filtered by a high pass filter. Can be seen in figure, that the interest sign was treated and it was centered in zero.

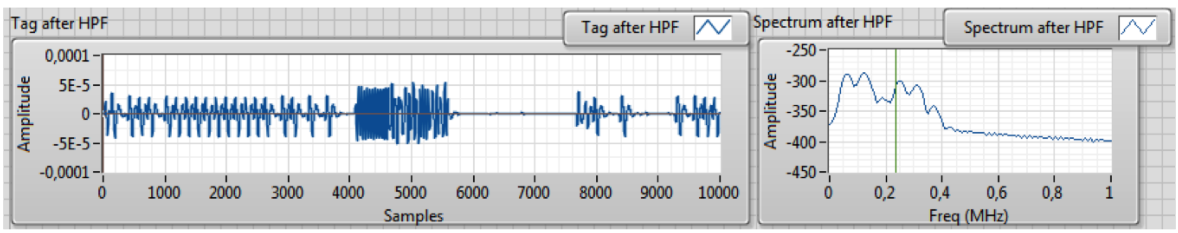

Figure 4.20: Signal after pass by high pass filter.

After finalisation the envelope detector and filters process, which treat the interest sign, this one is ready to be decoded.

4.5.2 Autocorrelation

The autocorrelation [Bro06] is a mathematical function, which allows to detect standards and repetitions in signals. This function can measure the correlation relation between a variable, in determined period time, with itself, in other period of time. Thus, it is useful for detecting variables, sequences and frequencies in signals with noise, which makes this function cructial in signal processing.

So, it can be said that the autocorrelation is the linear dependence of some variable with itself, in two different time periods. Because of this reason, the autocorrelation (4.5) [Mata] depends of h (the time lag between times) and the y_0, which is the lag zero convariance.

$$\rho_h = Corr(y_t, y_{t-h}) = \frac{y_h}{y_0} \tag{4.5}$$

In this dissertation, the autocorrelation was used to detect the RN16 and the PC, EPC and PacketCRC commands from tag. Therefore, a known sequence was used for the autocorrelation algoritm compare with the signal from tag. This way, with this algoritm can be detected the index where RN16 ou PC, EPC and PacketCRC start.

To develop the autocorrelation in LabVIEW code, the matlab code avaiable in [Matb] was used. So, can be seen in Figure 4.21 an example of autocorrelation detection and then in Figure 4.22 can be seen the signal in detail, after pass by autocorrelation process. It should be noted that complete pilot tone is not present in Figure 4.22.

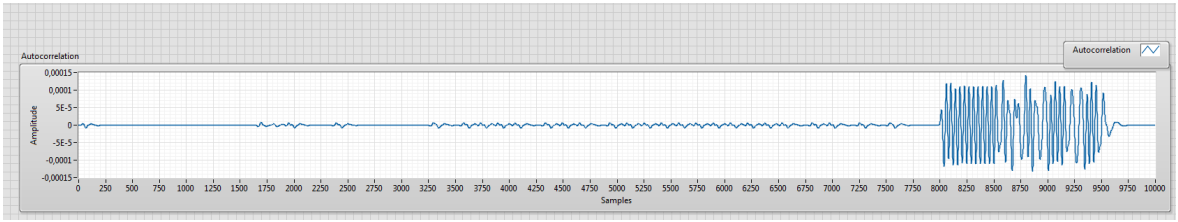

Figure 4.21: Signal after autocorrelation process.

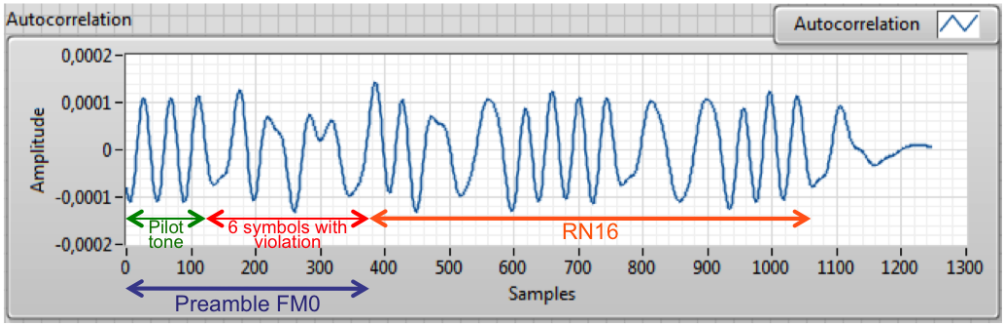

Figure 4.22: Signal detected by autocorrelation.

4.5.3 FM0 Decoding

In FM0 decoding part decodes the information sent by tag, because the data arrives after autocorrelation part.

The first thing to be done, to decode the tag information, it to know the tag specifications. In this case, a DR value of 64/3, a TRcal value of 90.2 μs, and consequently a BLF value of 236.5 kHz (2.4), with pilot tone was used. Then, the (4.6) to calculate how many samples a symbol has was used.

$$Number of samples = \frac{Fs}{\text{BLF}} \tag{4.6}$$

So, the result obtained was 42.3 samples. Nevertheless, from Table 2.18, the minimum and maximum number of samples of each symbol can be calculated, and this way an efficient detection of each symbol can be done. Thus, using the Table 2.18, to calculate the minimum and maximum number of samples, of each symbol, the (4.7) was used.

$$Number of samples = \frac{Fs}{\text{BLF} + 2.5\%} \tag{4.7}$$

To sum up, was calculated a minimum number of samples of 41.34 and a maximum of 43.46 samples. In Figure 4.23 can be seen the relationship between of number of samples and each symbol, in FM0 encoding.

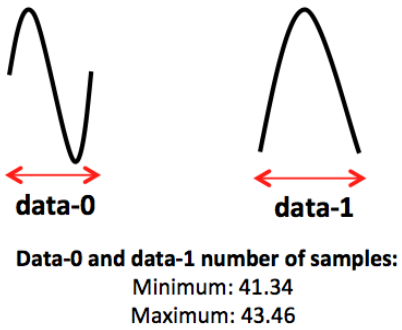

Figure 4.23: Relationship between symbols and number of samples.

It can easily be concluded that in data-0 symbol exists two zero spots, and in data-1 symbol exists one zero spot, excluding the first one. This conclusion is a big help to implement the algorithm to do the FM0 decoding. To develop this algorithm it is fundamental to know the number of samples of each symbol.

In summarised form, in algorithm it is verified if transitions in zero exist, so if one transition until 44 samples (43.46 round up) exists, it is a data-1 symbol, and if two transitions until 44 samples exist, it is a data-0 symbol. Furthermore, if no transition exist until 44 samples, it is a violation symbol. As a result of this algorithm, all tag information can be decoded.

In Figure 4.24, an example of RN16 detection can be seen, after passing by the tag information decoding, autocorrelation and FM0 decoding.

4.6 Application Use Case (Spectrum Analyzer) Implementation

To implement the spectrum analyzer and spectrogram application, two relevant LabVIEW blocks were used, the Fast Fourier transform (FFT) block and the spectrogram block. The

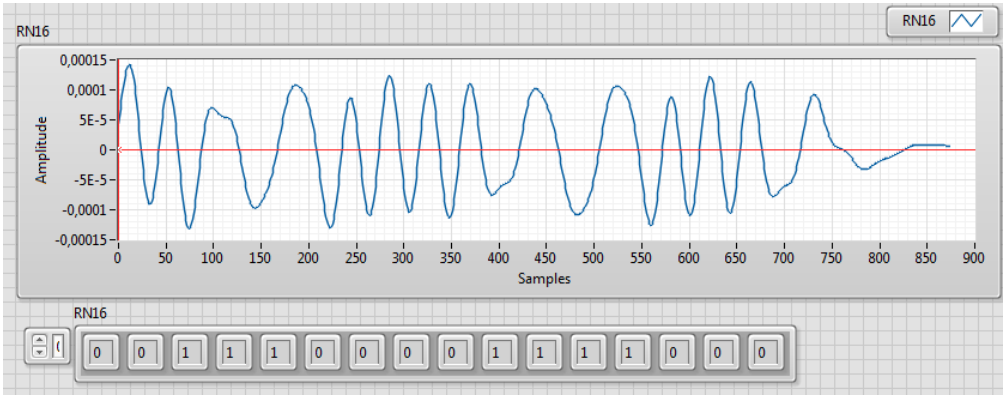

Figure 4.24: Example of RN16 detection after pass by the tag information block, autocorrelation and FM0 decoding.

FFT [Tod] technique is very important in digital signal processing because it calculates the Discrete Fourier Transform (DFT). This way, the FFT decomposes in different frequencies components a sequence of values. So, using this simple LabVIEW block, the power spectrum can be obtained. Figure 4.25 shows the LabVIEW code, which used the FFT power spectrum block (block with PS/PSD name).

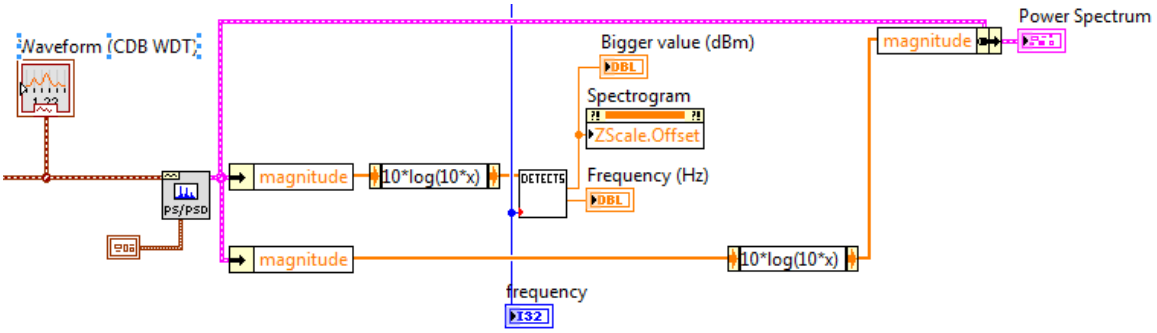

Figure 4.25: LabVIEW code responsible for calculate the power spectrum.

The spectrogram block calculates the intensity variation of the power spectral density, in LabVIEW block, and the respective LabVIEW code can be seen in Figure 4.26.

Besides these two important blocks, the biggest amplitude value in dBm and frequency was required to find, because it is important to know in which dBm value the signal is present. In Figure 4.25 can be observed the detects block, which is responsible for doing the calculation of maximum dBm value detected, and the respective frequency.

This way, with this simple LabVIEW code it is possible to build a power spectrum and spectrogram application.

4.7 RF-DC measurement system

To implement the RF-DC measurement system a LabVIEW was used, as can be seen in Figure 4.28. For this purpose, the NI PXI 5652 was activated. After, the a_1 and b_1 were read

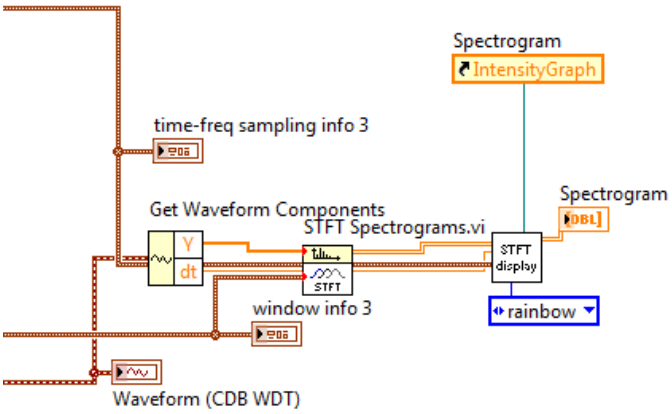

Figure 4.26: LabVIEW code responsible for generate the spectrogram.

from RX modules, it was required to calculate the S_{11} and the efficiency. These two results were obtained using (4.8) and (4.9). It should be noted the power values used to calculate the efficiency are in Watts.

$$S_{11} = \frac{b_1}{a_1} \tag{4.8}$$

$$Efficiency = \frac{\frac{V^2}{R}}{P_{in}} \tag{4.9}$$

A block to calculate the best result of each power value was made. The code is very simple, because only the bigger value of efficiency is found in the efficiency array. Finally, a block to save all information about each measure was made and the LabVIEW code can be seen in Figure 4.27.

The main results obtained in the course of this dissertation will be shown in the next chapter.

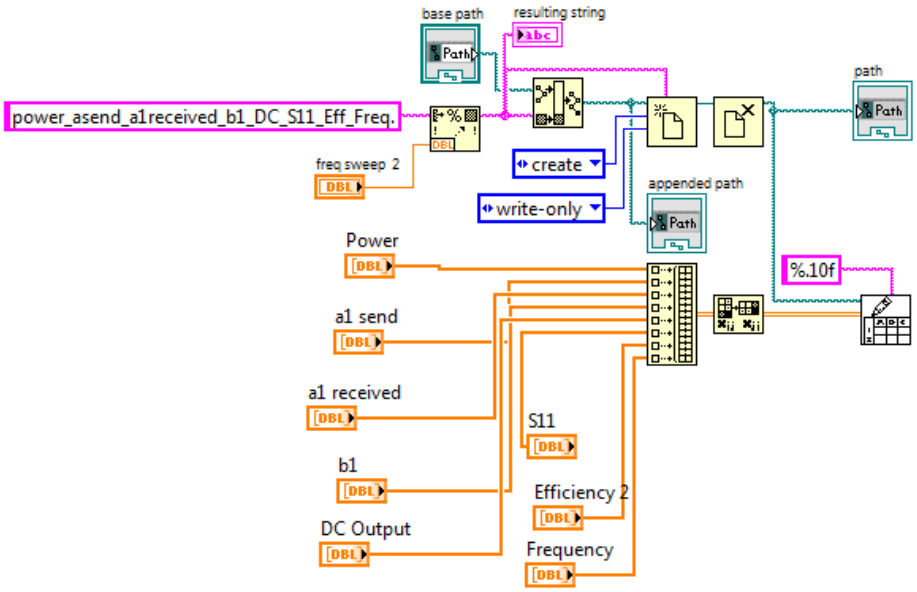

Figure 4.27: LabVIEW code of save data in a file.

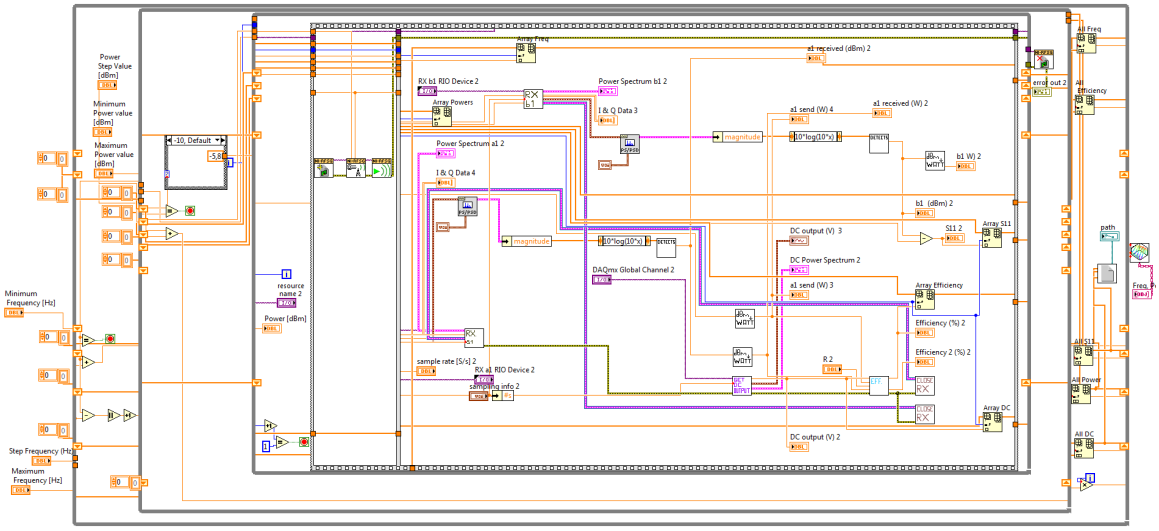

Figure 4.28: LabVIEW code of RF-DC measurement system.

Chapter 5

Results

This chapter presents the results obtained in this dissertation, in stimulus-response architecture, as well as, in real-time interrogator emulation architecture. All measurements made will be presented and a comparion between the two architectures, and thus better understand these results. The results of spectrum analyzer and spectrogram application and the RF-DC measurement system are presented too.

5.1 Commands Validation

The first thing to be done to verify if the system was well developed, was verify if the commands were well done. In the first place, the number of samples of preamble (used in R→T communication) was calculated and then, in oscilloscope, the number of samples of preamble matches with the equivalente time duration of preamble was verified.

As it was explained in subsection 2.5.4, the preamble is composed by delimiter, data-0, RTcal and TRcal. The preamble used was the preamble built in Table 4.1. Thus, like it was presented in Table 4.1, the total duration of preamble is 16270 samples, which corresponding to 162.7 μs.

Therefore, after calculation of the theoretical preamble time, the practical measurement was executed, using an oscilloscope in laboratory. To do this, the preamble was sent from PXI equipment, using LabVIEW programming, to VSG. Figure 5.1 proves that the preamble time was successfully achieved, so the preamble duration obtained was 162.8μs.

After preamble duration verification, a verification of the process was made by sending a Query command. So, it was verified if the sequence of preamble, Query command had the right duration.

The same calculation process was applied to verify the preamble and Query command duration. The data-0 and data-1 values obtained in Table 4.1 were used, and the total duration of preamble and Query command is 586700 samples, which corresponds to 586.7 μs . It should be noted the preamble has 16270 samples, as presented before, and the Query command has 42400 samples, which has 6 data-1 symbols (2800 samples each symbol) and 16 data-0 symbols (1600 samples each symbol). In Figure 5.2 can be seen the confirmation value of 586.7 μs for preamble and Query command together.

Figure 5.3 shows all communication sequence and the tag response. First of all, the preamble command can be seen, then, the Query command, and, finally, the Continuous Wave (CW). Consequently, the RN16 is observed, which is the tag response command.

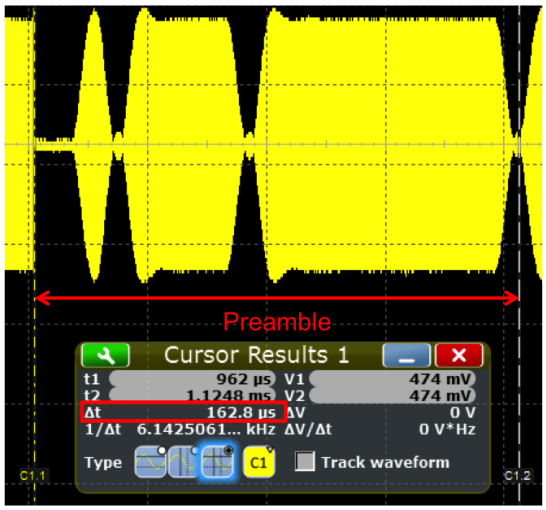

Figure 5.1: Preamble duration verification.

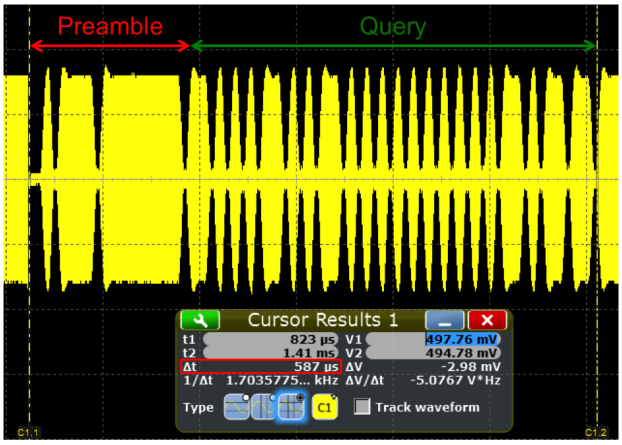

Figure 5.2: Preamble and Query command duration verification.

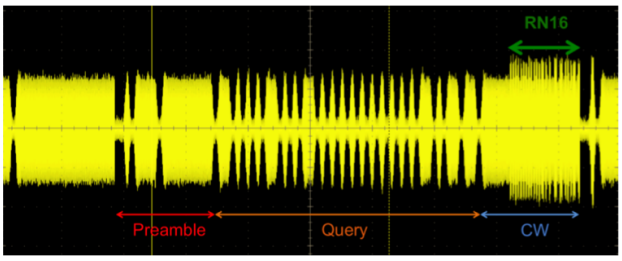

Figure 5.3: Tag response validation.

It should be noted that this verification was made for frame-sync and ACK commands in (R→T communication) and the same logical thinking was applied.

To test the frame-sync, the same frame-sync of subsection 4.1.1 was used. Thus, the frame-sync should have 72.5 μs and Figure 5.4 proves that this goal was achieved, by oscilloscope measurement.

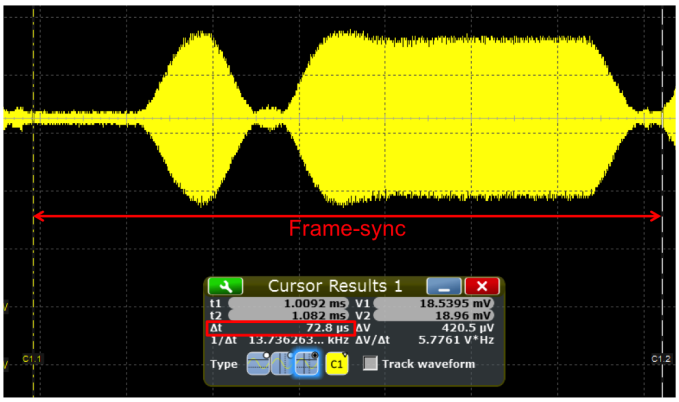

Figure 5.4: Frame-sync duration verification.

After frame-sync validation, the ACK command was tested, and to do this the same ACK command was used, which was present in subsection 4.1.1. This example of ACK command is composed by nine data-0 symbols and nine data-1 symbols. That is why, in this example, the ACK command has a duration of 396 μs. Therefore, the frame-sync and ACK command together make a duration of 468.5 μs. Figure 5.5 shows the duration of frame-sync and ACK command duration, measure in osciloscope.

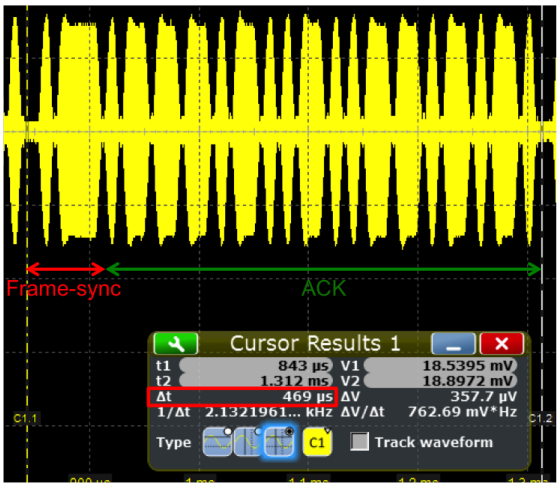

Figure 5.5: Frame-sync and ACK duration verification.

The preamble duration was fulfilled, the Query command duration was fulfilled and the tag replies with the RN16 command, so can be conclued that the commands validation has been successfully implemented. The frame-sync and ACK command were fulfilled too.

5.2 Stimulus-Response Architecture Results

As it was detailed in chapter 3, the stimulus-response architecture is composed by several elements. Figure 5.6 shows the stimulus-response setup used in laboratory to build this architecture, which has the VSG, the VSA, transmission and reception antennas and the tag.

It is noted that, in this figure, the PXI platform does not appear, but is connected by ethernet with VSG and VSA.

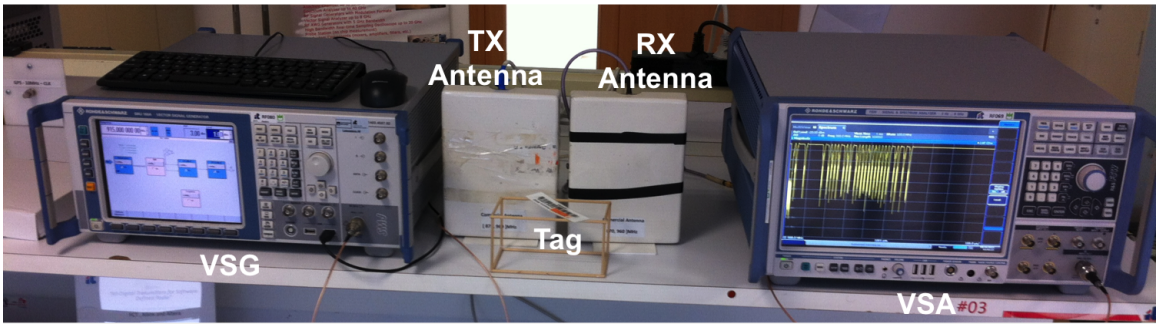

Figure 5.6: Stimulus-response architecture setup.

After this architecture was setup, its LabVIEW code was used, as explained in section 3.1. In Figure 5.7 can be seen the LabVIEW user interface of this architecture.

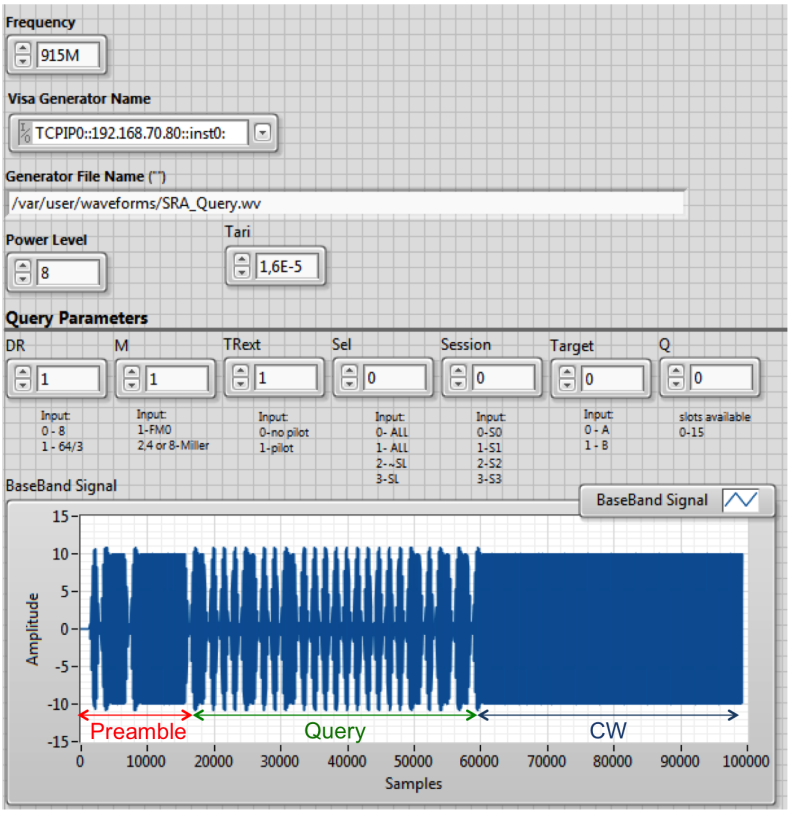

Figure 5.7: Stimulus-response architecture user interface.

As can be seen in Figure 5.7, in this interface, the user has the possibility to choose the Query command parameters and to see immediately the commands that will be sent.

In Figure 5.8 can be seen the VSA user interface, in LabVIEW code, which contains a chart with preamble and Query command sent to tag, and then can be seen the tag reply

with RN16 command. Below this chart, can be seen the RN16 decoding and the constitution of ACK command.

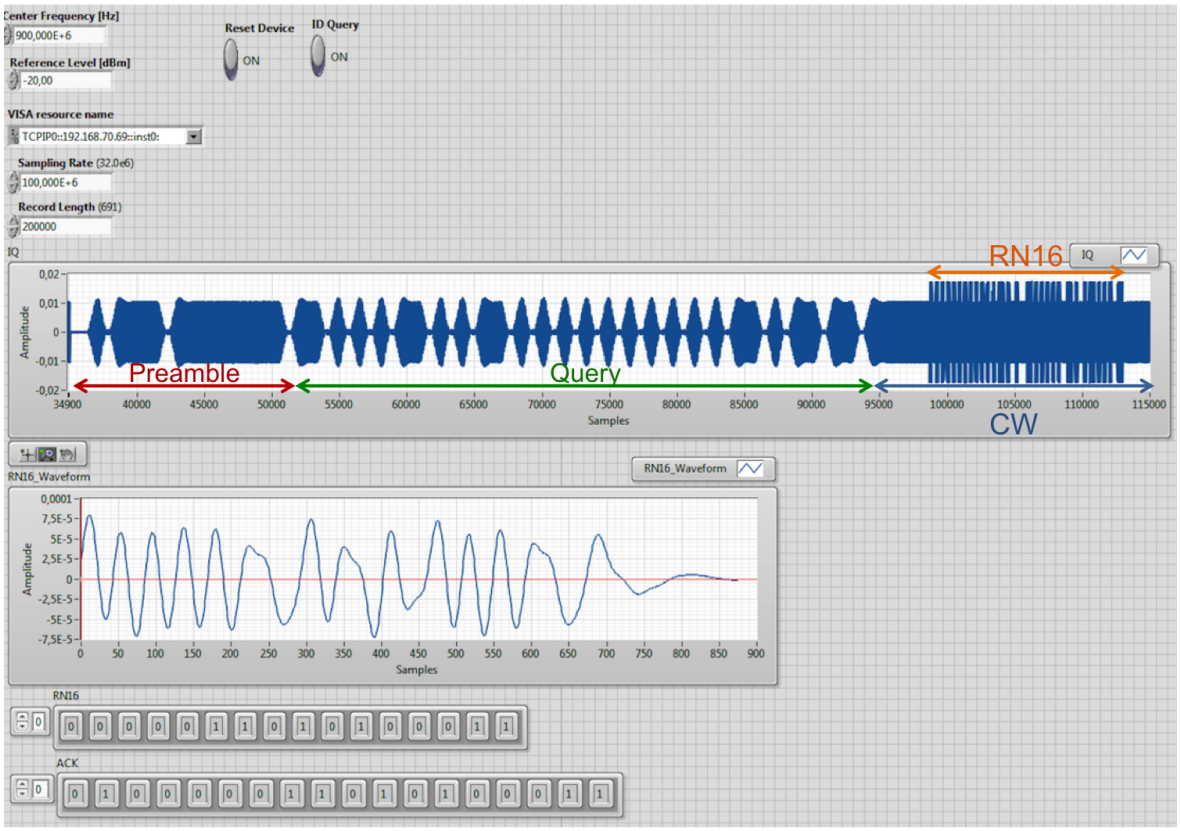

Figure 5.8: VSA user interface.

5.2.1 Distance Measures for Reader and Tag Communication

To measure the maximum distance and the minimum power which tag replies, two methods [Nik09] were used and block diagram presented in Figure 5.9. In first method is used a constant value of distance and the power is variable. In second method power is constant, but the distance to the tag is variable .

To apply these methods, the friis equations for free space propagation (5.1) and (5.2) are used. The relationship between these two equations gives the (5.3). In this equations, it is necessary to know the definition of some terms, Equivalent Isotropically Radiated Power (EIRP), the P_{tag} is the tag sensitivity, the λ is the wavelength, the r_{tag} is the tag maximum range, the P_{min} is the minimum power, the G_t is the gain transmitting antenna and the d is the distance to the tag.

$$P_{tag} = \text{EIRP}(\frac{\lambda}{4\pi r_{tag}})^2, \text{EIRP} = P_{reader} + G_t + CableLosses \tag{5.1}$$

$$P_{tag} = P_{min} G_t (\frac{\lambda}{4\pi d})^2 \tag{5.2}$$

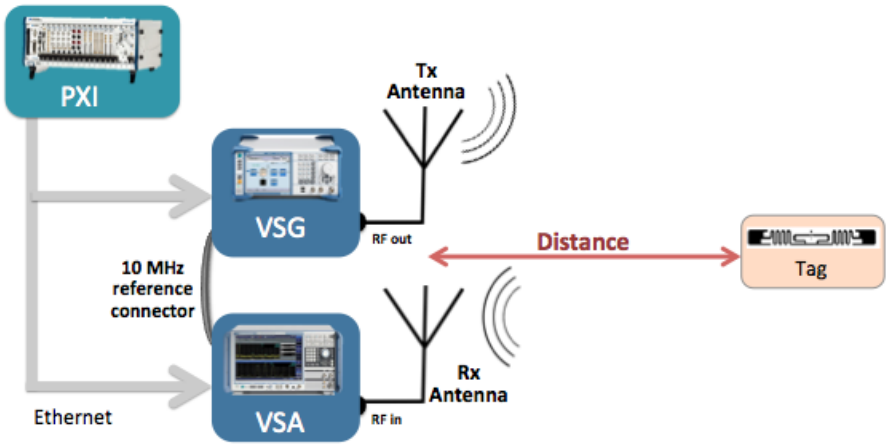

Figure 5.9: Measurement method to find the maximum distance and the minimum power which tag replies in stimulus-response architecture.

$$r_{tag} = d\sqrt{\frac{\text{EIRP}}{P_{min}G_t}} \tag{5.3}$$

These methods were used because they gives two important pieces of information, the minimum power needed for tag reply and the maximum distance that tag replies.

Before applying these methods, some measures were made and the results obtained for the Alien tag ,in Table 5.1, and for the ID Solutions tag, can be seen in Table 5.2. To obtain these results, a low power value was used and then was observed the maximum distance that tag replies. After that, the power value was increased in little steps until maximum power value of VSG and then was observed the maximum distance that can communicate with the tag, for each value of power. It is noted that a spectrum analyzer was used to verify the exact power value, for each case, and for this reason, was used the power values present in Tables 5.1 and 5.2. It should be noted too, that the same power values were used for both tags, because this way, the comparison between these two, can be seen more easily. Only the minimum power values which tag replies are different, and the maximum power values are equal for both tags, because it is the maximum power limit available by the equipment.

Power (dBm)	-12.4	-10.4	-10	-7.4	-6.1	-5.7	0.6	1.6	3.6	8.5
Distance (cm)	7.5	8.2	12.4	19	28	39	42	47	62	92

Table 5.1: Alien tag power and distance results for stimulus-response architecture.

Power (dBm)	-12.6	-10.4	-10	-7.4	-6.1	-5.7	0.6	1.6	3.6	8.5
Distance (cm)	7	8	12	17	20	31	40	45	67	90

Table 5.2: ID Solutions tag power and distance results for stimulus-response architecture.

Observing the results in Figure 5.10 it is possible to verify the influence of the increasing power in tag reply.

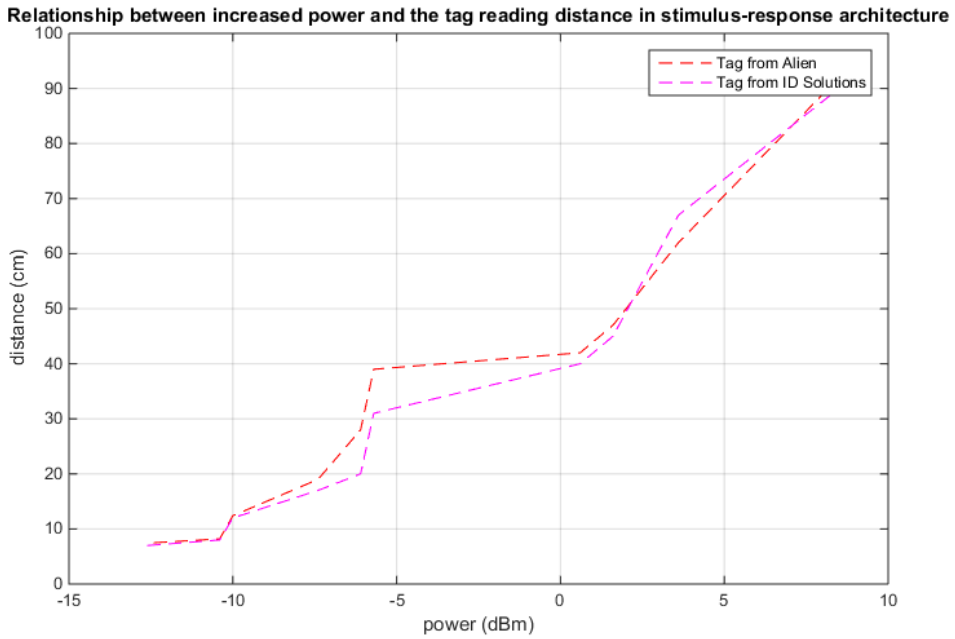

Figure 5.10: Relationship between increased power and the tag reading distance in stimulus-response architecture, for both tags.

After that, the tag sensitivity basis of (5.2) was calculated for both tags. The tag sensitivity values obtained and the values of each equation parameter are present in Table 5.3.

Tag	c (m/s)	Frequency (MHz)	G_t (dBi)	P_{reader} (dBm)	d (m)	P_{min} (dBm)	P_{tag} (dBm)
Alien	3.10^8	915	7	4.6	0.3	-5	-19.21
ID Solutions	3.10^8	915	7	4.6	0.3	-5.5	-19.71

Table 5.3: Tags results for fixed distance and variable power method for stimulus-response architecture.

Tag	Frequency (MHz)	Gt (dBi)	d_{max} (m)	EIRP (dBm)	P_{min} (dBm)	r_{tag} (m)
Alien	915	7	0.75	9.6119	1	1.80
ID Solutions	915	7	0.70	9.6119	1.2	1.78

Table 5.4: Tags results for fixed power and variable distance method for stimulus-response architecture.

It should be noted that these measurements were not made in anechoic chamber, as usual in these test scenarios because it was difficult to transfer all the equipments there. Comparing the tag sensitivity results for both tags (Alien: -19.21 dBm, ID Solutions: -19.71 dBm) in this architecture, with theoretical value (-20 dBm [Tec14c]), can be concluded that the results are very close to the theoretical value. Regarding maximum range obtained for both tags,

the practical value and the theoretical value have little difference (Alien: r_{tag}=1.80 m and d_{max}=0.75 m, ID Solutions: r_{tag}=1.78 m and d_{max}=0.750 m,). However, in these calculations the cable losses were not considered, which justifies these differences.

5.2.2 Short Architecture Conclusion

In fact, the stimulus-response architecture was not the best choice to implement the RFID reader, because the communication times between reader and tag were not accomplished. For this reason, only the first step of communication was completed. First, the Query command was sent from PXI, to the VSG. This initialization command starts the communication between reader and tag. After this command was sent, from PXI to VSG, in VSG it was necessary to select the file that contains this command. From that moment, it was esily realized that this step would be a big limitation to fulfill the times between the command sent from the reader to the tag, because the times are on the order of microseconds. The RN16 was obtained and decoded, hence the EPC would be decoded too, because the process is equal, however it was not possible to obtain the EPC because of the reasons explained before.

Nevertheless, as was explained in chapter 3, the first step of communication was completed, because, after sending a Query command to tag, the tag answered with RN16 command. This response command from tag, the RN16, was observed in PXI through communication with VSA. To obtain the VSA data, with tag response, it was necessary to make immediate capture from this equipment, and this control was made in PXI, through human control.

Thus, due to the fact that it is necessary to select, in VSG, the file which contains the commands to send to tag, and it is also necessary to control in PXI, the data from VSA, the time between the tag and the reader can not accomplished. This limitation can be overcome with a system where the transmission is made in real time without requiring human control during the whole communication.

Regarding tags, can be concluded that the measures to calculate the tag maximum range and the tag sensitivity went well, because the practical values were close to the theoretical values. The maximum distance was increased when the power value was increased.

However, with this architecture, it was proved that it is possible to send a Query and receive and decode the RN16 command from tag. So this architecture is possible to make RFID tag tests distances measurements(maximum distance and minimum power, which tag can reply), in laboratory, using this application in plataform PXI, and the only thing that it can not do is get the EPC.

5.3 Real-Time Interrogator Emulation Architecture Results

This architecture is easily built, because the RF modules are connected to the PXI chassi. Figure 5.11 shows the setup of this architecture.

As can be seen, this architecture is composed by the PXI, both RF modules (NI 5792 and NI 5793), the transmission and reception antennas and the tag. In Figure 5.12 shows the LabVIEW interface, and it is possible to observed the last part of the Query command, the continuous wave and the RN16 command, which is the tag reply. The RN16 decoding, the ACK command built and, at the end the sending of the ACK command can be seen.

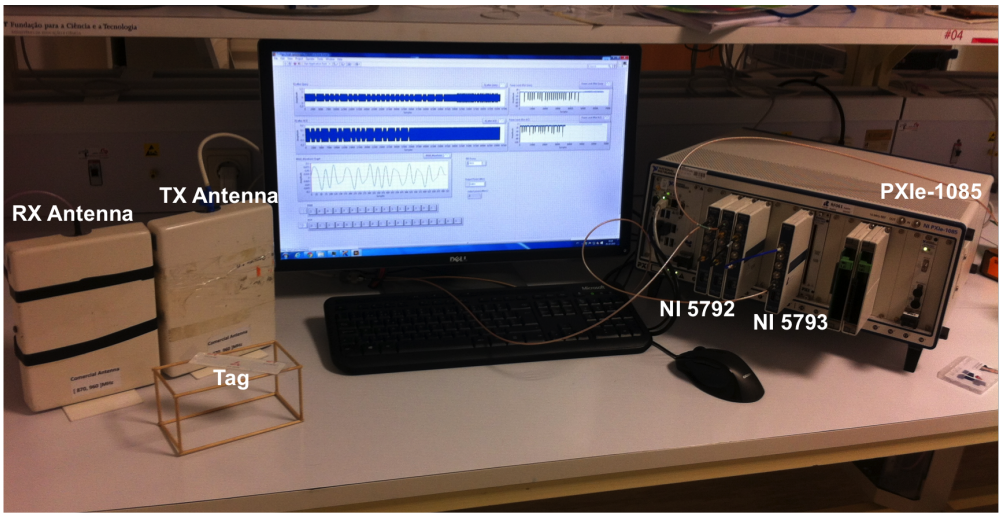

Figure 5.11: Real-time interrogator emulaton archictecture setup.

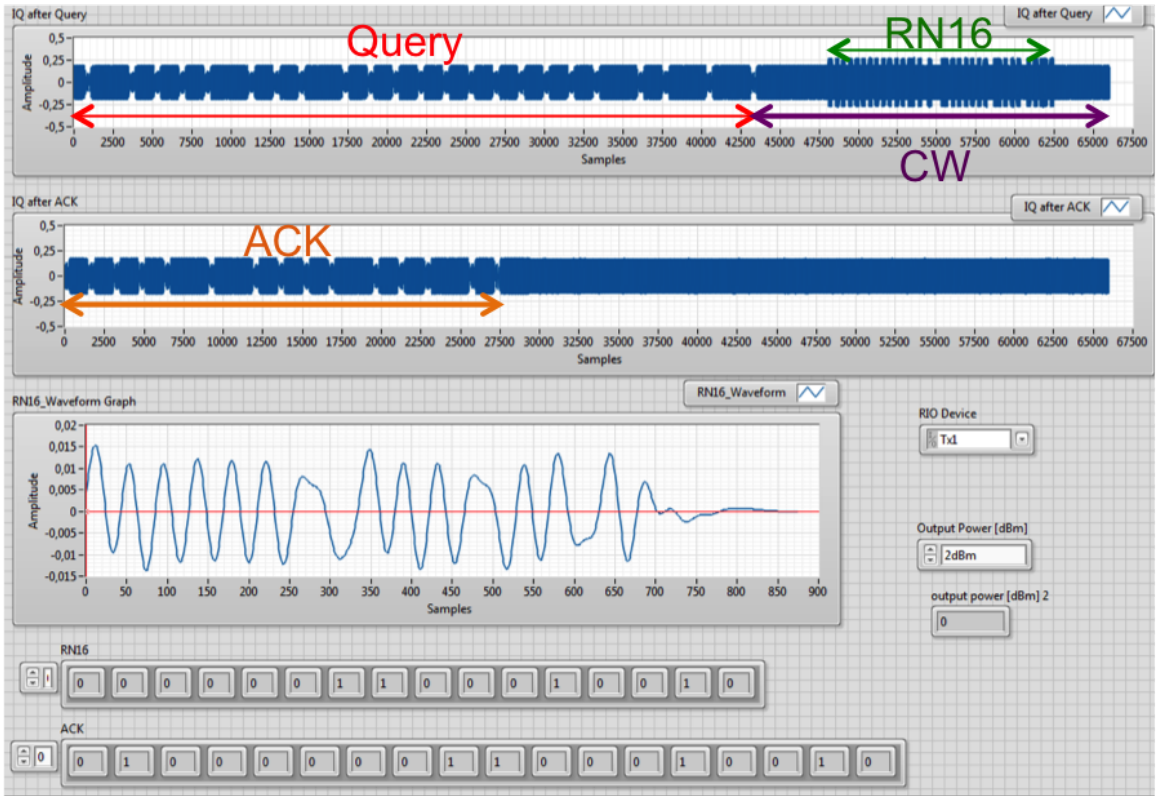

Figure 5.12: Real-time interrogator emulaton archictecture result.

5.3.1 Distance Measures for Reader and Tag Communication

In this architecture, the same measure method was used as the stimulus-response architecture to measure the minimum power and to find the maximum range which tag can reply. Figure 5.13 shows how this measurement method works in this architecture.

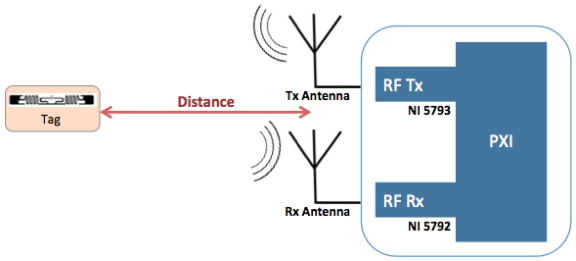

Figure 5.13: Measurement method to find the maximum distance and the minimum power which tag replies in real-time interrogator emulation architecture.

So, like in stimulus-response architecture, measures were made about maximum power and maximum range for both tags, which can be seen in Tables 5.5 and 5.6, and in Figure 5.14, the respective graph can be seen.

Power (dBm)	-10	-8	-4.8	-2.8	-1	-0.5	3.3	4.7	7.7	8.9
Distance (cm)	9.3	20	39	40	44	47	55	73	84	95

Table 5.5: Alien tag power and distance results for real-time interrogator emulation architecture.

Power (dBm)	-9.3	-8	-4.8	-2.8	-1	-0.5	3.3	4.7	7.7	8.9
Distance (cm)	10.5	25	35	39	45	49	61	72	85	108

Table 5.6: ID Solutions tag power and distance results for real-time interrogator emulation architecture.

The tag sensitivity and the maximum range were calculated in this architecture too, for both tags, using the same procedure. In Tables 5.7 and 5.8 results can be seen.

Tag	c (m/s)	Frequency (MHz)	G_t (dBi)	P_{reader} (dBm)	d (m)	P_{min} (dBm)	P_{tag} (dBm)
Alien	3.10^8	915	7	4.6	0.3	-5.4	-19.61
ID Solutions	3.10^8	915	7	4.6	0.3	-5.2	-19.41

Table 5.7: Tags results for fixed distance and variable power method for real-time interrogator emulation architecture.

Tag	Frequency (MHz)	Gt (dBi)	d_{max} (m)	EIRP (dBm)	P_{min} (dBm)	r_{tag} (m)
Alien	915	7	0.71	9.6119	-5.4	1.78
ID Solutions	915	7	0.7	9.6119	-5.2	1.72

Table 5.8: Tags results for fixed power and variable distance method for real-time interrogator emulation architecture.

It can be concluded that the practical values for tag sensitivity and for maximum range (Alien: -19.61 dBm, ID Solutions: -19.41 dBm) are very close to theoretical values (-20

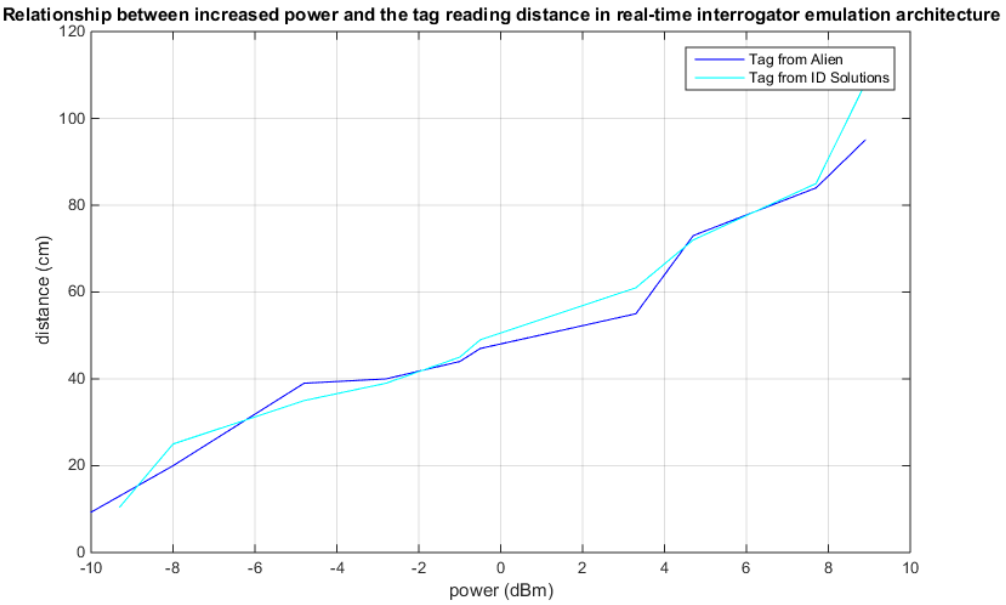

Figure 5.14: Relationship between increased power and the tag reading distance in real-time interrogator emulation architecture, for both tags.

---

dBm [Tec14c]), like in stimulus-response architecture. Once again, the cable losses were not take into account for these calculations, so the little difference in maximum range (Alien: r_{tag}=1.78 m and d_{max}=0.71 m, ID Solutions: r_{tag}=1.72 m and d_{max}=0.70 m,), can also be in principle justified by this fact.

5.3.2 Short Architecture Conclusion

In this architecture, the same limitation occurred, as mentioned before, because the time needed to send the data (commands) to FPGA is in milliseconds. So, the time in microseconds (T1 and T2) was expired and it was not possible to fulfil the entire protocol to obtain the EPC. Although, the RN16 command was obtained from tag, and this one was decoded. Thus, the same process to get and decode the RN16 command from tag is equal to get and the EPC from tag, and, this way, it can be concluded that only the T2 time was not fulfilled, in this architecture.

As was mentioned before, the FPGA processing was essential to fulfil the T2 time, but it was intended to prove that this time was not obtained mathematically. To conclude that the time to send data to FPGA is in milliseconds, some tests and calculation are made. First several tests were made to understand which is the right time to receive the data from RX module (NI 5792) and this way minimize the T2 time. Then, after understanding which is the right time to start the RX module capture, it was concluded that this time of capture is important to minimize the T2 time. Finally, the maximum T2 time (20Tpri) according to Table 2.17 and (2.3) was also calculated to verify that ACK command was not sent just in time. Table 5.9 shows the value of each parameter to calculate the T2 result.

Thus, the maximum time the tag to reply would be in 84.56 μs, which corresponds to 8456 samples. In Figure 5.12, it can be seen that to capture the entire RN16, many samples

TRcal (μs)	DR	BLF (MHz)	Tpri (μs)	T2 (μs)	T2 (Number of samples)
90.2	64/3	0.2365	4.228	84.56	8456

Table 5.9: T2 calculation.

are required to be captured. Even if (this test was made) the number of samples captured, by RX module, was minimized, it always required more or less 20000 samples. This way, it is not possible to decode the RN16, create the ACK command, send again through the TX module (NI 5793) and capture by RX module, in less than 8456 samples. The objective of this calculation is to explain that even if all decoding code was optimized, the limitation time is already overtaken by FPGA capture in RX module and in sending data in TX module.

It can be concluded that the results obtained have good distance values, as well as, good power values. In tags results, the conclusion is that the practical and theoretical value are very close, so the measures results went well.

However, as was presented, the RN16 command was obtained from tag. So with this architecture it is possible to have a LabVIEW application, which allows RFID tags tests and measures, to obtain the maximum distance and the minimum power, which the tag can give. In this regard, the tag tests and measures results were presented, according to this architecture.

To summarize, it can be said that this architecture presents a good behavior for an application which provides tag tests and measure, with a simple setup and it is user-friendly.

5.4 Comparison Between Stimulus-Response and Real-Time Interrogator Emulation Architectures

A comparison between two architectures was made to have an overview about system performance. Table5.10 shows the tags results for both architectures. As can be seen in Figure5.10 the behavior of tags in both architectures are very close.

Stimulus-response architecture	Alien	Power (dBm)	-12.4	-10.4	-10	-7.4	-6.1	-5.7	0.6	1.6	3.6	8.5
		Distance (cm)	7.5	8.2	12.4	19	28	39	42	47	62	92
	ID Solutions	Power (dBm)	-12.6	-10.4	-10	-7.4	-6.1	-5.7	0.6	1.6	3.6	8.5
		Distance (cm)	7	8	12	17	20	31	40	45	67	90
Real-time interrogator emulation architecture	Alien	Power (dBm)	-10	-8	-4.8	-2.8	-1	-0.5	3.3	4.7	7.7	8.9
		Distance (cm)	9.3	20	39	40	44	47	55	73	84	95
	ID Solutions	Power (dBm)	-9.3	-8	-4.8	-2.8	-1	-0.5	3.3	4.7	7.7	8.9
		Distance (cm)	10.5	25	35	39	45	49	61	72	85	108

Table 5.10: Comparision between tags results in stimulus-response and real-time interrogator emulation architectures.

Comparing the tags sensivity results for both architectures can be said that the results are very closely, as can be seen in Table 5.11 and the conclusion it is that both architectures

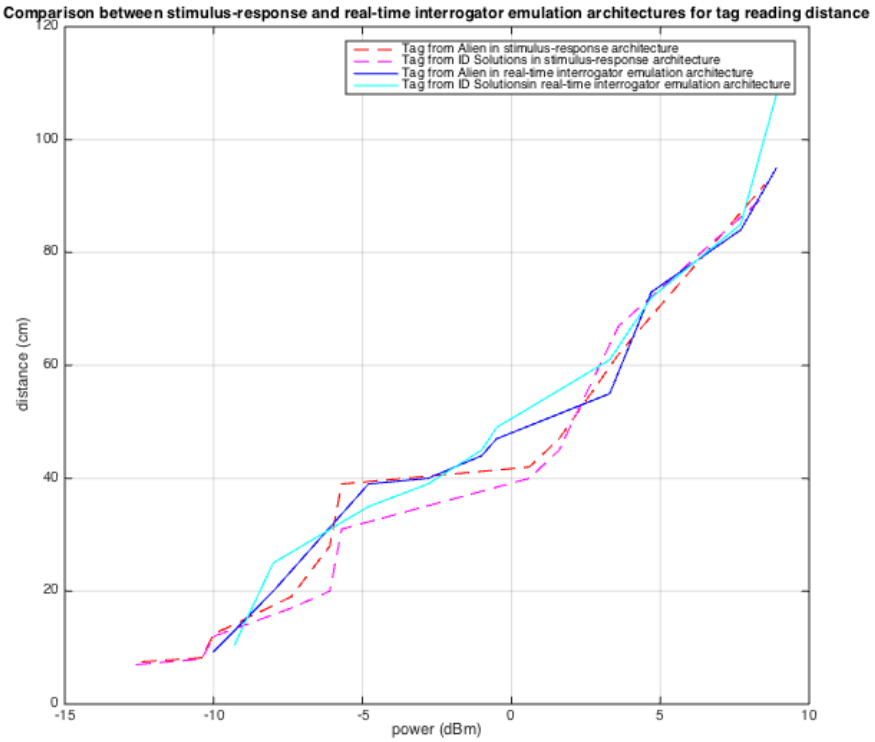

Figure 5.15: Comparison between stimulus-response and real-time interrogator emulation architecture for tag reading distance.

Stimulus-response architecture	Alien	P_{tag} (dBm)	-19.21	d_{max} (m)	0.75	r_{tag} (m)	1.80
	ID Solutions	P_{tag} (dBm)	-19.71	d_{max} (m)	0.70	r_{tag} (m)	1.78
Real-time interrogator emulation architecture	Alien	P_{tag} (dBm)	-19.61	d_{max} (m)	0.71	r_{tag} (m)	1.78
	ID Solutions	P_{tag} (dBm)	-19.41	d_{max} (m)	0.70	r_{tag} (m)	1.71

Table 5.11: Tags sensivity and maximum range obtained results for both architectures.

have similar performance.

Considering the dissertation objectives, in both architectures were accomplished. Although, as was mentioned before, only the EPC was not obtained in both architectures. Comparing these two architectures, the real-time interrogator emulation has better behavior, because has not the file limitation (as explained before) as stimulus-response architectures has, which makes this architecture more useful for measurement and tests in laboratory.

5.5 Power Transmit Mask

It was established to fulfill a mask of dense-interrogator environment. So, to prove that, this milestone was fullfiel, a spectrum analyzer was used. In Figure 5.16, the result of this measure can be seen, although the theorical limits appear in red and the practical results in white.

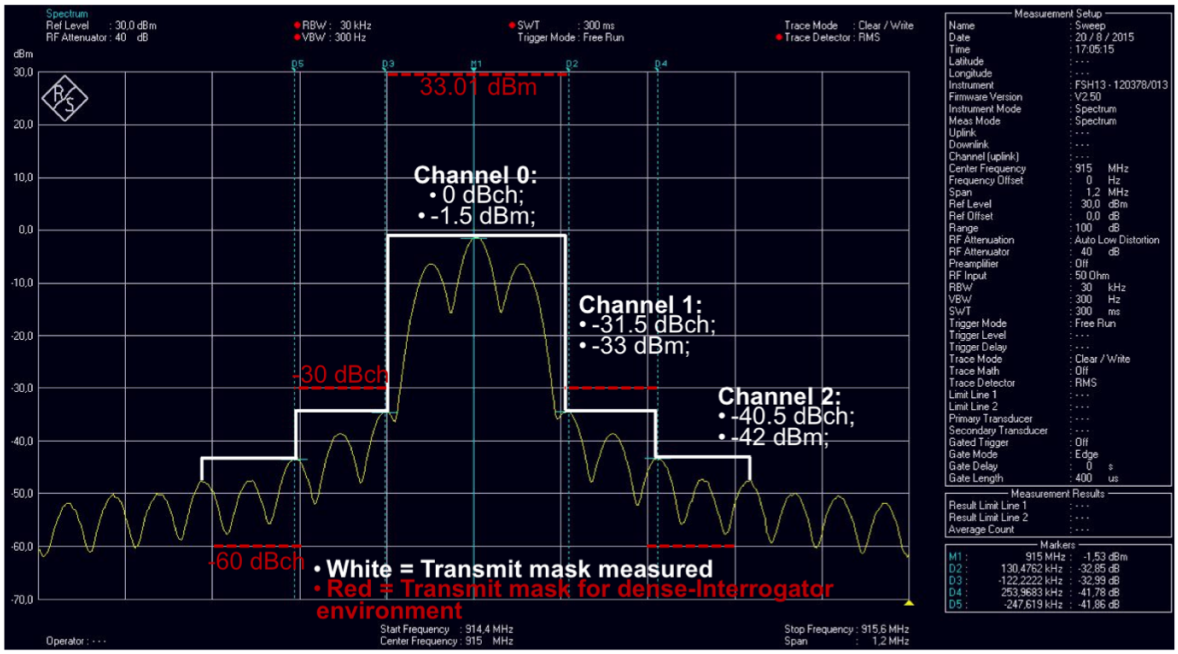

Figure 5.16: Power transmission mask fulfilled.

Looking at Figure 5.16, and analyzing it, the conclusion is that the sign is below of maximum limit of 33.01 dBm, and in the second channel the sign is below the maximum limit of 30 dBch. In Figure 5.17 it can be seen that bandwidth of the transmission channels was also fulfilled, because the theorical value is 500 kHz and a distance of 222.3 kHz was obtained.

Only in channel 2, the maximum limit was exceeded. However, when this limitation was noted, it was attempted to get a better filter to improve this condition. Although, after many tries, the conclusion was that if other filters were used, other parameters would be exceeded. Nonetheless, the decision was to used this filter, because in all other filters scenarios, this filter had the best behavior.

To conclude, in both architectures, the power maks was fulfilled.

5.6 Application Use Case (Spectrum Analyzer) Results

The spectrum analyzer and spectrogram application system has a very simple setup, which just contains the receiving antenna, connected to the NI 5792, and the PXI platform. The setup can be seen in Figure 5.18.

To test the system, an extra antenna was required to send a signal. This antenna was connected to VSG and transmitted an RFID signal at 915 MHz. Then, the spectrum analyzer application was started and the spectrum behaviors around the band of interest have

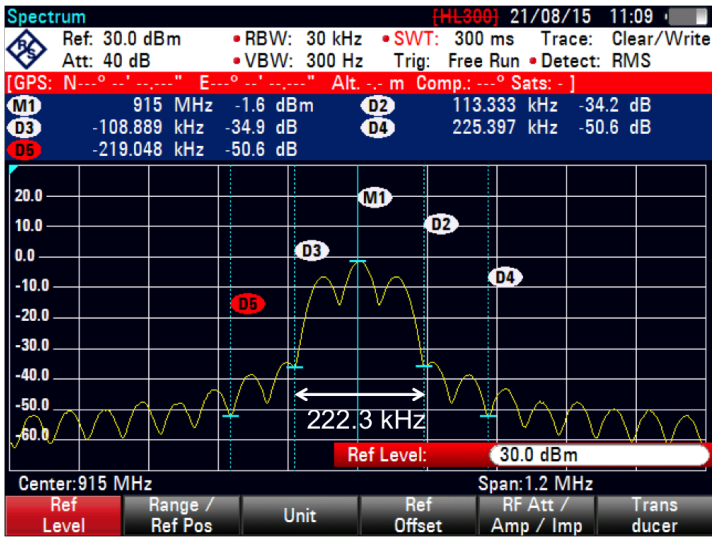

Figure 5.17: Power transmission mask bandwidth.

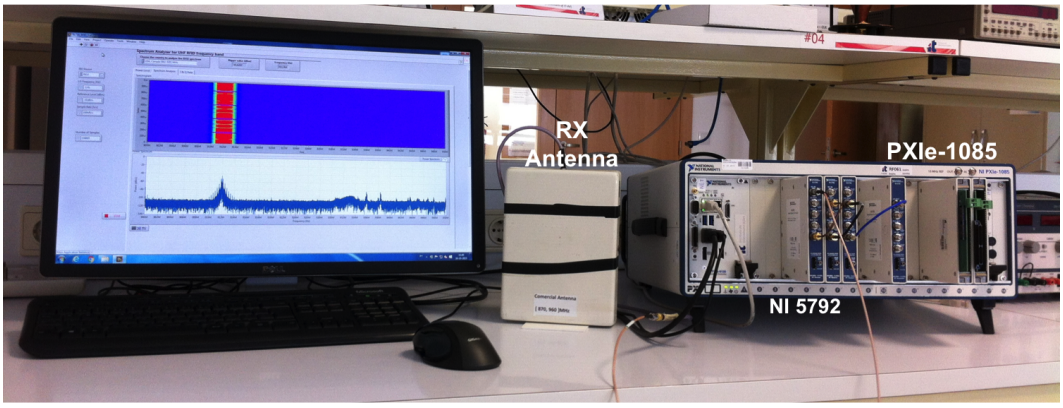

Figure 5.18: Setup of spectrum analyzer and spectrogram application system.

---

been analyzed. It is possible to observe, in Figure 5.19, the result of the real-time captured spectrum behavior (signal at 915 MHz, like it was expected), in power spectrum graph and in spectrogram form.

As was mentioned before, this application was made to choose the UHF RFID frequency band in worldwide, so the user interface has the list of each UHF RFID frequency band to be chosen, for each case that the user wants, and it can be seen in Figure 5.20. After detecting the signal, a test was made to calculate the maximum range that this application can read a signal, and the maximum value obtained was 21.2 meters.

In summary, this application was well implemented, having an user-friendly interface and a simple setup, it is possible to see the UHF RFID signals in power spectrum and spectrogram for a significant distance.

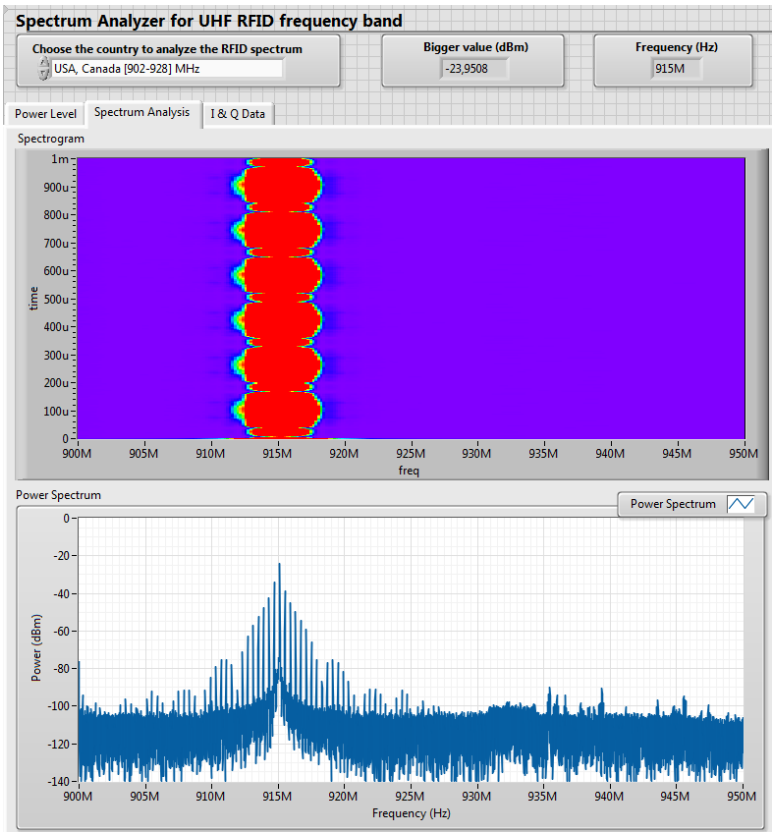

Figure 5.19: Power spectrum and spectrogram display result.

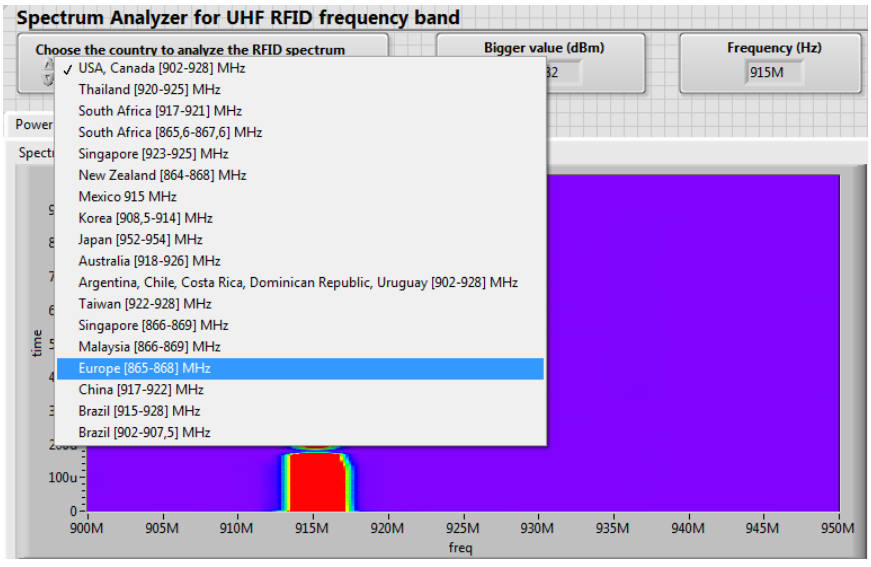

Figure 5.20: User interface of spectrum analyzer and spectrogram application.

5.7 RF-DC measurement system

The RF-DC measurement system has a simple setup too. Figure 5.21 shows the setup of this system. A RF-DC circuit [Bel14] was connected to test the system. In order to understand the behavior of this system the results were compared with the experimental results in [Bel14], which can be seen in Figures 5.22 and 5.23. Table 5.12 shows the results in detailed.

It can be concluded that the results obtained were very similar.

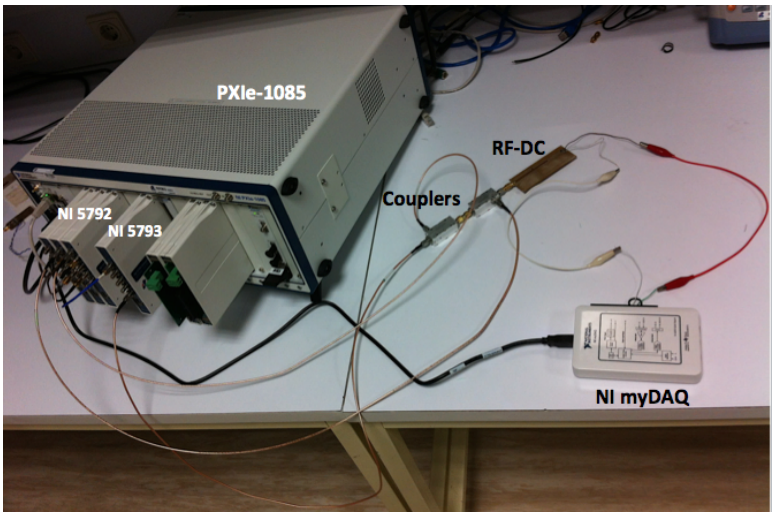

Figure 5.21: Setup of RF-DC measurement system.

	Frequency (MHz)	P_{in} (dBm)	Vout (V)	S_{11}	Efficiency (%)
RF-DC Measurement System Results	939	-10	0.52	-10.38	9.10
Experimental Results in [Bel14]	939	-10	0.53	-10.75	11.2
RF-DC Measurement System Results	1878	-10	0.48	-28.09	6.7
Experimental Results in [Bel14]	1878	-10	0.49	-10.39	5.9

Table 5.12: Comparison results between RF-DC measurement system and experimental results in [Bel14].

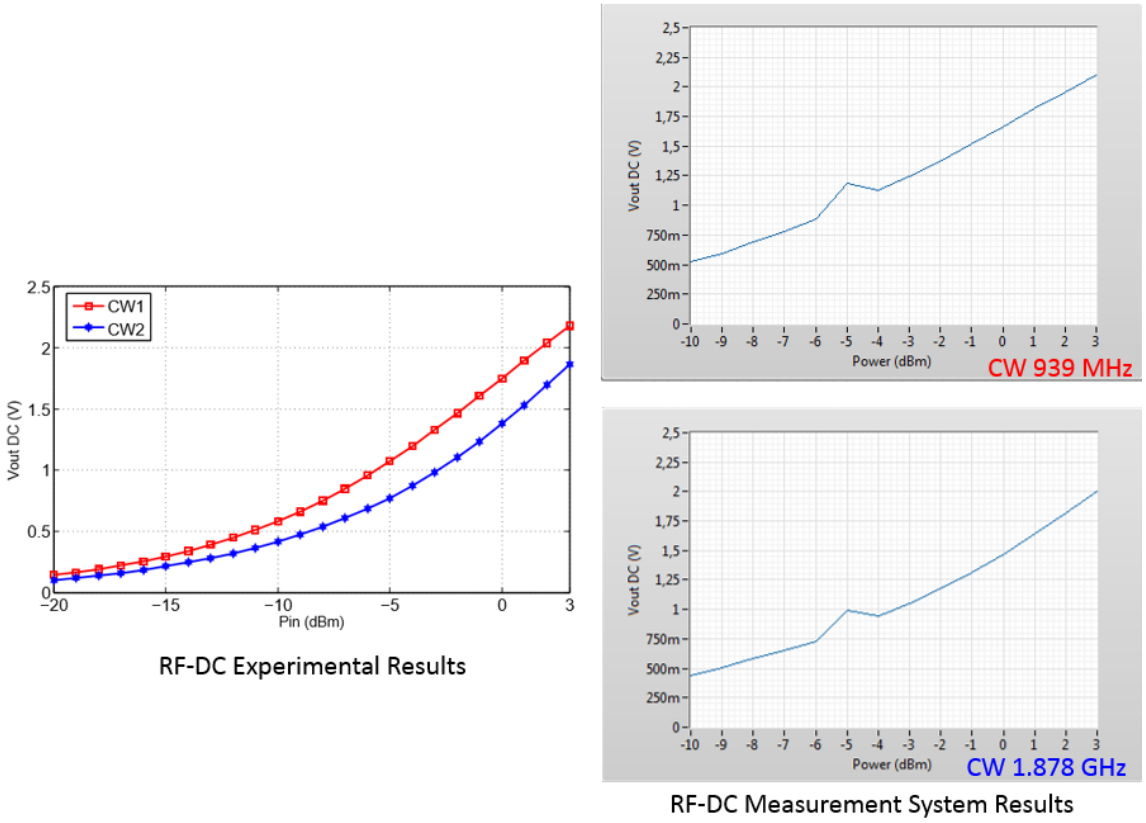

Figure 5.22: Comparison between RF-DC measurement system results and experimental results in [Bel14] for Vout values.

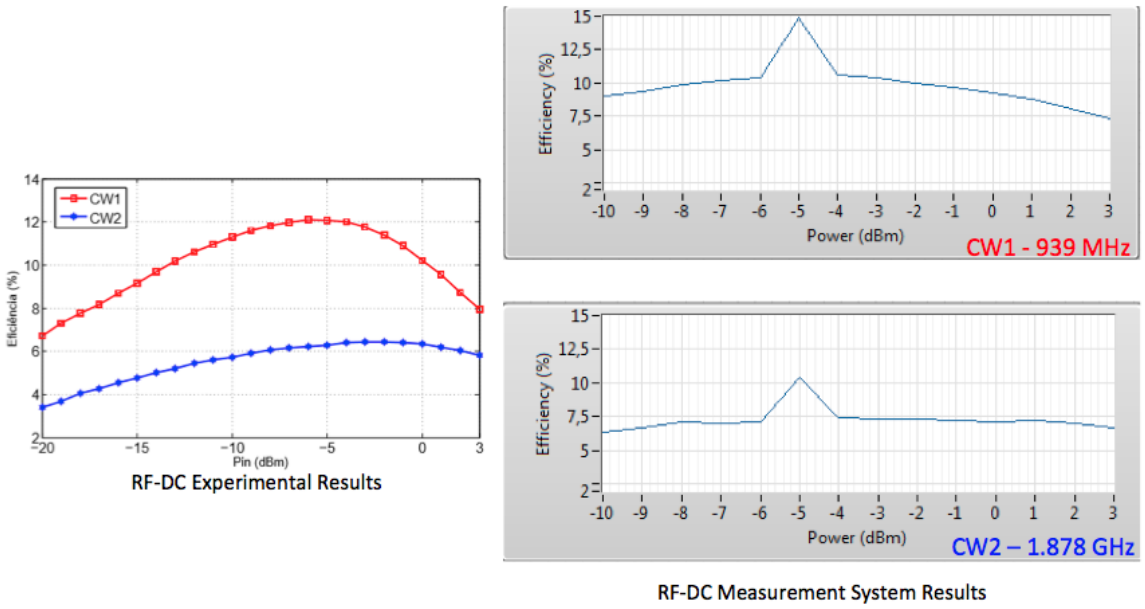

Figure 5.23: Comparison between RF-DC measurement system results and experimental results in [Bel14]I for efficiency values.

Chapter 6

Conclusions and Future Work

6.1 Conclusion

The main objectives defined for this dissertation were clearly achieved. The system allowed to test tag functionality, in both architectures. Not only the maximum distance that the tag can reply, but also the minimum power needed for tag reply was achieved, also in both architectures and the tags result obtained for both architectures were similar. The power spectrum and spectrogram application was well implemented, giving a great overview of the UHF RFID spectrum and it was a useful application case of the RFID reader.

Regarding RFID reader, it can be stated that the only thing that missed in the system was to get the tag EPC, because all steps in RFID reader were well implemented, besides this one. As was mentioned before, these steps were not achieved in both architectures. The reason why this did not occur in stimulus-response architecture is because it is necessary in VSG to select the files, and, obviously, the time limit of tag reply is exceeded. The same limitation occured in real-time interrogator emulation architecture, because the time to send and process the data to FPGA is bigger than the maximum time that tag can wait to reply.

Although not having achieved the expected results in stimulus-response architecture, since there was a fail to fulfill the communication time between the tag and the reader, it was tried to overcome this difficulty looking for other architecture, the real-time interrogator emulation architecture. However, as mentioned, the same limitation occurs, but due to another reason. It can be concluded that the big advantage of real-time interrogator emulation architecture, comparing to the stimulus-response architecture is the fact of this architecture having the RF modules connected to the PXI, which makes this system easier to interact and to process with tag.

With regard to RFID reader, the conclusion is that the system specifications and all the system steps were accomplished, since the power mask was fulfilled, the tag replied with a RN16 and the system decodes the RN16 command.

Finally, the RF-DC measurement system gave some important parameters values about RF-DC circuits to improve their efficiency, as was expected, but a calibration method is required to improve the system.

6.2 Future Work

For future work, it is important to try to explore a way to put the file sent by PXI for VSG without requiring human control. Thus, the limitation of time communication commands, between the reader and tag, is outdated.

In the end of this dissertation, a little bit about PXI FPGA was explored, in order to understand how it works. Nevertheless, more time is required to understand efficiently how PXI FPGA works. This possibility was studied, because it is believed that processing the data in FPGA the time limitation is overdue.

Regarding power spectrum and spectrogram application, these could be tremendous assets adding to a persistent chart because the preservious version is preserved and, this way, more information is given to the user.

The RF-DC measurement system will be optimized, using a rigorous calibration method, because it is one of the following research steps.

Appendices

Appendix A

Article for CONFTELE 2015, 10^{th} Telecommunications Conference

RFID Characterization System based on LabVIEW

M. Jordão, D. Ribeiro, P.M. Cruz, N.B. Carvalho
Instituto de Telecomunicações, Departamento de Eletrónica, Telecomunicações e Informática
Universidade de Aveiro, Campus Universitário de Santiago
Aveiro 3810-193, Portugal
marinajordao@ua.pt

Abstract— **This paper describes a RFID characterization approach using LabVIEW. The work is focused on RFID characterization, wireless power transmission and electromagnetic energy harvesting applications. The use of PXI module and the implementation of a LabVIEW code for mixed-domain (RF and DC) characterization and modeling is presented.**

Keywords—Mixed-domain; PXI; LabVIEW; RFID; Wireless Power Transmission; Energy Harvesting; RF-DC;

I. INTRODUCTION

[1] A characterization approach based on specific PXI instrumentation is developed using measurement solutions for RFID, RF-DC converters, and so on. These test and measurement solutions are important to guarantee the optimization of circuits, mainly when the energy efficiency is to be maximized, being such a key point in wireless power transmission and electromagnetic energy harvesting. A mixed-domain measurement test bench was developed, which combines synchronous measurements of radio-frequency (RF) and DC ports. In order to use these characterization systems in useful applications the first development was to apply it to RFID (radio-frequency identification) circuits. In this sense, the excitation of an RFID tag should be done following a convenient protocol. This is why the first approach was to design an RFID reader that could be embedded into the characterization instrument. For this purpose, an RFID reader and the respective LabVIEW code has been developed, in order to demonstrate the applicability of modular instrument. Two architectures have been implemented, one based on a stimulus-response strategy and another for a real-time interrogator emulation [1].

The RFID reader uses International Standards Organization (ISO) 18000-6C RFID communication protocol [2], which operates in the 860-960 MHz frequency range. In downlink is used Pulse Interval Encoding (PIE) encoding with the On/Off Key (OOK) modulation. In the uplink it is used Bi-phase space (FM0) coding.

II. AUTOMATED RFID READER BLOCKS

In order to explain the overall implemented system we will describe each sub-system individually.

[1] This work is funded by National Funds through FCT – Fundação para a ciência e a Tecnologia under the project PEst-OE/EEI/LA0008/2013; UID/EEA/50008/2013 and by Instituto Telecomunicações under project CREaTION (ref. EXCL/EEITEL/0067/2012)

A. PXI platform

The PXI platform from National instruments (NI) is a robust computer with high performance. This system is designed to provide reliable and easily configurable measurements solutions. The system used in our lab uses a pack of software and capturing and generator RF signals that makes it suitable for the proposed RFID characterization system development. Fig. 1 presents such a platform.

Figure 1. PXI platform

The LabVIEW programing is a graphical programming developed by NI. It was used in this development because of its simplicity and compability with most of the selected sub-systems. LabVIEW language follows a data flow model, which makes it very functional for data acquisition and handling of information.

B. RFID Tag (DUT)

Radio-frequency identification (RFID), is a technology that uses RF signals for identification purposes. This identification method allows to store a serial number that identifies a person, object or another type of information within the tag. The RF waveform approach followed used a backscatter solution where the RF signal transmmited by the "reader" is modulated in amplitude and received back for demodulation. In order to implement such a "reader" a waveform design should be made according to the RFID protocol, [2].

C. Receiver and Transmitter Front-ends

The PXI platform has the ability to add different types of front-ends to work like receivers and transmitters and has the possibility of processing the data with FPGAs. To demonstrate the extent of the test system was used the external VSG and VSA connected (via Ethernet) to the PXI. Thus, it was used the VSG and VSA in a stimulus-response architecture to implement the RFID reader.

For the real-time emulation architecture two modules from

NI, NI 5792 and NI 5793 have been employed. The NI 5792 and NI 5793 are a RF receiver and transmitter, respectively, adapter modules, which are designed to connect to the PXI platform. These modules are internally connected to a FlexRIO FPGA module.

III. RFID READER

As mentioned before, it was implemented two different architectures. It is proposed to build an RFID reader for the Ultra High Frequency (UHF) range between 902-928 MHz (used in the United States of America) and in a dense-interrogator environment. This choice was made because two reasons. First, because it is more difficult to fulfill the system specifications with adjacent channels, in comparison with channels separated by 600 kHz, as in the case of the European UHF RFID range. Secondly, because it is more challenging to fulfill the power mask of the dense-interrogator environment, than a single-interrogator environment, it is only necessary to develop stipulated standards by regulators, or then, multiple-interrogator environment, in which the readers occupy just some of the channels. Figure 2 shows the RFID reader block diagram.

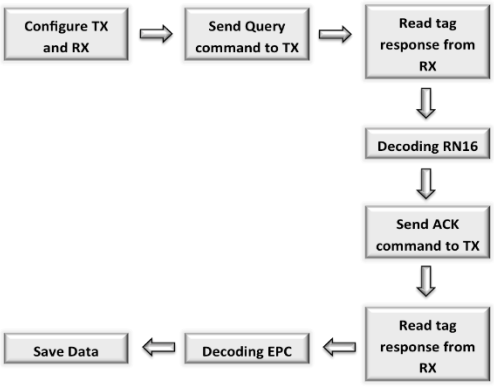

Figure 2. RFID reader block diagram

The communication between the reader and the tag should fulfil a group of several commands imposed by the standard. In Figure 3, it can be observed an example for a complete reader sequence and tag reply. The RFID reader sets the data rate by means of the preamble command that initiates the communication between the reader and the tag.

The encoding of information that goes from the reader to the tag is made up of two symbols, the data 0 and data 1. These symbols are obtained by PIE encoding, and the Type A Reference Interval (*Tari*) value can change between 6.25 us and 25 us. The *Tari* number is a time interval for data-0 in Interrogator-to-Tag signalling. Communication between the reader and the tag is initiated by a preamble followed by a query command. Figure 4 shows the detailed composition of the preamble sequence.

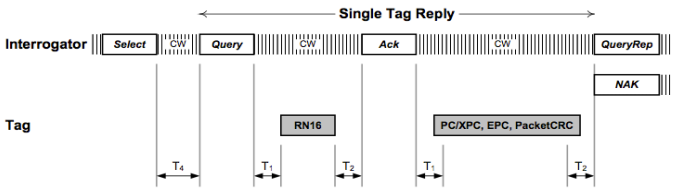

Figure 3. Commands sequence between the reader and the tag

Figure 5 shows the construction of the preamble in LabVIEW. The preamble command is just one of several other commends necessary for the RFID testing and identification, which have been created in the implemented PXI platform.

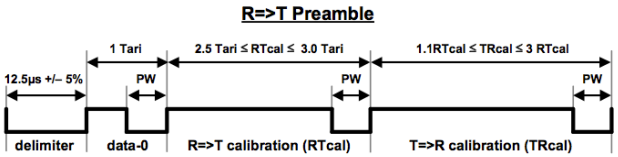

Figure 4. Frame Preamble scheme

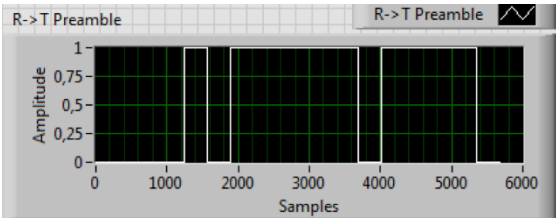

Figure 5. Frame Preamble scheme results in LabVIEW

A. *Stimulus-Response Architecture*

To develop an RFID reader, using LabVIEW programing, the first approach followed the stimulus-response architecture.

In such an architecture, the VSG (acting as reader transmitter) interrogates the tag with a "query" command, and, in parallel, sends a digital marker to trigger the VSA (acting as reader receiver). This way, the VSA captures the signal replied back by the tag and process the information in the PXI processor (host computer). It has been chosen as a first approach because it is easy to implement.

Figure 6 shows a simple block diagram of the RFID reader in a stimulus-response architecture.

In fact, this architecture was not the best choice to implement the RFID reader, mainly because the communication time between reader and tag cannot be accomplished. Due to this reason, only the first step of communication has been completed. Firstly, the PXI (host computer) configures the VSG to send a "query" command. This command starts the real communication between reader and tag. After some specific tests, we noticed that this kind of implementation will pose several limitations to fulfill the necessary timing between the commands to be exchanged between reader and tag, because the times were in the order of milliseconds, while the time slot to be accomplished according to the standard should be in the order of few microseconds.

Anyway, the first step of communication was completed, since after sending the "query" command to tag, it has replied

with RN16 command, as expected. This replying command from tag (RN16) was received in the VSA (emulating reader receiver) and processed in the PXI host computer. After these steps, the RN16 received data should be processed in the host computer and sent back to the tag as an "acknowledge" command. It is exactly in this point where the RFID standard is jeopardize, because the timing responses have been completely violated.

To overcome this failure in the implemented stimulus-response architecture, it would be required a system that can process the data in real-time without any human control in the middle of the commands set. However, this real-time implementation is not possible to be realized in this architecture, but it was tested and validated the first set of reader commands and associated tag replies.

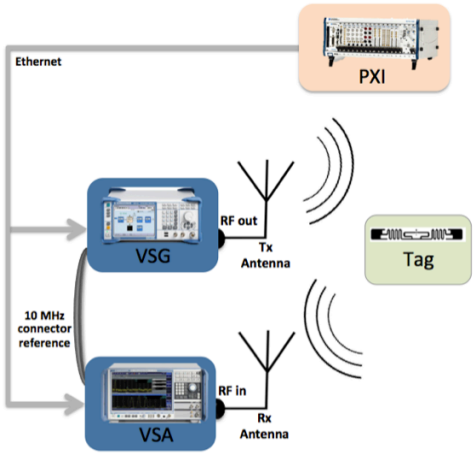

Figure 6. Stimulus-response architecture

B. *Real-Time Interrogator Emulation Architecture*

Since with the previous stimulus-response architecture it was not possible to fulfill the communication timings between reader and tag, it was necessary to study and evaluate other alternatives. The option that has been though considered different transmitter and receiver RF front-ends, which allow sending commands between reader and tag in an almost real-time condition. Therefore, it was decided to implement the new version of the RFID reader system with the FPGA-based RF front-end modules existent in the available PXI platform, see Fig. 1. This way we have used a FlexRIO module (NI-5793) for the transmitter and the module NI-5792 for the receiver, and both connected to the FPGA boards inserted in the PXI chassis. The NI-5792 and NI-5793, RF receiver and transmitter, respectively, are both adapter modules designed to work in FPGA module. Thereby, it was chosen the real-time interrogator emulation architecture to the RFID reader system.

Figure 7 shows the real-time interrogator emulation architecture. The reason to choose such an architecture is because the RF modules are connected to FPGAs, and in this way, being able to decode and retransmit the required commands within several microseconds. It was verified that some of the limitations of the previous architecture have been overtaken in the current real-time interrogator implementation.

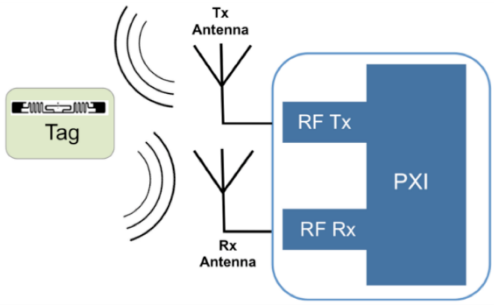

Figure 7. Real-Time Interrogator Emulation architecture

Nevertheless, there were some additional issues found in the proposed architecture that also preclude the imposeed severe timings between commands. The main reason for that to happen will be discussed in the next section .

IV. RESULTS

To validate the RFID characterization system it was necessary to test all the individual blocks parts of the reader and tag communication. The main specifications to be accomplished by the RFID reader are in depicted Table 1.

Table 1. RFID reader specifications

Reader carrier frequency	915 MHz
Bandwidth of the transmission channel	500 kHz
Distance between channels	None, because the transmission channels are adjacent
Maximum output power	4 W - Effective Isotropic Radiated Power (EIRP)
Delta frequency	1 MHz
Environment	Dense-Interrogator
Modulation	OOK
Encoding	PIE
Coding	FM0

A. *Transmission Validation*

First, it was built the baseband signal of "query" command. Then, it was checked whether the duration of this command was valid or not, and if the tag replied to this command with RN16 code. Figure 8 shows the tag response (RN16), after sending a "query" command.

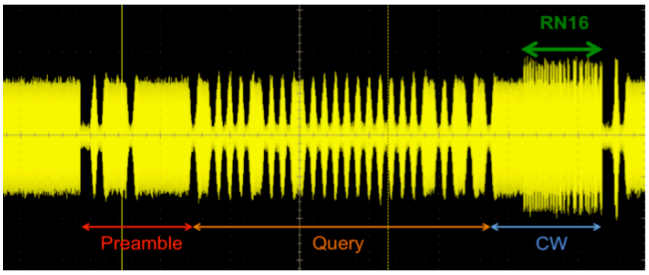

Figure 8. Real-time interrogator reader and tag commands exchange

B. Power Transmission Mask

It was necessary to then verify the power of transmission mask in a dense-interrogator environment can be fulfilled or not. To make this assessment there was the need to use a low-pass filter in the transmitter chain. Figure 9 shows the power mask results. The transmitted signal is between the transmission channel bandwidth (maximum frequency is 500 kHz). The transmitted signal is below the allowed power limit of 2 Watt as imposed by the national regulator (ANACOM). The transmitted signal respects the attenuation imposed by protocol.

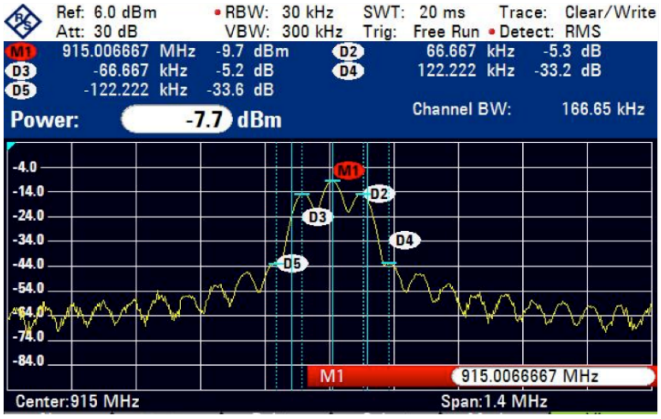

Figure 9. Power Mask

C. Reception Validation

To carry out the decoding of the received information from the tag it was necessary to obtain the signal envelope by doing the square of the signal, pass in a low-pass filter, then decimate and a high-pass filter, check [3] for more details. As mentioned, the square of the signal followed by a low-pass filter to remove higher frequency components returns the signal envelope. Then, the signal is decimated by a factor of 10, to reduce the number of samples to process, and finally, the high-pass filter was implemented to remove the DC component, since we are only interested in the few MHz components. After that, to detect the RN16, an autocorrelation function was employed. The autocorrelation can detect the sequence that is intended through the comparison with a sequence already known. Figure 10 shows all system working flow. It is possible to observe the "query" command, the RN16 reply from the tag and the "ACK" command created at the reader by decoding the RN16 received data. However, it was not possible to obtain the EPC tag (ID). The reason for this to happen in the real-time interrogator emulation architecture, is due to the fact that the time required to extract samples for decoding the RN16 exceeds the maximum time that the tag will wait for an "ACK" command. So, even if the RN16 decoding algorithm is optimized, due to this limitation, it is impossible to put the system to operate without using the processing of the information in a real-time manner, [4]. For instance, implementing all these coding and decoding loops inside one of the FPGA blocks available in the PXI platform, but this is out of the scope of the current work.

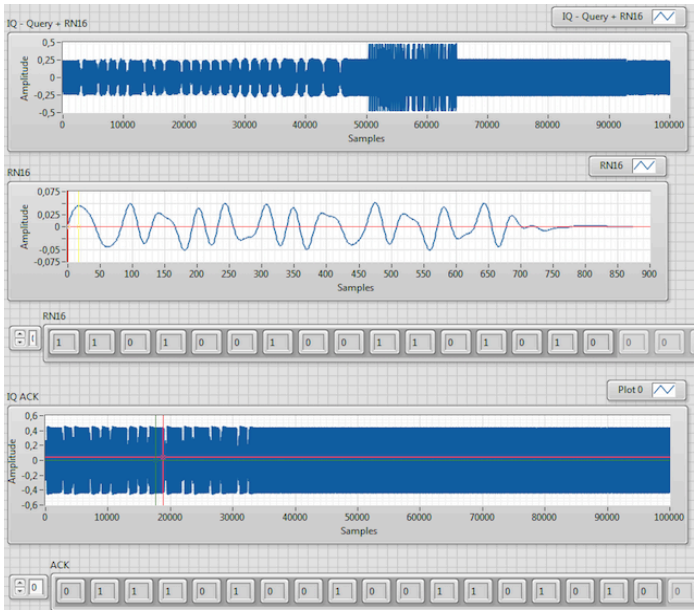

Figure 10. Query command, RN 16 tag reply and ACK command

D. Maximmum system range

After performing some measurements, it was concluded that the system responds to a minimum power of -9 dBm for a fixed distance of 5.5 cm. For a maximum power of 30 dBm (1 Watt) the system can respond up to an average distance of 93 cm.

The RFID reader is capable to work in different carrier frequency to be defined/changed by the user.

V. CONCLUSIONS

The LabVIEW-based RFID reader developed in this paper was step forward in the design of mixed-domain (RF-to-DC) characterization tools. This system will be the key sub-system of a complete mixed-signal multi-domain characterization solution. The big difficulty in this work was to try to overcome the very severe timing limits defined in the RFID standard for the reader data processing and respective tag replies. Future work includes developing and improving the proposed RFID characterization system in the NI LabVIEW Real-Time Module.

REFERENCES

[1] National Instruments, "Advanced RFID Measurements: Basic Theory to Protocol Conformance Test " in IEEE Transactions on Industrial Electronics, Dez. 19, 2013

[2] EPC™ Radio-Frequency Identification Protocols Identity Protocols Generation-2 UHF RFID Protocol for Communications at 860 MHz – 960 MHz Version 2.0.1, EPCglobal Inc., Apr-2015.

[3] João Santos. RFID para a gama UHF baseado em Software-Defined Radio. Master's thesis, Departamento de Eletrónica, Telecomunicacões e Informática. Universidade de Aveiro, 2014.

[4] Pavel V. Nikitin, V. Seshagiri Rao, "LabVIEW-Based UHF RFID Tag Test and Measurement," *IEEE Transactions on Industrial Electronics*, vol. 56, no. 7, pp. 2374-2381, July 2009.

Appendix B

Poster for CONFTELE 2015, 10^{th} Telecommunications Conference

RFID Characterization System based on LabVIEW

Marina Jordão, Diogo Ribeiro, Pedro Cruz and Nuno B. Carvalho

Departamento de Eletrónica, Telecomunicações e Informática, Instituto de Telecomunicações, Universidade de Aveiro, Aveiro, Portugal

Abstract

This poster describes an RFID characterization approach using LabVIEW. The work is focused on RFID characterization, wireless power transmission and electromagnetic energy harvesting applications. The use of PXI module and the implementation of a LabVIEW code for mixed-domain (RF and DC) characterization and modeling is presented. For this purpose, an RFID reader and the respective LabVIEW code has been developed, in order to demonstrate the applicability of modular instrument.

RFID Reader

Goals

- Developed an RFID Reader for the Ultra High Frequency (UHF) in PXI from NI using LabVIEW code.
- Used International Standards Organization (ISO) 18000-6C RFID communication protocol.
- Used the VSG, VSA, NI 5792 and NI 5793 like front-ends.

Specifications

Reader carrier frequency	915 MHz
Bandwidth of the transmission channel	500 kHz
Distance between channels	None, because the transmission channels are adjacent
Maximum output power	4W – Effective Isotropic Radiated Power (EIRP)
Delta frequency	1 MHz
Environment	Dense-Interrogator
Modulation	OOK
Encoding	PIE
Coding	FM0

Command sequence between the reader and the tag

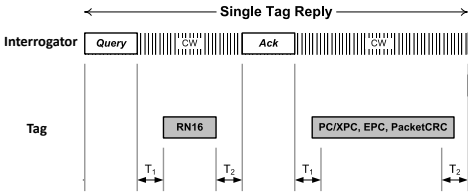

T1 - Time from Interrogator transmission to Tag response for an *immediate* Tag reply.
T2 - Time from Tag response to Interrogator transmission.

RFID Reader Architecture

Stimulus Response Architecture

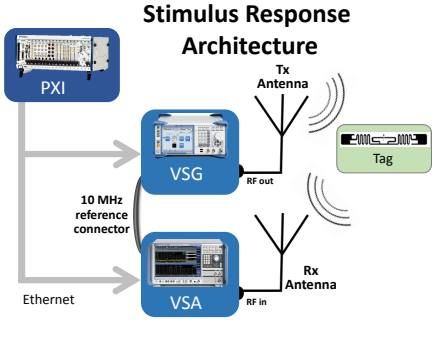

Real-Time Interrogator Emulation Architecture

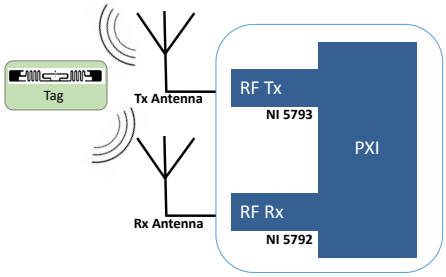

Block Diagram

RFID Reader Block Diagram

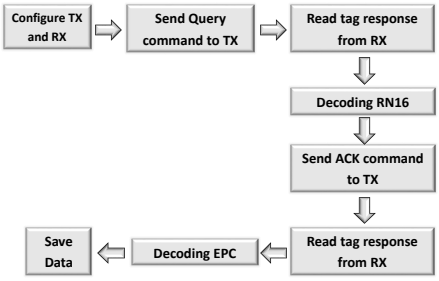

Results

Tag response (RN16) after sending a Query command

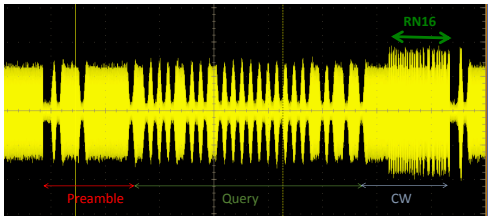

Power Transmission Mask

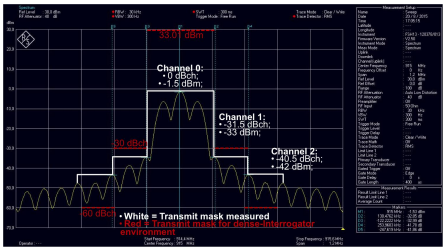

RN16 Decoding

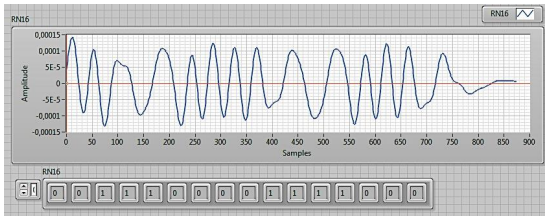

Conclusion

- The LabVIEW-based RFID reader developed in this paper was step forward in the design of mixed-domain (RF-to-DC) characterization tools.
- This system will be the key sub-system of a complete mixed-signal multi-domain characterization solution.
- After performing some measurements, it was concluded that the system responds to a minimum power of -9 dBm for a fixed distance of 5.5 cm. For a maximum power of 30 dBm (1 Watt) the system can respond up to an average distance of 93 cm.
- The big difficulty in this work was to try to overcome the very severe timing limits defined in the RFID standard for the reader data processing and respective tag replies.
- Future work includes developing and improving the proposed RFID characterization system using FPGA implementation.

This work is funded by National Funds through FCT Fundo para a ciência e a Tecnologia under the project PEst-OE/EEI/LA0008/2013; UID/EEA/50008/2013 and by Instituto Telecomunicões under project CREaTION (ref. EXCL/EEITEL/0067/2012)

Bibliography

[Ana09] Anacom. Quadro Nacional de Atribuição de Frequências, 2009.

[Ban94] David Bantz. Industrial Scientific and Medical (ISM) Bands. `http://www.wirelesscommunication.nl/reference/chaptr01/dtmmsyst/ism.htm`, 1994.

[Bel14] Daniel Gil Belo. Otimização de Sistemas de Transmissão de Energia sem Fios. Master's thesis, Electronics, Telecommunications and Informatics Department, Aveiro University, 2014.

[Bro06] Piet M. T. Broersen. *Automatic Autocorrelation and Spectral Analysis*. Springer, 2006.

[Cis08] Cisco. *Wi-Fi Location-Based Services 4.1 Design Guide*. Americas Headquarters, Cisco Systems, May 20, 2008.

[Col] Eric C. Coll. *Wireless Fundamentals*. Teracom Training Institute Ltd.

[Dob07] Daniel Dobkin. *Communications Engineering Series: The RF in RFID - Passive UHF RFID in Practice*. Elsevier Inc., 2007.

[EPC13] EPC. EPC information. `http://www.epc-rfid.info`, 2013.

[GS1] GS1. Mode of operation of RFID systems. `http://www.gs1.ch/en/gs1-system/the-gs1-system/epcglobal/radio-frequency-technology/mode-of-operation-of-rfid-systems`.

[GS115] GS1. EPC Radio-Frequency Identity Protocols Generation-2 UHF RFID: Specification for RFID Air Interface Protocol for Communication at 860 MHz and 960 MHz. April, 2015.

[Har13] Doug Harper. myDAQ Resources. `http://physics.wku.edu/phys318/tag/day01/`, January 27, 2013.

[Ins] National Instruments. O que é o NI myDAQ? `http://www.ni.com/mydaq/what-is/pt/`.

[Ins98] National Instruments. *LabVIEW: User Manual*. January 1998.

[Ins06] National Instruments. *RF and Microwave Signal Generators with Modulation Capability*. National Instruments, `http://www.datasheetarchive.com/dl/Datasheet-080/DASF0014100.pdf`, 2006.

[Ins07] National Instruments. Sources of Error in IQ Based RF Signal Generation. January 09, 2007.

[Ins13a] National Instruments. Advanced RFID Measurements: Basic Theory to Protocol Conformance Test. December 2013.

[Ins13b] National Instruments. *LabVIEW: Getting Started with LabVIEW*. National Instruments, `http://www.ni.com/pdf/manuals/373427j.pdf`, June, 2013.

[Ins13c] National Instruments. *User Manual and Sepecifications NI 5792R: RF Receiver Adapter Module*. National Instruments, `http://www.ni.com/pdf/manuals/373947b.pdf`, May 13, 2013.

[Ins13d] National Instruments. *User Manual and Sepecifications NI 5793R: RF Transmitter Adapter Module*. National Instruments, `http://www.ni.com/pdf/manuals/373949b.pdf`, May, 2013.

[Ins14a] National Instruments. What is I/Q Data? February 06, 2014.

[Ins14b] National Instruments. O que é o PXI? February 24, 2014.

[Ins15a] National Instruments. Creating RFID Applied Tag Performance Tests. 2015.

[Ins15b] National Instruments. *PXI Express, NI PXIe-1085 Series User Manual*. National Instruments, `http://www.ni.com/pdf/manuals/373712f.pdf`, February, 2015.

[JA] RF Monolithics John Anthes. OOK, ASK and FSK Modulation in the Presence of an Interfering signal.

[JCR14] Viktor Bana Justin Church, Jeremy Q. Bagley and John D. Rockway. Metamaterial Wireless Power Transfer System. *URSI*, 2014.

[Jou] RFID Journ. RFID Frequency Asked Question. `https://www.rfidjournal.com/faq/show?67`.

[Jou15] RFID Journal. RFID Journal Introduces Internet of Things Conference. `http://www.rfidjournal.com/articles/view?12416`, 2015.

[KAT] KATHREIN. Indoor Directional Antenna Vertical Polarization Half-power Beam Width. `http://www.belnetmon.bn.by/doc/936675c.pdf`.

[Mata] MathWorks. Autocorrelation and Partial Autocorrelation. `http://www.mathworks.com/help/econ/autocorrelation-and-partial-autocorrelation.html`.

[Matb] MathWorks. Cross-correlation. `www.mathworks.com/help/signal/ref/xcorr.html`.

[MKS11] Neeraj Mohan Mandeep Kaur, Manjeet Sandhu and Parvinder S. Sandhu. RFID Technology Principles, Advantages, Limitations & Its Applications. *International Journal of Computer and Electrical Engineering, Vol.3, No.1*, February, 2011.

[Nik09] Pavel V. Nikitin. LabVIEW-Based UHF RFID Tag Test and Measurement System. *IEEE Transactions on Industrial Electronics, Vol. 56, No 7*, July 2009.

[Pra08] Pedro Isidoro Prata. Sistemas de Localização para Ambientes Interiores bbaseado em RFID. Master's thesis, Electronics, Telecommunications and Informatics Department, Aveiro University, 2008.

[RFI09] RFIDiom. What is RFID? `http://www.rfidiom.com/rfid-technology-introduction/`, 2009.

[Rob05] Mark Roberti. The History of RFID Technology. `http://www.rfidjournal.com/articles/view?1338`, January 16, 2005.

[San14] Joo Santos. Leitor RFID para a gama UHF baseado em Software-Defined Radio. Master's thesis, Electronics, Telecommunications and Informatics Department, Aveiro University, 2014.

[Tan08] Li Tan. *Digital Signal Processing: Fundamentals and Applications*. Elsevier Inc., 2008.

[Tec14a] Alien Technology. *ALN-9640 Squiggle Inlay*. `http://www.alientechnology.com/wp-content/uploads/Alien-Technology-Higgs-3-ALN-9640-Squiggle.pdf`, 07 February 2014.

[Tec14b] Alien Technology. *ALN-9654 G Inlay*. `http://www.alientechnology.com/wp-content/uploads/Alien-Technology-Higgs-3-ALN-9654-G.pdf`, 27 May 2014.

[Tec14c] Alien Technology. *Higgs 3: EPC Class 1 Gen 2 RFID Tag IC*. `http://www.alientechnology.com/wp-content/uploads/ALC-360%20Higgs3%202014-12-21.pdf`, December 21, 2014.

[The04] Les Thede. *Practical Analog and Digital Filter Design*. Artech House Inc, 2004.

[Tod] Todd. The Fast Fourier Transform: A Mathematical Perspective. `http://www.ces.clemson.edu/~janoski/reu/2008/FFT-book.pdf`.

[VDHP07] Albert Puglia V. Daniel Hunt and Mike Puglia. *RFID-A Guide to Radio Frequency Identification*. John Wiley & Sons Inc., 2007.

[VF13] Ovidiu Vermesan and Peter Friess. *Internet of Things: Converging Technologies for Smart Environments and Integrated Ecosystems*. River Publishers, 2013.

[VTS13] Andrea Ferrero Valeria Teppati and Mohamed Sayed. *Modern RF and Microwave Measurement Techniques*. Cambridge, 2013.

[XA15] Minghua Xia and Sonia Aissa. On the Efficiency of Far-Field Wireless Power Transfer. *IEEE TRANSACTIONS ON SIGNAL PROCESSING, VOL. 63, NO. 11,*, JUNE 1, 2015.

[YZC09] Laurence T. Yang Yan Zhang and Fiming Chen. *RFID and Sensor Networks: Architectures, Protocols, Security and Integrations*. CRC Press, 2009.

[ZT94] Glenn Zelniker and Fred Taylor. *Advanced Digital Signal Processing: Theory and Applications*. Marcel Dekker Inc, 1994.